NASA-CR-200985

Final Report
Grant No. NAS3-27418
October 19, 1994 - March 31, 1996

COST MODELS FOR MMC MANUFACTURING PROCESSES

Submitted to:

Mr. Glen M. Williams, Contracting Officer
Technology Support Branch, MS 500-306
National Aeronautics and Space Administration
Lewis Research Center
21000 Brookpark Road
Cleveland, OH 44135

Submitted by:

Dana M. Elzey
Research Assistant Professor

Haydn N. G. Wadley
Associate Dean for Research

SEAS Report No. UVA/528509/MSE96/101
May 1996

DEPARTMENT OF MATERIALS SCIENCE AND ENGINEERING

SCHOOL OF
ENGINEERING
& APPLIED SCIENCE

University of Virginia
Thornton Hall
Charlottesville, VA 22903

Cost Models for MMC Manufacturing Processes

Dana M. Elzey and Haydn N. G. Wadley

Final Report: NASA Contract NAS3-27418

for the period 10/19/94 - 3/31/96

1.0 Introduction to QCM and Motivation for its Development

Advanced materials offer exciting possibilities for the development of new technologies and for achieving further improvements in current technology. The attraction of these advanced materials is the performance edge they promise over conventional materials. Usually however, there is a substantial price penalty to be paid for the extra performance. In considering the application of advanced materials, it is thus the affordability, i.e. the combination of price and performance, (and not the performance alone), which must be the deciding factor.

The high cost of new materials derives primarily from low production volumes and poorly characterized manufacturing processes (leading to process inefficiency, high product variability and low process yield). Production volumes are ultimately regulated by the demand for the new material, although they may be stimulated initially by government subsidies in materials research and development. Poor characterization refers to inadequate understanding of the relationship between material properties, process conditions, equipment design and the microstructure and properties of the finished product and is an inevitable feature of relatively immature processing technologies. The inadequacy is reflected both in a dearth of reliable experimental observations and in theoretical models for predicting material changes taking place during processing. Experimental data is expensive to obtain and when available, usually covers only a small "window" in the total process-material space; the issue of affordability cannot be reliably addressed for potential applications outside this window.

This lack of information regarding novel materials and processes places persons responsible for directing R&D efforts (i.e. industry managers and government program sponsors) in the difficult position of having to down-select from competing technologies with little information to guide them. This research has focussed on one possibility for providing quantitative information on the affordability of relatively immature materials and their associated manufacturing processes. The approach is known as QCM, or Quality-Cost Modeling; it differs from conventional manufacturing process cost modeling in that it incorporates material models (allowing key microstructural features of the finished product to be related back to the process conditions used) to predict quality, process efficiency and yield, rather than assume values for these quantities. Cost is based on the cost of 'raw' materials, the actual process cycle imposed (which determines the energy consumed), the predicted efficiency with which starting material actually ends up in the final product (material use efficiency,

MUE), capital costs (amortized over the production period) and the cost of consumables (materials used, but not intended for incorporation in the final product).

The QCM tool is intended to be a relatively simple-to-use device for obtaining a first-order assessment of the quality-cost relationship for a given process-material combination. The QCM curve is a plot of cost (in units of $/kg of final product) versus quality (an index indicating microstructural quality, i.e. absence of defects, cracks, interfacial degradation, etc., or performance, i.e. a set of properties such as strength, toughness, etc.), which is unique for a given process-material combination. The QCM curve indicates the tradeoff between cost and performance, thus enabling one to evaluate affordability. Additionally, the effect of changes in process design, raw materials, and process conditions on the cost-quality relationship can be evaluated. Such results might indicate the most efficient means to obtain improved quality at reduced cost by process design refinements, the implementation of sensors and models for closed loop process control or improvement in the properties of raw materials being fed into the process.

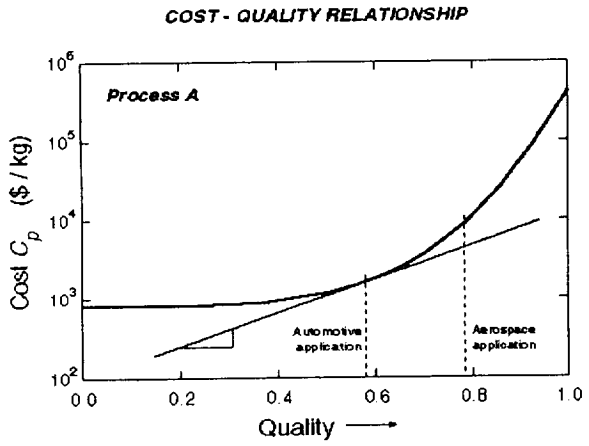

FIGURE 1. Characteristic QCM curve defining the affordability space for a given material-process system.

QCM also allows alternative processes for producing the same or similar material to be compared in terms of their potential for producing competitively priced, high quality material. Aside from demonstrating the usefulness of the QCM concept, this is one of the main foci of the present research program, namely to compare processes for making continuous fiber reinforced, metal matrix composites (MMC's). Two processes, low pressure plasma spray (LPPS) deposition and tape casting are considered for QCM development.

QCM addresses several of the key cost issues mentioned previously: factors leading to the inefficient conversion of raw materials and resources into high quality material can be identified and numerical simulations used to observe the sensitivity of the process to changes in material and processing strategy. Critical cost-and quality-drivers can be identified and prioritized according to their influence on affordability. The cost/benefit ratio of various alternatives for reducing costs (including new process cycle designs, changes to the raw material, redesigning or upgrading process equipment, see Fig. 2) can be evaluated. The influence of production volume on the cost/kg of material can be estimated. Since the models serve to crystallize the current state of understanding of the relationships among process variables, evolving microstructural features, performance-defining attributes and cost-drivers, they also address the issue of understanding processing-performance relationships.

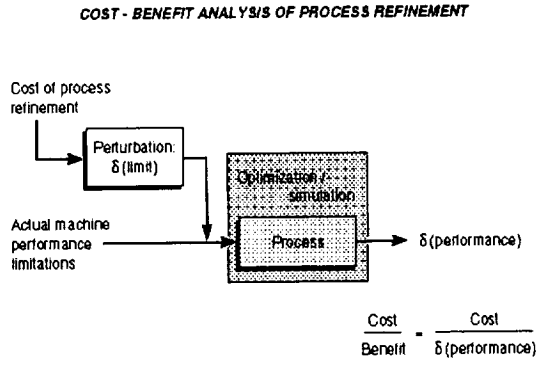

FIGURE 2. The potential for improving affordability by process refinement can be assessed using QCM.

The following consists of a more detailed look at the design of the QCM approach, followed by discussion of the application of QCM to each of the selected MMC manufacturing processes along with results, comparison of processes, and finally, a summary of findings and recommendations.

2.0 QCM Architecture

At a high level, a material manufacturing process can be viewed as a system which consumes energy while transforming the (micro)structure (and possibly also the shape) of 'raw' material(s) into a finished product. The final microstructure determines the properties (performance) of the material. Thus the processing conditions and the initial material state determine the performance of the finished product (here, the material).

Now consider a model (or set of models) which simulate the evolution of the material's microstructure from some given initial state as a function of a set of time-dependent process conditions (also given), see Fig. 3. Such models are often referred to as process or process-structure models. As shown in Fig. 3, input to the process models consists of a set of process conditions, equipment design parameters, and the amounts and properties of starting and consumable materials. (Consumable materials are not intended for the final product, but assist the transformation in some way.)

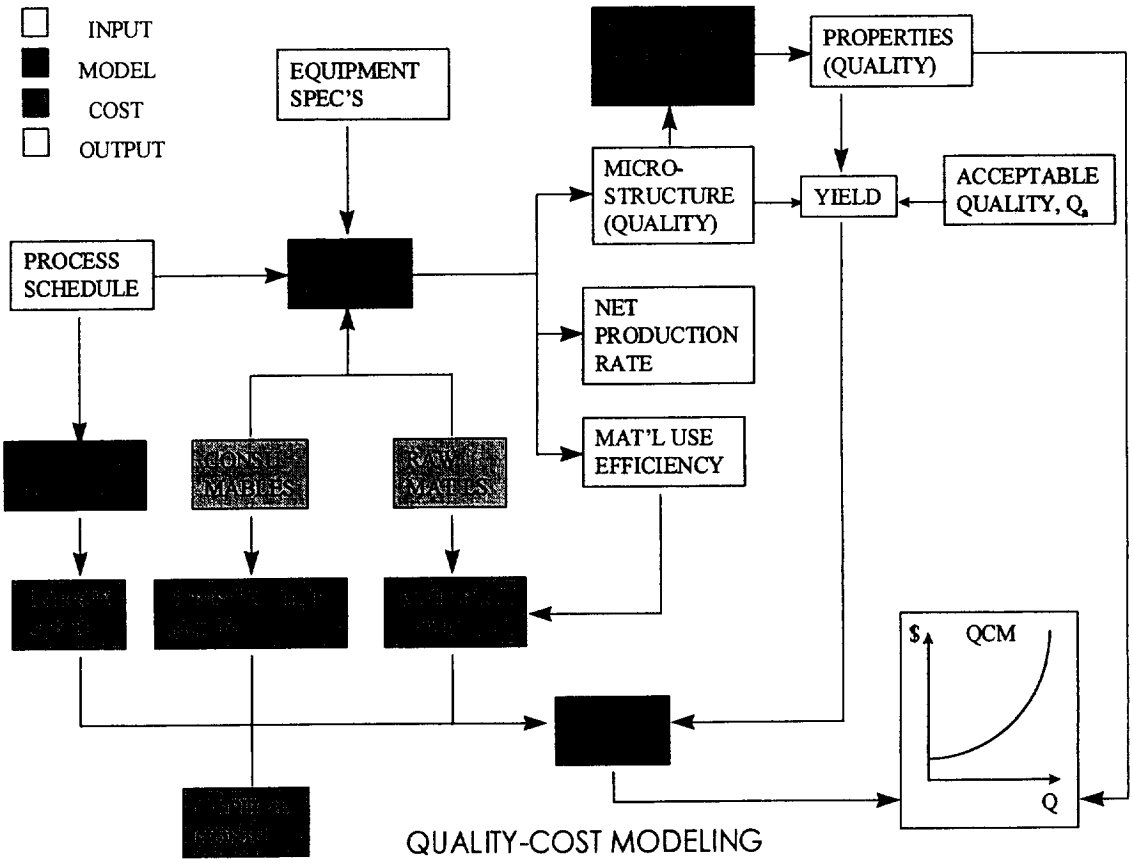

FIGURE 3. Flowchart illustrating the QCM concept: process and cost models are combined to simulate the influence of process and material on affordability.

In addition to the final microstructure, the models provide as output, the production rate (kg/hr) and the MUE (material use efficiency, defined as the fraction of 1 kg of starting material ending up in the finished product). The MUE

bears an important influence on the cost of the final product - if the efficiency is say, 0.5, then for every kg of product, one must pay for 2 kg of starting material .

The quality of the finished product may be characterized in terms of its microstructural features or these may be used to predict the actual properties (such as yield strength, poisson's ratio, thermal conductivity, etc), by means of structure-property models. In either case, a quality index may be calculated, which is a number in the range 0 to 1, which indicates the 'goodness' of the actual material relative to some ideal. It is expressed as a weighted sum of dimensionless properties (or microstructural state variables). Comparison of the predicted quality with a user-supplied specification for minimum acceptable quality, allows determination of process yield; the given batch will be unacceptable (yield = 0) if it does not meet or exceed the stated specification. Repeated simulation, with statistically determined input (simulating variability in the quality of starting materials, process control inaccuracy, etc.), allows prediction of process yield.

The cost of the final product is rather simpler to predict than its quality - it consists of the costs of the starting materials (which must account for the MUE), c_m, consumable materials (gases, fuel, catalysts, binders, etc.), c_c, energy, c_e, and capital investment, c_{cap}

$$C = c_m + c_c + c_e + \frac{c_{cap}}{m} \qquad \text{(EQ 1)}$$

where m is the production volume, thus representing the amortization of the capital investment over the time of production.

Since the processing conditions are known as a function of time (e.g. the temperature of a sintering furnace), the total energy requirement for each piece of processing equipment is obtained as the integral of the power consumption for that device. The power consumption is given as a function of the process variable (e.g. temperature in the case of the sintering oven) by so-called resource models. Thus resource models convert process cycles into energy requirements. Multiplying by the cost of electric (or other energy) gives the energy-related costs.

With quality and cost determined for a given set of strarting materials, processing conditions and equipment design specifications, a point is plotted on a plot of cost vs quality (Fig. 1). Repeating the numerical experiment for varying conditions leads finally to a picture of the reachable quality for a given cost. The limit, or edge of this affordability space is the desired cost-quality curve.

3.0 Plasma Spray Deposition

3.1 Process Overview

High temperature plasmas can be used to melt metallic (or ceramic) powders, thus creating a jet spray of molten matrix droplets. Plasma torches are typically either of the DC Arc or of the RF Induction type. DC Arc spraying is preferred for the application of protective barrier coatings, such as those used for the protection of gas turbine blades. RF Induction is generally preferred for manufacturing MMC's because of lower particle velocities (typically less than 50 m/s), and therefore higher melting capacity (g powder/min) due to the longer residency time of each particle in the plasma. Figure 4 shows a detail of the RF Induction Coupled plasma spray torch. It consists of a confinement tube (in which the plasma is generated), surrounded by a water-cooled copper conductor. Alternating current passes through the conductor, inducing an EMF along the tube axis. As the RF power is increased, thereby increasing the potential within the confinement tube, the resistivity of a gas introduced at the top of the torch axis (e.g. Ar, H_2, N_2, air) can be overcome, creating a plasma, i.e. a partially ionized gas in which free electrons are available to conduct current and to produce RF induction heating. Heat transfer from the plasma, either by loss of kinetic energy or by reassociation reactions in diatomic gases such as hydrogen, provides heat to melt the powder particles, which are also injected along the torch axis.

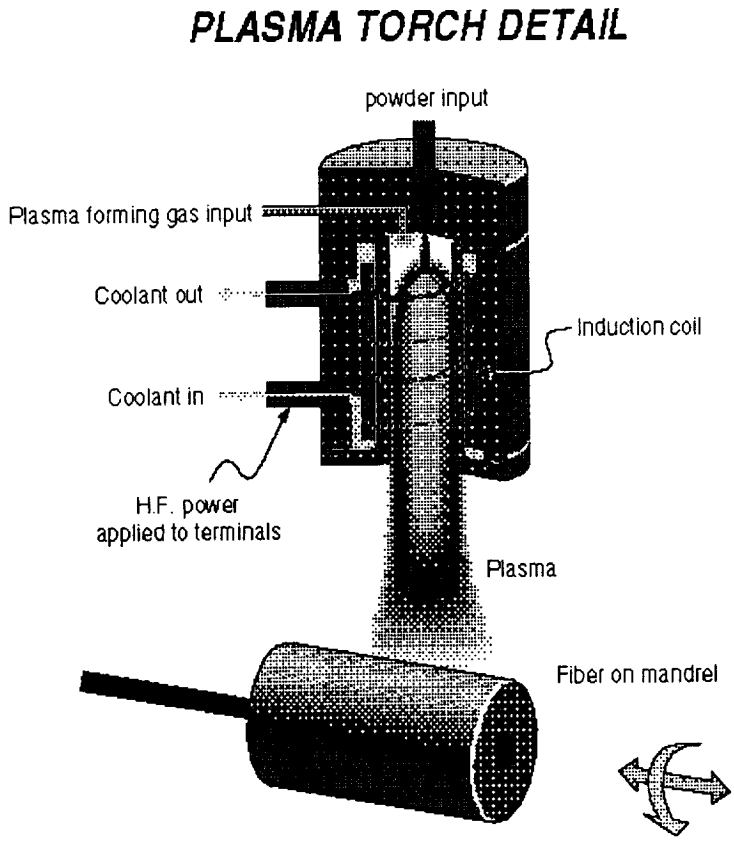

FIGURE 4. Schematic of the low pressure plasma spray deposition process for manufacturing MMC monotape.

Figure 5 illustrates the steps needed to produce a composite component: first, monotapes are produced by passing a single layer of parallel, uniformly spaced ceramic fibers beneath a fine spray of plasma-melted metal/alloy droplets. Following deposition to the desired thickness, the tapes are cut and stacked to produce a laminate of specified macroarchitecture (ply orientation, stacking sequence, etc.). The laminate is then placed within a container, evacuated, and consolidated to full density and final shape by the application of pressure and heat, typically within a hot isostatic press (HIP). The performance of the end-product is determined by its shape and by the final microstructure, which is affected only by the spray deposition and consolidation steps. Figure 5 identifies the process variables (i.e. those variables which can be adjusted by the operator during the process), microstructural state variables and some of the process cost elements. The process leading to a shaped MMC component may be broken down into three steps: plasma spray creation, spray deposition, and consolidation. Here, only the spray creation and deposition process steps (leading to creation of a single MMC monotape) are considered. The consolidation process will of course add to the cost of the finished component and will influence its quality. The objective of the plasma spray creation and deposition models is to simulate the evolution of microstructural variables which are most sensitive to the process conditions used and which most strongly affect the final properties. The selection of critical microstructural features and first-order effects is based on experimental observations and information available in the open literature.[1-3]

1. M.I.Boulos, "RF Induction Plasma Spraying", J.Thermal Spray Tech., 1(1), 33 (1992).

2. P.Proulx, J.Mostaghimi and M.I.Boulos, "Plasma-Particle Interaction Effects in Induction Plasma Modeling Under Dense Loading Conditions", Int.J.Heat Mass Transfer, 28(7), 1327 (1985).

3. M.P.Freeman and J.D.Chase, "Energy Transfer Mechanism and Typical Operating Characteristics for the Thermal RF Plasma Generator", J.Appl.Phys. 39(1), 180 (1968).

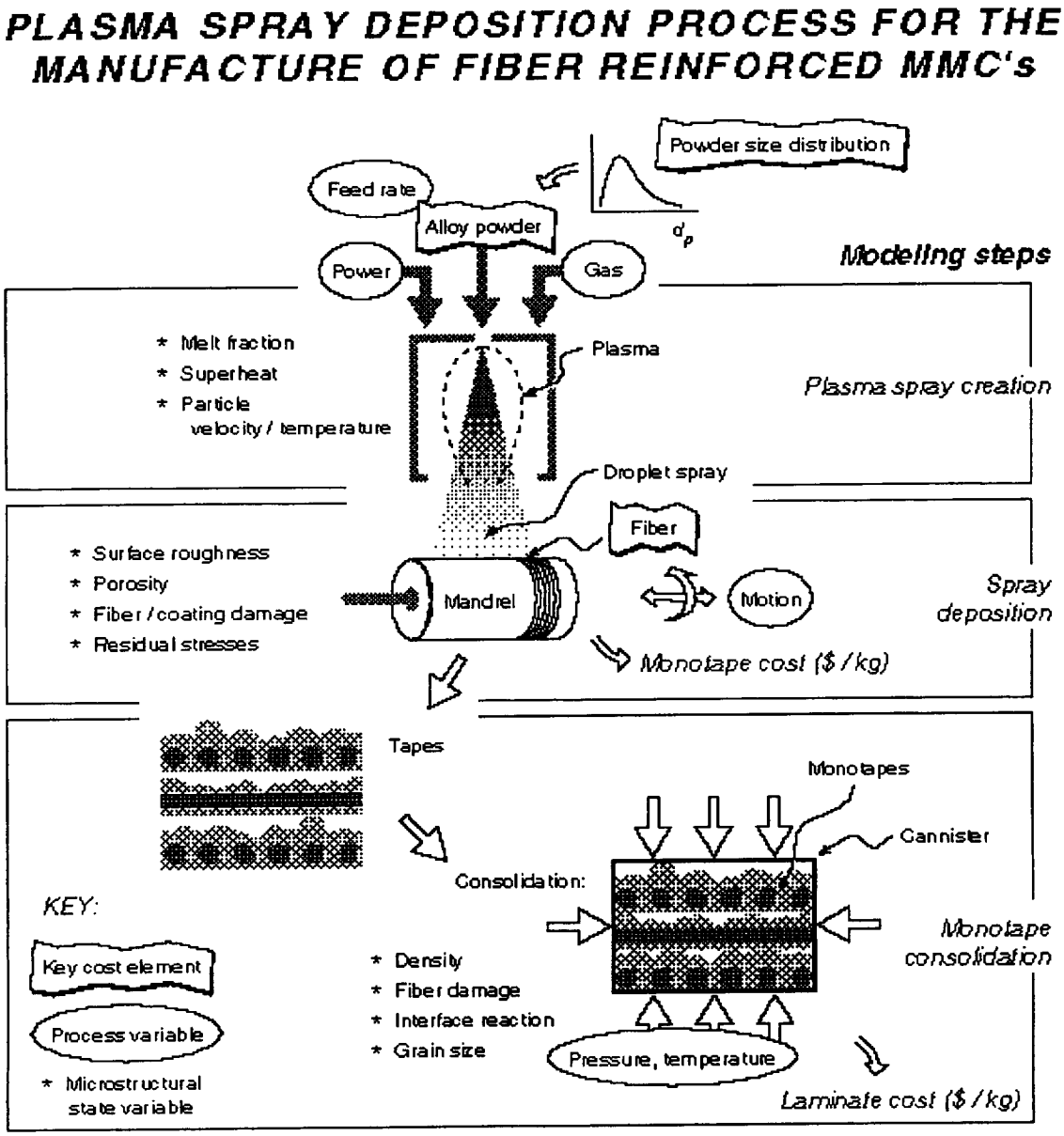

FIGURE 5. Process steps, variables and material parameters during plasma spray deposition of MMC's.

Figure 6 illustrates a number of factors affecting the (microstructural) quality and performance of MMC monotapes produced by plasma spray deposition. The process models developed for calculating material quality include the effects of fiber thermal shock, (and in effect, spalling, which is related to thermal shock), porosity, and interfacial reactivity. Other effects, which may be important under some circumstances, have been neglected, but could be included in further refinements.

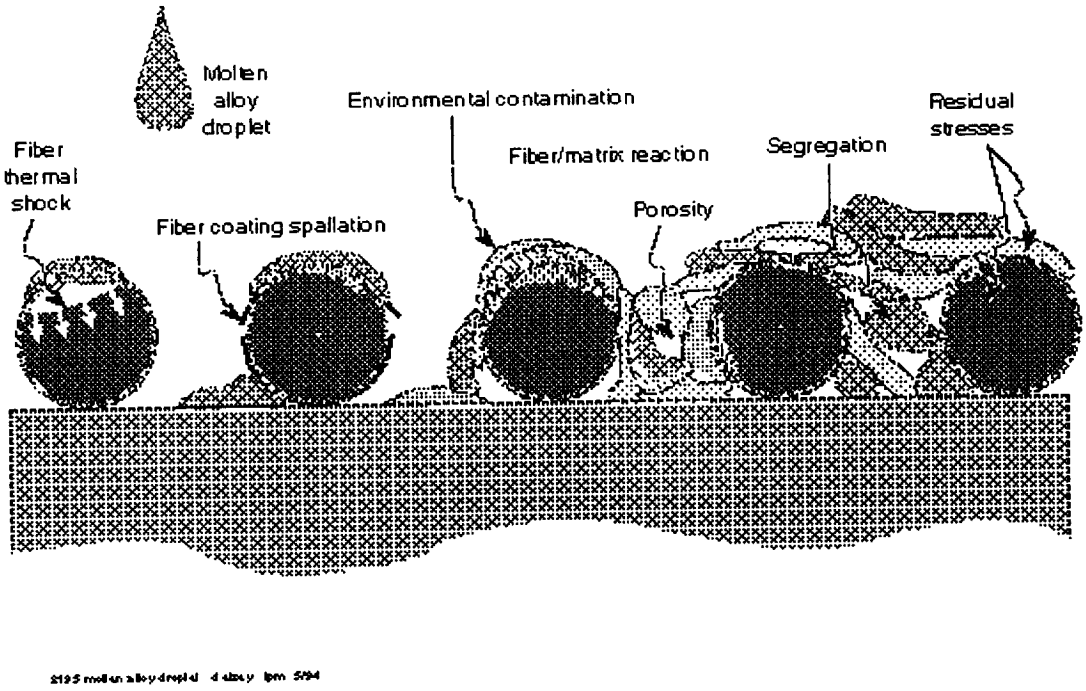

FIGURE 6. Factors and microstrucutral features affecting the quality of plasma sprayed MMC monotapes during deposition.

3.2 Process Parameters

Table 1 lists variables associated with the plasma spray deposition process. Process variables are input chosen by the user; they are arbitrary, but are considered fixed for the duration of a process schedule. Equipment design parameters specify features of the processing facility, which may be changed by modification of the equipment design and are also model input. Geometric variables, such as powder size distribution and fiber spacing are user-input. The fiber volume fraction, specified by the user, is the volume fraction of fiber desired in the fully consolidated composite.

TABLE 1. Plasma Spray Process Parameters

Variable Type	Variable Name	Symbol	Units
Process Variables	Carrier gas flow rate	q_{cg}	slpm
	Central gas flow rate	q_{mg}	slpm
	Sheath gas flow rate	q_{sg}	slpm
	Powder flow rate	$\dot{m}$	g/min
	RF Power	P	kW
	Preheat temperature	T_s	$^{\circ}C$
	Spray distance	l_s	cm
	Radius of injection probe orifice	r_i	mm
Equipment design parameters	Plasma tube radius	r_T	mm
	Deposit length	l_D	cm
	Mandrel diameter	d_M	cm
	Mean powder size	d_p	μm
	Powder size std. deviation	σ_{dp}	μm
Geometric parameters	Fiber diameter	d_F	μm
	Fiber spacing	λ_s	μm
	Fiber vol. fraction	$\bar{v}_F$	--
	Interfacial reaction zone thickness	δ_R	μm
Microstructural state variables	Matrix relative density	D	--
	Thermal shock damage	ω_s	--
	Dimensionless reaction zone thickness	$\bar{\delta}_R = \frac{\delta_R}{\delta_a}$	--
Quality Indices	Matrix relative density	D	--
	Cumulative thermal shock damage	Ω_s	--

TABLE 1. Plasma Spray Process Parameters

Variable Type	Variable Name	Symbol	Units
Efficiency and Production	Monotape quality	Q_{ps}	--
	Melting efficiency	η_l	--
	Material use efficiency	η_m	--
	Spray duration	t_s	min
	Tape thickness	δ_T	mm
	Deposition rate	$\dot{m}_{dep}$	g/min
	Production rate	$\dot{m}_{prod}$	g/min
Cost	Materials costs	c_m	$/kg
	Consumables costs	c_c	$/kg
	Energy cost	c_e	$/kg
	Capital costs	c_{cap}	$/kg
	Monotape cost	C	$/kg

Microstuctural variables are tracked as a function of time - their final values depend on the material's initial state and the specified process conditions. For the plasma spray process, these variables charcterizing the microstructural state include the relative density of the matrix, interfacial reaction zone thickness and thermal shock damage to the fiber and/or its coating.

Quality indices are dimensionless numbers, each having a range of 0 to 1 (0 being the lowest quality, 1 the best). They represent the microstructural state in normalized state space. The quality of the final MMC monotape is obtained as a weighted sum (weight factors are user-defined) of the quality indices. Cost variables have already been introduced in equation 1.

Finally, Table 1 lists variables associated with process efficiency and production rate. The material use efficiency has been introduced previously; it is defined as the fraction of 1 kg of starting material which ends up in the final product. The melting efficiency is the fraction of powder mass which melts as it passes through the plasma torch. The spray duration, t_s, is the time required for the given spray conditions to produce a monotape of sufficient thickness, δ_T, such that the user-specified fiber volume fraction, $\bar{v}_F$, is obtained.

Table 2 lists material properties needed for the metallic matrix, ceramic fiber, the interfacial zone (between the fiber and matrix), plasma and mandrel.

TABLE 2. Material Properties

Constituent	Property	Symbol	Units
MATRIX			
Solid	Thermal conductivity	k_s	W/mK
	Thermal diffusivity	a_s	m^2/s
	Density	ρ_s	g/cm^3
	Specific heat	cp_s	J/gK
	Emmisivity	ε	--
	Melting point	T_m	K
	Latent heat of melting	h_m	J/g
Liquid	Thermal conductivity	k_l	W/mK
	Thermal diffusivity	a_l	m^2/s
	Density	ρ_l	g/cm^3
	Specific heat	cp_l	J/gK
	Emmisivity	ε	--
	Boiling point	T_b	K
	Latent heat of vaporization	h_v	J/g
	Surface tension	σ_s	MPa
	Dynamic viscosity	μ_p	g/ms
FIBER	Elastic modulus (longitudinal)	E_F	GPa
	Reference strength	σ_0	GPa
	Weibull modulus	m	--
	Thermal conductivity	k_F	W/mK
	Coefficient of thermal expansion	α_F	$^\circ C^{-1}$
PLASMA	Density	ρ_{PS}	g/cm^3
	Specific heat	Cp_{PS}	J/gK
	Thermal conductivity	k_{PS}	W/mK
	Dynamic viscosity	μ_{PS}	g/ms
INTERFACE	Pre-exp. constant	κ_0	$m\sqrt{s}$
	Activation energy	Q_i	J/mol
MANDREL	Melting temperature	T_{mm}	K

3.3 Models for QCM of Plasma Spray

As shown in Fig. 3, the models needed to perform QCM include process, structure-property, cost and resource models. If the microstructural state is used as a measure of material quality, as is done here, then structure-property models can be omitted. The models are described next, beginning with process models (from which the quality indices are obtained), followed by resource and cost models.

3.3.1 Process (Quality) Models

The plasma spray deposition process is modeled in two steps: spray creation and deposition.

3.3.1.1 Plasma Spray Creation

During plasma spraying, the metal/alloy powder which is to form the composite matrix is introduced into the plasma where the powder particles are accelerated and heated. The plasma, which is typically argon or an argon/hydrogen mixture, is generated by RF induction. Particle heating takes place by conduction and convection, with radiative losses to the surroundings. The plasma, initially at a temperature of around 10^4 K (before powder is introduced), is quickly cooled when the powder mass flow begins. At steady state, the plasma reaches an (unknown) equilibrium temperature.

Given the distribution of powder sizes, the initial particle velocity and temperature, the RF power, and an initial guess for the plasma equilibrium temperature, the model calculates the total energy absorbed by heating of the powder particles. It then uses an energy balance (energy available from the plasma = energy absorbed by particle heating, melting and vaporization + radiative losses) to determine if the guessed equilibrium temperature is correct. The model searches iteratively for the equilibrium temperature until conservation of energy is satisfied. Although the model is a one-dimensional idealization, the predicted temperature agrees well with mean temperatures obtained from more complicated 3-D mesh-type models.

The velocity history of a particle of size, d_p, is obtained from the solution of the momentum equation

$$\frac{du_p}{dt} = -\frac{3}{4}\left[C_D(u_p - u)|u_R|\frac{\rho_{ps}}{\rho_p d_p} + g\right] \qquad \text{(EQ 2)}$$

where u_p and u are the particle and plasma velocities, respectively, $u_R = u_p - u$ is the relative velocity, g is the acceleration due to gravity and C_D is the drag coefficient for a spherical particle in a viscous plasma. The following approximation, due to Lesinski et al[1], has been used for calculating the drag coefficient:

TABLE 3. Drag Coefficient

$$C_D = \begin{cases} 0 & \text{Re} = 0 \\ \dfrac{24}{Re} & 0 < Re \le 0.2 \\ \dfrac{24}{Re}(1 + 0.1875Re) & 0.2 < Re \le 2 \\ \dfrac{24}{Re}(1 + 0.11Re^{0.81}) & 2 < Re \le 21 \\ \dfrac{24}{Re}(1 + 0.189Re^{0.62}) & 21 < Re \le 200 \\ \dfrac{24}{Re}(1 + 0.0987Re^{0.75}) & 200 < Re \le 500 \end{cases}$$

where Re, the Reynolds number, is defined as

$$Re = \frac{\rho_{PS} u_R d_p}{\mu_{PS}}. \qquad \text{(EQ 3)}$$

The particle temperature history is determined from the energy balance equation

$$\frac{dT}{dt} = \frac{\pi d_p^2 h_c}{c_p}(T_{PS} - T) - \pi d_p^2 \sigma \varepsilon (T^4 - T_0^4) \qquad \text{(EQ 4)}$$

where T is the particle temperature at time, t, h_c is the plasma-particle heat transfer coefficient, T_{ps} is the plasma temperature, T_0 is ambient temperature, σ is the Stefan-Boltzmann constant, and ε is the emmisivity. The heat capacity of the particle as a function of temperature is

$$c_p = \begin{cases} \dfrac{\pi d_p^3}{6}\rho_s c p_s & T \ne \begin{pmatrix} T_m \\ T_b \end{pmatrix} \\ \dfrac{\pi d_p^3}{6}\rho_s h_m & T = T_m \\ \dfrac{\pi d_p^2}{6}\rho_s h_v & T = T_b \end{cases}$$

The heat transfer coefficent is approximated in terms of the Reynold's number

$$h_c = \frac{k_{PS}}{d_p}(2 + 0.515Re^{0.5}) \qquad \text{(EQ 5)}$$

with the temperature-dependent plasma thermal conductivity approximated for an Ar plasma by

$$k_{PS} = 0.0165 + 0.262\left(\frac{T}{10^4}\right) - 0.024\left(\frac{T}{10^4}\right)^2 \qquad \text{(EQ 6)}$$

for T < 6000 K, or

$$k_{PS} = 0.074 + 0.372\left(\frac{T}{10^4}\right)^3 - 0.248\left(\frac{T}{10^4}\right)^6 \qquad \text{(EQ 7)}$$

for T > 6000 K.

Figure 7 illustrates a typical particle temperature history; the temperature of the 50 μm diameter titanium particle increases until its melting point (1800 K) is reached. The particle melts at constant temperature due to the latent heat of melting, followed by superheating of the liquid until the boiling point is reached at 2500 K. Evaporation, and consequent loss of mass, occurs if the boiling point is reached prior to exiting the torch. The final diameter of the particle at impact is calculated based on the amount of mass lost.

1. J.Lesinski, R.Gagne and M.I.Boulos, "Gas and Particle Velocity Measurements in an Induction Plasma", Proc. 5th Int. Symp. Plasma Chem., B.W.Heriot, ed., vol. 2, pp. 527-533, Int. Union of Pure and Appl. Chem., Edinburgh, Scotland, UK, Aug. 10-14, 1981.

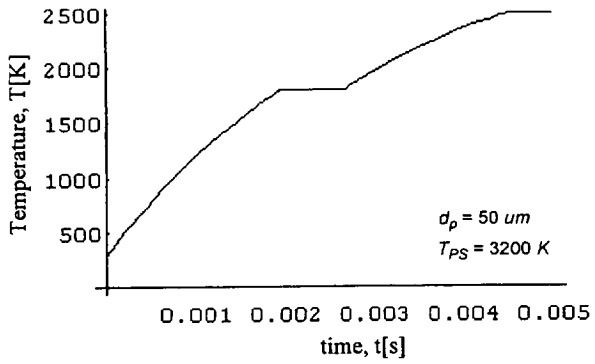

FIGURE 7. Typical temperature history: in this case a 50 μm diameter Ti powder particle moves through a plasma at a mean temperature of 3200 K.

The time required to completely melt the particle is given by

$$t_m = t_s + \frac{1}{dx/dt} \qquad \text{(EQ 8)}$$

where t_s is the time to reach the melting point and x is the melt fraction. The time rate of change of melt fraction is found using EQ 4:

$$\frac{dx}{dt} = \frac{\pi d_p^2 h_c}{c_p}(T_{PS} - T_m) - \pi d_p^2 \sigma \varepsilon (T_m^4 - T_0^4) \qquad \text{(EQ 9)}$$

Similarly, the particle size once the boiling point (T_b) has been reached is given by

$$\frac{dd_p}{dt} = \frac{\pi d_p^2 h_c}{c_p}(T_{PS} - T_b) - \pi d_p^2 \sigma \varepsilon (T_b^4 - T_0^4) \qquad \text{(EQ 10)}$$

Once the plasma equilibrium temperature and the temperature and velocity histories of an individual particle (in a powder size distribution) is determined, the temperature, velocity, diameter and liquid fraction of the particle at impact with the substrate can be predicted, which are then available as input to the deposition model. Rather than calculate the velocity and temperature history of each particle, the distribution is discretized into say, 20 bins, each of which is then represented by an average particle size, d_{pi}. The diameter (and hence the volume) of each representative particle at impact is determined by how much mass is lost by evaporation in flight. Given the final volume of the i^{th} particle, v_i, the material use efficiency is obtained as

$$\eta_m = \frac{\sum_{i=1}^{N} n_i \cdot \rho_s v_i}{\dot{m}} \qquad \text{(EQ 11)}$$

where N is the number of bins, n_i is the number of particles in bin i, ρ_s is the density of the matrix material and $\dot{m}$ the mass flow rate. The melting efficiency, η_l, is also obtained as

$$\eta_l = \frac{\sum_{i=1}^{N} n_i \cdot \rho_s v_i \cdot \bar{v}_{li}}{\eta_m \cdot \dot{m}} \qquad \text{(EQ 12)}$$

where , $\bar{v}_{li}$ is the melt fraction of the i^{th} particle, and η_m is the material use efficiency.

The number of particles in the ith bin, n_i, is determined from

$$n_i = N_p \cdot \varphi_{dp}(d_{pi}) \cdot \delta d_{pi} \qquad \text{(EQ 13)}$$

where $\varphi_{dp}(d_p)$ is the probability density function for particle size, so that $\varphi_{dp}(d_{pi}) \cdot \delta d_{pi}$ represents the probability that the i^{th} particle has a size between d_{pi} and $d_{pi} + \delta d_{pi}$, and N_p is the total number of particles processed per second:

$$N_p = \frac{\dot{m}}{\int_0^\infty \varphi(x)\frac{\pi x^3}{6}\rho_s dx}. \qquad \text{(EQ 14)}$$

The energy absorbed by a single particle, q, during flight is given by the sum of the energies needed to raise the temperature of the particle to the melting point, to melt the particle, to raise the temperature to the boling point, and finally to supply the latent heat of vaporization. By summing the energy absorbed/time of flight over all particles in the discretized particle size distribution, the total power absorbed during spraying is obtained:

$$P = \sum_{i=1}^{N} n_i q_i(d_{pi}) \qquad \text{(EQ 15)}$$

where n_i is given by EQ 13. This must be balanced with the RF power input (times a factor representing the efficiency of the plasma in converting electrical energy into available heat) to determine the plasma equilibrium temperature.

3.3.1.2 Plasma Spray Deposition

The formation of the monotape by the impact, spreading and freezing of particle droplets is too complex to be modeled in detail, at least for the present purpose. Instead, a model developed by Majdeski[1] is used to calculate the final splat diameter of molten particles selected from the particle size distribution. The model idealizes the impacting droplet as a disk having a dimensionless radius, ξ. As the droplet impacts and spreads, it begins to soildify where it is in contact with the cooler substrate. Assuming perfect adhesion wherever the droplet contacts the flat substrate, the time-dependence of the dimensionless splat size, ξ, is described by the following 2nd order ODE:

$$\frac{d^2\xi}{dt^2} = -\frac{3}{2c_1\varphi\xi^2\xi'}\left\{\frac{2\varphi\xi\xi'^2}{We} + \frac{(\xi\xi')^2}{\varphi Re} + \xi\xi'^3\right\} \quad \text{(EQ 16)}$$

in which the factor, φ, is given by the integral equation

$$\varphi = \frac{1}{6c_1^2\xi^2}\left\{1 - \bar{m}_s - \hat{c}\left[\sqrt{t} + 2\int_0^t \xi\xi'\sqrt{t-\tau}\,d\tau\right]\right\} \quad \text{(EQ 17)}$$

Here, the constant, $\hat{c}$, is

$$\hat{c} = 6c_1^2\kappa\left(\frac{\rho_s}{\rho_l}\right)\sqrt{\frac{c_1}{Pe}} \quad \text{(EQ 18)}$$

and the dimensionless *Peclet* and *Weber* numbers are

$$Pe = \frac{u_p d_p}{\alpha_s} \quad \text{(EQ 19)}$$

$$We = \frac{\rho_{PS} u_p^2 d_p}{\sigma_s} \quad \text{(EQ 20)}$$

1. J.Madejski, Solidification of Droplets on a Cold Surface, Int.J.Heat Mass Transfer, 19, 1009 (1976).

The freezing parameter, κ, is given implicitly by

$$\kappa = \frac{2}{\sqrt{\pi}}\left\{\frac{\bar{T}_0}{Erf\left(\frac{\kappa}{2}\right)e^{\kappa^2/4}} - \frac{\bar{T}_P\sqrt{\frac{k_{PS}c_{pPS}\rho_{PS}}{k_s c_{ps}\rho_s}}}{Erfc\left(\frac{\kappa}{2}\sqrt{\frac{\alpha_s}{\alpha_l}}\right)}e^{-\frac{\kappa^2\alpha_s}{4\alpha_l}}\right\} \quad \text{(EQ 21)}$$

with dimensionless substrate and particle temperatures, $\bar{T}_0$ and $\bar{T}_P$:

$$\bar{T}_0 = \frac{k_s(T_m - T_{sub})}{\alpha_s\rho_s h_f} \quad \text{(EQ 22)}$$

$$\bar{T}_P = \frac{k_s(T_l - T_m)}{\alpha_s\rho_s h_f} \quad \text{(EQ 23)}$$

Using Majdeski's model to calculate the dimensionless splat size requires as input the particle temperature, T_l, velocity, u_p, and diameter, d_p, for each particle upon impact with the substrate (assumed flat and of known temperature, T_{sub}).

3.3.1.3 Relative Density

A weighted average of the (normalized) splat diameters, ζ, is then determined from.

$$\zeta = \frac{1}{\eta_m\dot{m}}\sum_{i=1}^{N}(n_i\rho_s v_i)\xi_i \quad \text{(EQ 24)}$$

ζ is then taken as an indicator of the deposit's relative density and surface roughness since, if ζ is large (relatively), impacting particles are able to flow extensively prior to freezing. Thus, voids, interstices in the surface, etc. are more likely to become filled, leading to higher relative density and lower surface roughness. For example, the relative density of the sprayed tape is expressed as a linear function of ζ:

$$D = D_0 + m_D(\zeta - 1) \quad \text{(EQ 25)}$$

where D_0 is the packing density which would be expected if all particles impacted in the unmelted condition, i.e. when $\zeta = 1$. Experience with EQ 24 shows that ζ reaches a maximum value of around 1.67, corresponding to complete melting and near-optimal flow prior to freezing.

Therefore, $\zeta = 1.67$ is taken as corresponding to full density in the sprayed tape. If $D_0 = 0.8$, the approximate relative density of randomly packed spheres having a distribution of sizes, this gives $m_D = 0.3$.

3.3.1.4 Fiber Thermal Shock

The impingement of molten particles onto much cooler fibers results in significant local thermal stresses, which can cause spalling of the interfacial coatings used to protect fibers during high temperature exposure. If very severe, the thermal stresses can also induce microcracking in the fibers themselves. Preheating of the fiber substrate is practically essential to minimize thermal shock damage.

When a hot particle impacts a cooler fiber, the surface of the fiber expands locally, placing it in compression, while underlying material (toward the fiber center) experiences tensile stresses. This leads to spalling by causing the surface coating to buckle as the surface goes into compression. Russell et al[1] have developed a simplified analysis of this problem by considering a fiber, at temperature, T_F, which is suddenly immersed in an infinite (liquid) medium of temperature, T_∞. After obtaining the temperature solution, in which only radial variation in temperature occurs, the three stress components were obtained as a function of radial position, time and the temperature difference, $\Delta T = T_\infty - T_F$. The axial stress which develops at the fiber's center, in dimensionless form, is given by

$$\bar{\sigma}_a = \frac{\sigma_a(1-\nu_F)}{\alpha_F E_F (T_F - T_\infty)} \qquad \text{(EQ 26)}$$

where ν_F is the fiber's Poisson ratio, α_F is the linear coefficient of thermal expansion, and E_F, is the fiber's modulus. The temperature solution depends on the rate of heat transfer from the liquid to the fiber and on the fiber's themal conductivity, k_F. The Biot number, defined as

$$Bi = h\frac{d_F}{2k_F} \qquad \text{(EQ 27)}$$

(where h is the heat transfer coefficient and d_F is the fiber's diameter), can be used to describe these conditions.

The axial stress at the fiber's center can be approximated in terms of Bi:

$$\bar{\sigma}_a = \qquad \text{(EQ 28)}$$

$$0.58 + 0.163[\log Bi - \sqrt{(\log Bi)^2 - 5.2\log Bi + 6.9}\,].$$

Combining EQ's 26, 27 and 28 provides a condition for the occurrence of fiber shock in terms of the difference in temperature between the fiber and the impacting droplet:

$$T_d - T_F \geq \frac{\sigma_F(1-\nu_F)}{\bar{\sigma}_a(Bi)\alpha_F E_F} \qquad \text{(EQ 29)}$$

where σ_F is the fiber strength. Thermal shock is seen to be controlled by the preheat temperature of the fiber, by properties of the fiber and by the heat transfer rate from droplet to fiber. The substrate preheat temperature should be kept high enough to avoid thermal shock, but excessively high preheat should also be avoided in order to minimize interfacial reactions and to minimize the risk of damage to the mandrel.

During spraying, if a particle causes EQ 29 to be satisfied, a damage parameter, ω_s, is set equal to 1, otherwise $\omega_s = 0$. The overall cumulative fiber thermal shock damage, Ω_s, is given by

$$\Omega_s = \frac{1}{N_p}\sum_{i=1}^{N} n_i \omega_s \qquad \text{(EQ 30)}$$

which cannot exceed 1 (the condition when all particles result in thermal shock).

3.3.1.5 Interfacial Reaction

At sufficiently high temperatures, diffusional rates become high enough that reactions between the metallic matrix and ceramic fiber can occur. The extent of these reactions can be roughly correlated with the thickness of the reaction zone at the interface, δ_R. The reaction thickness as a function of time obeys a parabolic relation

$$\delta_R = k_R\sqrt{t} \qquad \text{(EQ 31)}$$

where k_R, the reaction rate constant is

1. E.S.Russell, D.Y.Wei, Y.Pang and D.G.Backman, "Modeling of MMC Plasma Deposition Processing" in: Advanced Sensing, Modeling and Control of Materials Processing, eds. E.F.Matthys and B.Kushner, TMS Warrendale, PA), pp. 99-120 (1992).

$$k_R = k_0 e^{-\frac{Q_R}{RT}} \quad \text{(EQ 32)}$$

where k_0 is a constant, Q_R is the activation energy for the reaction, R is the Universal gas constant and T is the absolute temperature.

Usually, the reaction can be allowed to occur to some extent without significantly degrading the final properties of the composite. An allowable reaction zone thickness is designated, δ_a, representing a limiting thickness, below which no degradation in properties is assumed to occur. Defining a dimensionless thickness, $\bar{\delta}_R = \delta_R/\delta_a$, the interfacial quality is unaffected for $\bar{\delta}_R \le 1$. If it is assumed that the interfacial quality falls off linearly with increasing dimensionless thickness over some range, $\Delta\delta_R$, a quality index, Q_R, (ranging from 0 (lowest) to 1 (highest)) can be defined:

$$Q_R = \begin{cases} 1 & \bar{\delta}_R \le 1 \\ 1 - \dfrac{(\bar{\delta}_R - 1)}{\Delta\delta_R} & 1 < \bar{\delta}_R \le 1 + \Delta\delta_R \\ 0 & \bar{\delta}_R > 1 + \Delta\delta_R \end{cases}$$

3.3.1.6 Overall Quality

With the quality indices for the microstructural state variables, relative density, fiber thermal shock and the interfacial reaction now available, the overall (monotape) quality, Q_{PS}, is determined from a weighted sum of the microstructural quality indices:

$$Q_{PS} = w_1 D + w_2 \Omega_s + w_3 Q_R \quad \text{(EQ 33)}$$

The weighting factors, w_i, which sum to 1, are user-specified and reflect the relative importance of each microstructural parameter in determining the final properties needed in the composite.

3.3.1.7 Spray Duration and Production Rate

Given the relative density of the plasma spray deposited matrix (D) (*see §3.3.1.3*), the thickness of a (porous) deposited matrix layer, δ_M, required to produce a specified fiber volume fraction, $\bar{v}_F$, in the finished (i.e. fully dense) composite is detemined from

$$\delta_M = \frac{\delta_F}{D}\left(\frac{1 + \bar{v}_F}{\bar{v}_F}\right) \quad \text{(EQ 34)}$$

where δ_F is the effective fiber thickness

$$\delta_F \equiv \frac{\pi d_f^2}{4\lambda_s} \quad \text{(EQ 35)}$$

and λ_s is the center-to-center fiber spacing. Physically, EQ 35 gives the thickness of a layer of fiber material (say SiC) whose volume is equivalent to that of the (actual) cylindrical fibers. The sum of EQS 34 and 35 gives the as-sprayed tape thickness. The time required to attain the needed thickness of matrix deposit depends on the actual deposition rate, $\dot{m}_{dep}$, (given by the product of mass flow rate through the torch, $\dot{m}$, and the material use efficiency, η_m), the volume of the deposit (deposit area times thickness) and the density of the matrix:

$$t_s = \frac{(l_D d_M \delta_M)\rho_s}{\dot{m}_{dep}} \quad \text{(EQ 36)}$$

where l_D and d_M are the deposit length and mandrel diameter, respectively.

The overall rate of MMC monotape production is the sum of the matrix deposition rate, $\dot{m}_{dep}$, and the rate at which fiber is incorporated into the tape, given by the total mass of fiber being coated divided by the spray duration:

$$\dot{m}_{prod} = \dot{m}_{dep} + \frac{(l_D d_M \delta_F)\rho_F}{t_s} \quad \text{(EQ 37)}$$

where δ_F is given by EQ 35.

3.3.2 Cost Models

Four cost elements are accounted for in estimating the cost of the plasma spray deposited monotape per kg: materials costs, c_m, the cost of consumables (i.e. materials which are used, but do not appear in the final product), c_c, energy costs, c_e and capital costs, c_{cap}. Each cost element is calculated per kg of as-sprayed tape. The costs associated with materials, consumables and energy are independent of production volume, but the capital costs are amortized over the time of production and so they decrease with each kg of monotape produced. The models used to calculate the four cost elements are developed next.

3.3.2.1 Materials Costs

The volume fraction of fiber (specified by the user) is $\bar{v}_F$ and hence the matrix volume fraction in the fully dense

composite is $\bar{v}_m = 1 - \bar{v}_F$. If the matrix powder cost is given by c_{powder} [$/kg] and fiber cost by c_{fiber} [$/kg], the material cost per kg of as-sprayed monotape is

$$c_m = \left(1 - \bar{v}_F \frac{\rho_F}{\rho_c}\right) \frac{c_{powder}}{\eta_m} + \bar{v}_F \frac{\rho_F}{\rho_c} c_{fiber} \qquad \text{(EQ 38)}$$

where $\rho_c = (1 - \bar{v}_F)\rho_p + \bar{v}_F \rho_F$, is the composite density.

3.3.2.2 Cost of Consumables

The only consumables required for the plasma spray process are the gases used to create the plasma, to provide sheath cooling within the torch tube and to transport the matrix powder into the torch. The cost of consumables per kg of finished tape is given by the cost of gas per minute divided by the tape production rate. If the carrier, sheath and central (plasma forming) gas flow rates (in units of *slpm*) are q_{cg}, q_{sg} and q_{mg}, respectively, with associated costs [$/liter], c_{cg}, c_{sg} and c_{mg}, the cost rate of consumables is $\dot{c}_{gas} = c_{cg} q_{cg} + c_{sg} q_{sg} + c_{mg} q_{mg}$. This gives for the cost of consumables per kg of monotape

$$c_c = \frac{\dot{c}_{gas}}{\dot{m}_{prod}} \qquad \text{(EQ 39)}$$

where the tape production rate is given by EQ 37.

3.3.2.3 Energy Costs

While some energy is required to manipulate the substrate and to operate the vacuum pumps, by far the greatest energy requirement is that associated with the RF torch. The RF power is either given as user input, or the spray creation model calculates the RF power needed to maintain a specified plasma equilibrium temperature (for a given powder material and flow rate). The RF induction coupled plasma exhibits an energy efficiency, η_e, of around 10-15%, i.e. for every kW consumed, roughly 0.1-0.15 kW actually goes into melting powder.[1] Thus, if P is the power setting, the cost rate [$/min] associated with energy consumption is

$$\dot{c}_e = \frac{P}{\eta_e} \bar{c}_E \qquad \text{(EQ 40)}$$

where $\bar{c}_E$ is the unit cost of electricity [$/kWh]. The energy cost per kg of monotape is then

$$c_e = \frac{\dot{c}_e}{\dot{m}_{prod}} \qquad \text{(EQ 41)}$$

3.3.2.4 Capital Costs

The major equipment items needed for an RF plasma spray facility (Fig. 8) include the processing chamber (a double-walled stainless steel vacuum-rated pressure vessel), the water-cooled RF plasma torch (with associated closed-loop cooling system and safety controls), powder feeder, liquid ring pump, power supply and temperature sensor (IR camera). Total capital cost is simply the sum of the costs of these items:

$$c_{cap} = \sum_i c_{capi} \qquad \text{(EQ 42)}$$

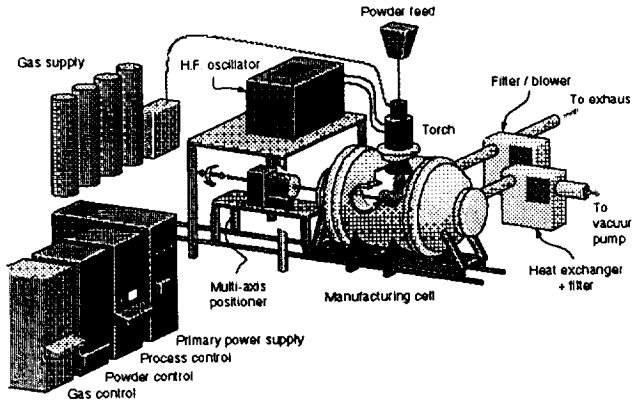

FIGURE 8. Major components of a typical RF plasma spray facility.

3.3.2.5 Total Monotape Cost per kg

EQs 38, 39, 41 and 42 provide the four cost elements, which are summed to obtain the total cost of plasma sprayed MMC monotape [$/kg]:

$$C = c_m + c_c + c_e + \frac{c_{cap}}{M_{prod}} \qquad \text{(EQ 43)}$$

The capital cost per kg of MMC monotape depends on the total mass of composite tape produced, M_{prod}. This simplified formula approximates the amortization of capital costs over the time of production. As can be seen, the first kg of MMC tape is quite expensive, since the capital costs

1. M.I.Boulos, "Thermal Plasma Processing", *IEEE Trans. on Plasma Sci.*, **19**(6), 1078 (1991).

are divided by one. It therefore totally dominates the cost of monotape at low production volumes. However, as the production volume increases, the capital cost per kg of tape drops, eventually becoming insignificant relative to the other costs.

3.4 Implementation

The quality and cost models described above have been implemented using *Mathematica*™.[1] The Mathematica program code for the plasma spray QCM is given in Appendix A.

3.5 Results

3.5.1 Quality-Cost Relationship

Figure 9 shows a cost-quality curve for the plasma spray deposition process. The plot shows the cost per kg to produce 1000 kg of monotape, normalized by the raw materials cost (C/c_m), versus the weighted microstructural quality (Q_{PS}). The highest quality, corresponding to a value of 1, represents a microstructure which contains no voids, has sustained no thermal shock damage (spalled coating, fiber microcracking) and has an interfacial reaction zone thickness which is below the acceptable limit.

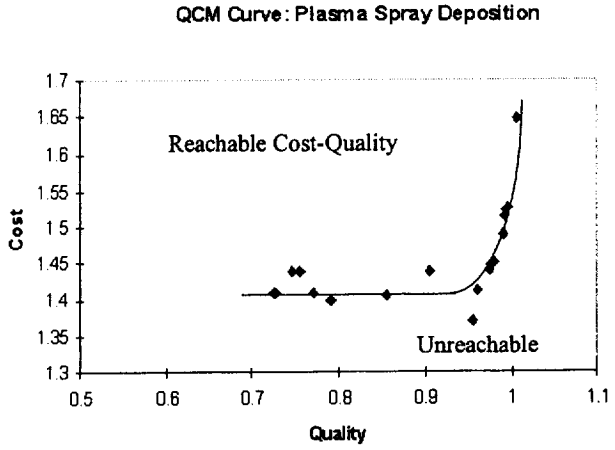

FIGURE 9. Cost-Quality curve for the RF plasma spray deposition process. Very high quality is achievable, but only at exponentially rising cost.

Each data point in Fig. 9 represents the result of one simulation using the QCM tool. The input data and output for these simulations are listed in a spreadsheet in Appendix B. The data were obtained for varying RF power, substrate preheat temperature, powder flow rate and powder size distribution. The fiber size, spacing and volume fraction were fixed at 142 μm, 355 μm (2.5 fiber diameters) and 0.4, respectively. Also fixed were the gas flow rates, q_{cg}, q_{sg} and q_{mg}, at 10, 35 and 5 *slpm*, respectively. The QCM curve for a composite tape having a smaller fiber volume fraction would be shifted to a lower cost ratio than that of the 40 vol% composite represented in Fig. 9.

The QCM curve in Fig. 9 indicates that the cheapest composite which could be produced by plasma spray deposition, regardless of quality, is about 1.4 times the cost of the raw materials. To this cost (which really represents the so-called 'technical costs') must be added the cost of labor, overhead, etc. Theoretically, the lowest possible cost is just the cost of the raw materials, in which case the cost ratio would be 1. This would be the case for large production volumes, for which the capital cost approaches zero. At 1000 kg total production, the capital costs ($227,500, see Appendix B) amount to roughly one fourth of the total tape cost.

A microstructural quality of about 0.95 can be reached with practically no increase in cost. The flatness of the QCM curve for $Q_{PS} < 0.95$ illustrates the likely benefit of process optimization, since only knowledge of the process-structure relationships are necessary to improve quality (at no additional cost).

It can also be seen that the plasma spray process is capable of producing very high quality material (at least in terms of the microstructural features considered by the QCM model), but at rapidly increasing cost. The exponential cost increase is caused by declining material use efficiency as one attempts to lower porosity in the deposit by increasing the RF power. The relative density can be pushed almost to 1 if sufficient superheat is achieved in the powder particles (which determines their ability to flow into and fill irregularities in the substrate surface). This is illustrated by Figure 10, which shows the relative density of

1. Mathematica, vers. 2.0, Wolfram Research, Inc.

the spray deposited matrix as a function of the RF power used to process the particles.

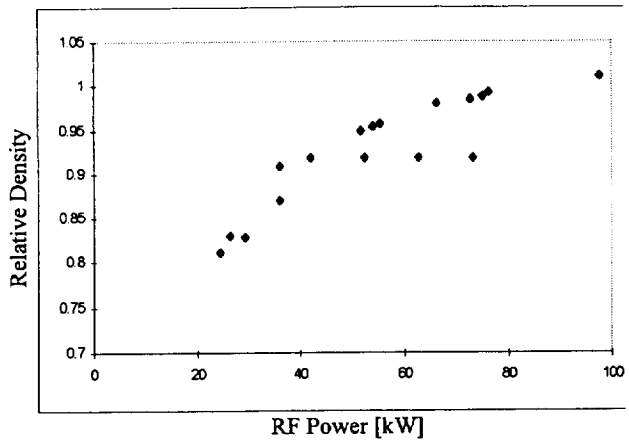

FIGURE 10. Influence of RF power (which controls the plasma equilibrium tmperature) on deposit density.

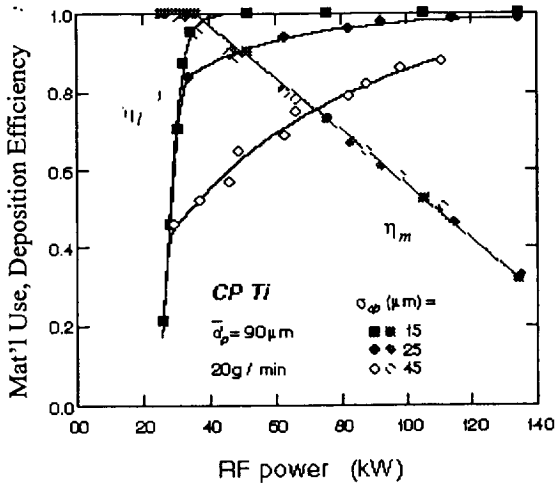

FIGURE 11. The trade-off between material use efficiency and melting efficiency as RF power is increased.

Another measure of the 'flow' character of the spray is the mass fraction of melted material at impact with the substrate, i.e. the melt efficiency, η_l. Thus, as RF power increases, η_l also increases, but because the smaller particles in the size distribution are becoming increasingly vaporized at higher temperatures, less mass actually reaches the substrate, i.e. the material use efficiency, η_m, declines. Figure 11 illustrates this trade-off between melting efficiency (and therefore quality) and material use efficiency (and thus cost). The mass flow rate was fixed at 20 g/min (0.044 lb/min) and the gas flow rate was 60 slpm (2.12 cfm) for all cases.

Figure 11 also shows the effect of widening the particle size distribution, keeping the mean particle size (90 μm) and powder flow rate (20 g/min) fixed. If the peak RF power that can be sustained by a given plasma torch is say, 100 kW, then the highest melting efficiency that can be reached is only around 85% for the widest size distribution. The increased concentration of very large particles decreases the mass which can be fully melted, thereby limiting the relative density (quality) that can be achieved.

A good combination of deposition and melting efficiency can be obtained for the smallest particle size variability ($\eta_l = \eta_m = 0.99$), but only over a very narrow range of RF power. It is unlikely that the model accurately predicts this optimal power setting, but the indication that it occurs over a limited range of settings properly reflects the difficulty of identifying optimal process conditions when spraying powders with a narrow size distribution. The intermediate size variability (± 25 μm) provides an adequate combination of efficiencies over a wider power range. It is also interesting to note that the tighter size distributions absorb less power while delivering improved efficiencies.

While the results of Fig. 11 might be used to show the advantage of processing with tighter particle size distributions, one must also consider the rapidly increasing costs associated with powders having more closely controlled particle size. As Fig. 12 shows, powder cost increases rap-

idly with decreasing mesh size; increased sieving to control the width of the size distribution further increases cost.

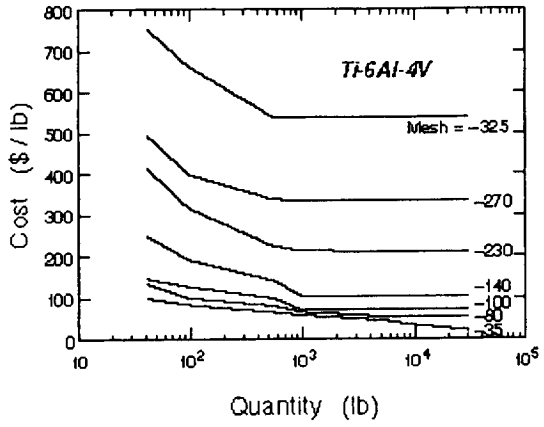

FIGURE 12. Cost of Ti-6Al-4V powder as a function of quantity and mesh size.

3.5.2 Cost Breakdown

The actual cost of as-sprayed MMC tape (per kg) is taken to consist of four cost elements: material, consumables, energy and capital costs. Figure 13 illustrates the cost breakdown for the 19 simulations presented in the appendix. The production volume was taken to be 10^3 kg, the cost of fiber, 1000 $/kg and the cost of powder, 250 - 350 $/kg, depending on the particle size. The figure shows clearly that the cost is dominated by material costs (powder and fiber) and by capital costs. Energy costs are totally insignificant and the cost of consumables is relatively unimportant.

It is interesting to note that although the quality-cost relatinship varies considerably for these 19 experiments, the cost breakdown is quite insensitive to all of the imposed variations in process variables. It may be concluded that process optimization is not the immediate solution to the high cost of plasma sprayed composite monotape. The costs of fiber and powder must first drop well below the values quoted above (which amount to around 600 - 700 $/kg of composite monotape) before investments in advanced sensing and process optimization can be expected to pay off. For the 1000 kg production volume, material costs (powder + fiber) would need to fall to around 300 $/kg of composite. This would not guarantee that the composite material would be competitive with conventional materials, but it would allow process design refinements and process optimization/control to have a tangible impact on composite cost.

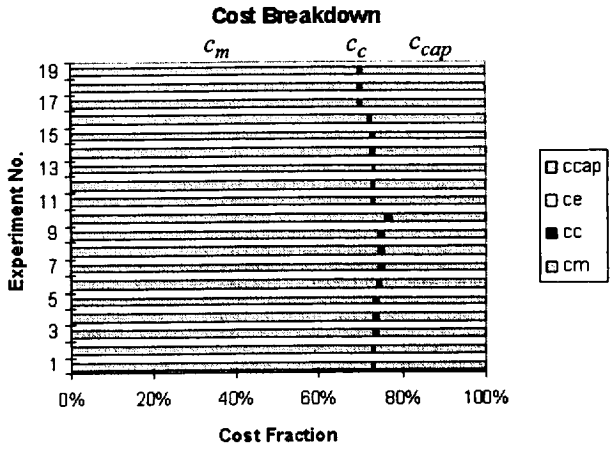

FIGURE 13. Fraction of tape cost by cost element. Total cost is dominated by material and capital costs.

3.5.3 Key Factors Affecting QC

Three performance-defining attributes of spray-deposited MMC monotapes have been identified and incorporated into the QCM tool: relative density, fiber thermal shock and reaction zone thickness.

The reaction zone thickness appears to be the least concern during plasma spraying, at least given the reaction kinetics of SCS-6 fiber (with its double-layer C coating) in a Ti-6Al-4V matrix. The QCM results included in Appendix B indicate that the spray duration needed to attain a tape thickness corresponding to a 40 vol% fiber composite is typically on the order of 10 minutes or less, so that even with the locally high transient temperatures reached as material passes directly beneath the plasma, there is insufficient time for significant diffusion to occur. Even lengthy preheating, say 1 hr, at 800 $^{\circ}C$ will cause little reaction zone growth. The factors which affect the spray duration most strongly are, in order of importance, the matrix powder flow rate, and RF power (increasing power leads to reduced material use efficiency and longer times to deposit a given amount of matrix).

Fiber thermal shock can be avoided if the temperature difference between the impacting droplets and the fiber sub-

strate is sufficiently low. Thus, thermal shock is controlled primarily by the substrate preheat temperature and to a lesser degree, the RF power and powder flow rate (which together control the plasma equilibrium temperature and the mean particle temperature). Increasing the powder flow rate (for a given RF power) lowers the melting efficiency and mean particle temperature, thereby reducing the extent of thermal shock damage. Increasing the preheat temperature improves the quality by enhancing droplet flow upon impact (particles take longer to freeze) and by reducing thermal shock damage. It is therefore essential to reach and maintain proper preheat temperature. Because of the low cost of energy, this provides improved quality with little associated cost penalty.

The relative density of the spray deposit is sensitive to the powder size distribution, mass flow rate, RF power, and substrate preheat temperature. All of these combine to influence the ability of impacting particles to flow and fill existing voids in the substrate. Figure 14 shows the influence of RF power on the plasma equilibrium temperature for a powder feed rate of 20 g/min. The key point is that the RF power must be adjusted to match the thermal characterisics and flow rate of the matrix powder to ensure a high melting efficiency (without extreme losses due to vaporization). It is therefore important to be able to model the interaction between powder feed rate, RF power and material properties or to sense the plasma equilibrium or mean particle temperature.

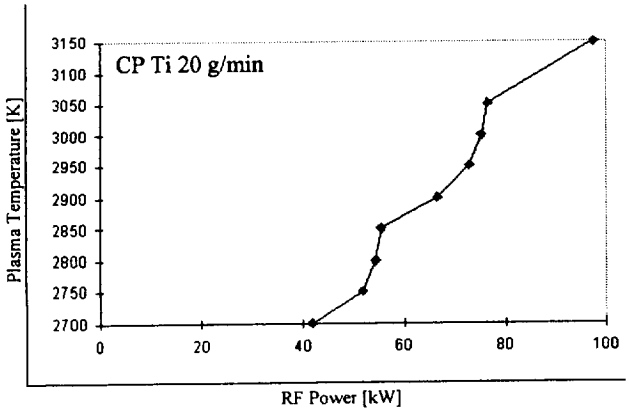

FIGURE 14. Influence of RF power on plasma equilibrium temperature at fixed powder mass flow rate.

4.0 Tape Casting Process

4.1 Process Overview

The tape casting process is a solid state processing route for producing MMC monotape precursor material. Because of this, processing temperatures are low relative to the melting points of the composite constituents, and so reactions between the fiber and matrix are avoided. Only the consolidation step (hot isostatic or vacuum hot pressing) following tape casting involves temperatures sufficiently high to cause significant interfacial reactivity. Tape casting is a variant of the slurry casting process, practiced for thousands of years in making clayware and whiteware pottery. The difference between slurry and tape casting lies in the intended shape of the product, being a flat, thin tape in the case of the latter process. Tape casting is widely used in the electronics industry for the manufacture of thin, monolithic ceramic substrates of high quality.

Figure 15 presents a schematic of the tape casting process for manufacturing MMC monotape. The process may be broken down into four sequential steps: slurry formulation, casting, drying (also called "stabilization"), and outgassing (technically known as "thermolysis"). The slurry formulation step consists of combining a metal/alloy powder with controlled amounts of organic materials which act as a carrier fluid for transport and shaping of the powder. The slurry formulation step determines the rheological (flow) properties of the powder slurry and hence its ability to infiltrate a fiber mat completely and uniformly. Typical slurries contain, in addition to the matrix powder, a binder (which flocculates, i.e. binds, the powder particles), a solvent (used to adjust the viscosity of the binder), a plasticizer (which improves the viscoelastic properties of the condensed binder by lowering its glass transition temperature) as well as other ingredients such as wetting agents, antifoaming agents and so forth.

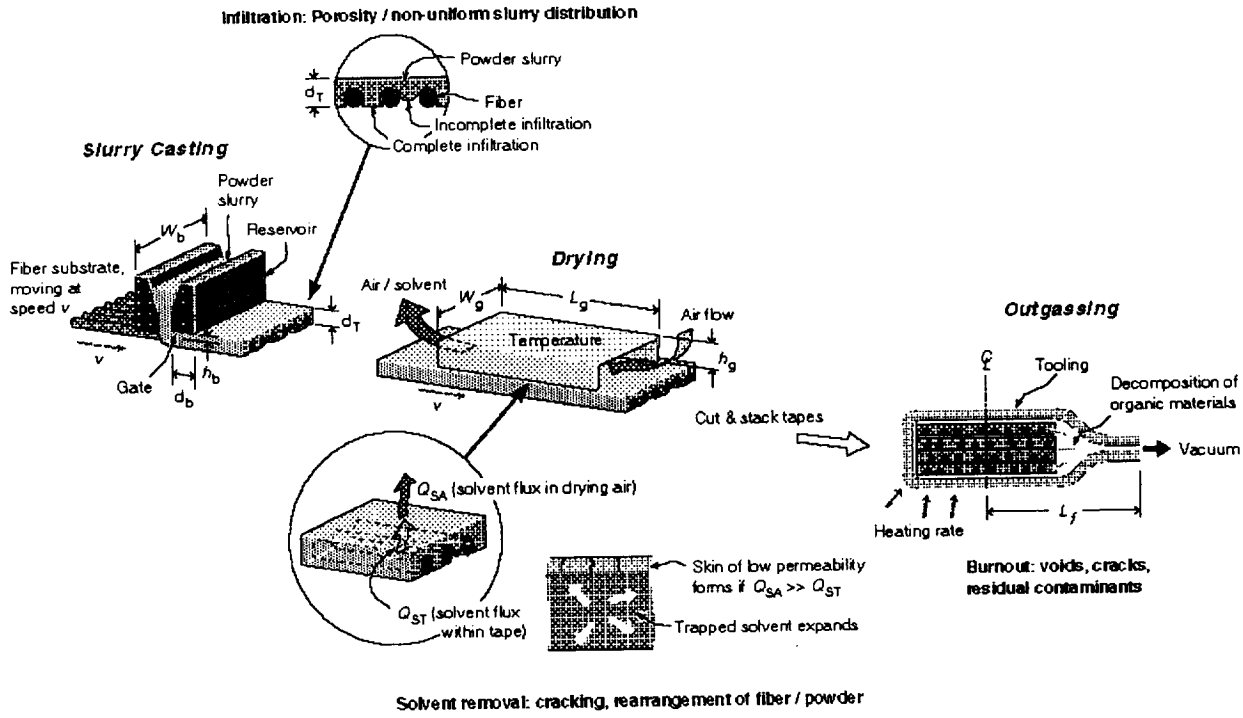

FIGURE 15. Schematic of the tape casting process for MMC monotape.

The formulated slurry is fed (under pressure due to the slurry's own weight or via an externally applied pressure) to a casting gate through which the fiber mat is passing. The speed of the fiber mat, the gate height and the slurry pressure are process variables, which are typically adjusted prior to the start of the process and remain unchanged during casting. The casting step influences the extent to which the fiber mat is infiltrated and the final tape thickness (which must be adjusted to control the volume fraction of fiber in the final composite).

After casting, the tape is passed through a low temperature oven in which a controlled amount of the volatile solvent is removed by evaporation. As solvent is removed, the slurry consistency changes from viscous (liquid) to rubbery (solid, but slightly tacky). The stabilized monotape is referred to as 'green' tape and can be used immediately, or stored in a freezer for later use. The temperature of the drying oven, the rate of air flow (usually in the opposite direction of the incoming tape) and the partial pressure of solvent in the air can be controlled to regulate the solvent removal rate. Figure 16 is representative of the structure of MMC monotape produced by the tape casting process. Inhomogeneities such as voids or clusters of large particle must be avoided to prevent rearrangement and bending of fibers during consolidation.

The final step in the manufacture of MMC tape is outgassing, in which the organic (slurry) components are removed by heating, typically to temperatures in the range 350 - 450 $°C$. The green tapes are usually cut to the desired shape and stacked to form a laminate and then placed within a metallic vacuum bag. The temperature is then increased to the outgas level and, under vacuum, the volatile components are removed. Thermal gravimetric analysis (TGA) or some other suitable method, is used to sense the current removal rate. Outgassing continues until the rate of removal is sufficiently low to guarantee an acceptable residual organic content. The temperature and pressure are control variables during outgassing.

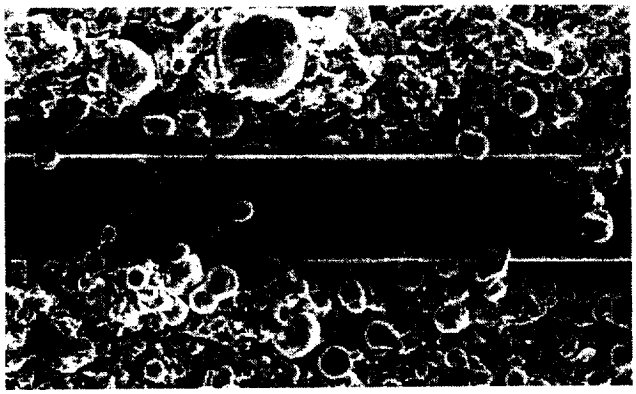

FIGURE 16. Typical microstructure of tape cast MMC monotape (Ti-6Al-4V/SCS-6).

The performance-limiting microstructural features of the finished (i.e. outgassed, but not consolidated) tape are porosity, internal cracks, poor fiber spacing and residual organic contaminents. The QCM tool for the tape casting process may be used to predict the cost required to produce material which is increasingly free of these defects and therefore of increasing product quality.

4.2 Process Variables

One of the complicating features of the tape casting process is the changing slurry composition; the initial mass fractions, determined by the slurry 'recipe', must be recalculated following casting due to the addition of fiber, then again after drying due to the removal of solvent and finally again after outgassing, due to removal of the organic components. A subscript/superscript system is used to track the mass and volume fractions of each component, through the various process steps: an '*s*' designates a variable associated with the slurry formulation step, '*b*' refers to material following casting, but prior to drying, '*g*' designates as-dried (green) tape, and '*f*' refers to outgassed (final) product (see Table 4).

TABLE 4.

PROCESS STEP	SUPERSCRIPT
Slurry formulation	*s*
Casting	*b*
Drying	*g*
Outgassing	*f*

While superscripts designate process steps, subscripts will be used to indicate the specific component in question, i.e.

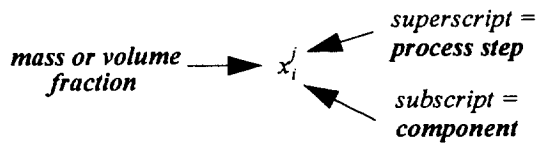

Thus, the mass fractions of the slurry components are designated $\overline{m}_i^s$, $\overline{m}_i^b$, $\overline{m}_i^g$, and $\overline{m}_i^f$, where *i* represents the component subscript (powder ('*p*'), fiber ('*f*'), binder ('*b*'), solvent ('*s*'), plasticizer ('*pl*'), deflocculant ('*d*'), and surfactant ('*w*')). The subscripts used are summarized in Table 5.

TABLE 5.

COMPONENT	SUBSCRIPT
Powder	*p*
Fiber	*f*
Binder	*b*
Solvent	*s*
Plasticizer	*pl*
Surfactant	*w*
Deflocculant	*d*
Slurry[a]	*S*
Carrier[b]	*C*
Tape[c]	*T*

a. includes all components except fiber

b. includes all components except powder and fiber

c. includes all components

Variables other than mass, volume fractions and tape density *will not use superscripts*. Material property subscripts indicate components, unless otherwise noted. Process and design variable subscripts indicate the process step with which the variable is associated, unless noted otherwise.

Figure 17 is a flow diagram for the slurry casting of MMC tape, indicating the steps in the process, process variables (input), material parameters (input), and the features of the product (which ultimately determine its quality) as it progresses from slurry to the final product (output). Table 6 is a list of the variables used in the tape cast QCM model (excluding mass and volume fractions).

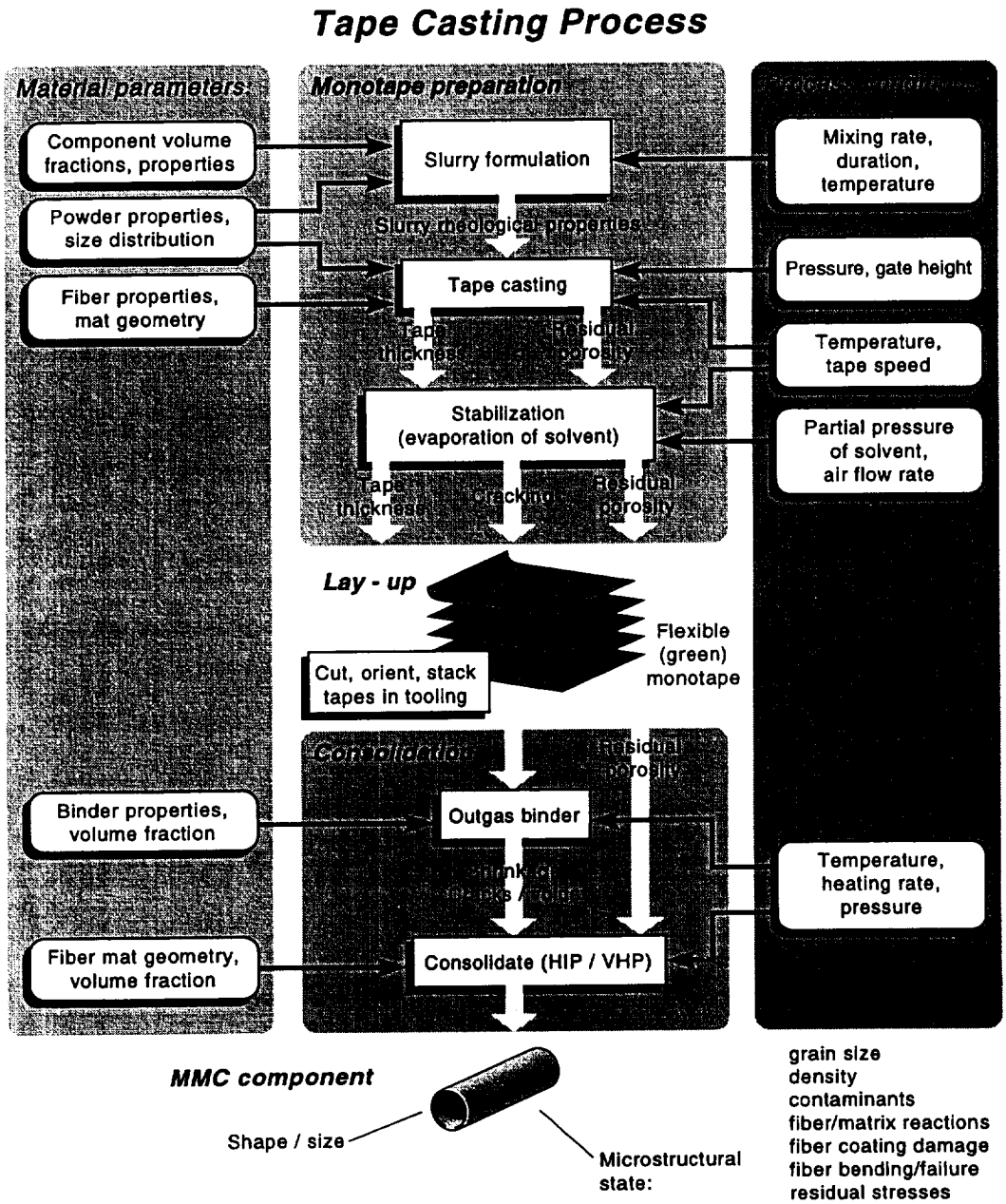

FIGURE 17. Flow diagram of the tape casting process for MMC's.

TABLE 6. Tape Casting Process Parameters

Variable Type	Variable Name	Symbol	Units
	Mixer batch size	M_s	kg
	Mixing time	t_s	hr
	Mixer rate	ω_s	rpm
	Tape speed	v_T	cm/s
	Gate height	h_b	mm
	Applied pressure	p_b	kPa
	Drying temperature	T_g	$°C$
	Air flow rate	q_g	slpm
	Outgas batch size	M_f	kg
	Outgas temperature	T_f	$°C$
	Heating rate	$\dot{T}_f$	$°C$ /s
	Exit pressure	p_f	Torr
	Mixer impeller dia.	d_{ml}	cm
	Casting reservoir depth	h_R	cm
Equipment design parameters	Casting gate thickness	δ_b	mm
	Gate width	w_b	cm
	Furnace length	L_g	m
	Furnace height	h_g	m
	Furnace width	w_g	m
	Outgas tooling length	L_f	cm
	Mean powder size	d_p	μm
	Powder size std. deviation	σ_{dp}	μm
	Fiber diameter	d_f	μm
	Fiber spacing	λ	μm
	Fiber vol. fraction	$\bar{v}_f$	--
	Infiltration depth	δ_I	μm
Microstructural state variables	Shrinkage strain	ε_s	--
	Residual contaminant mass fraction	$\bar{m}_{res}$	--
	Dimensionless infiltration depth	$\bar{\delta}_I = \frac{\delta_I}{d_f}$	--
	Casting quality	Q_b	--
	Solvent flux ratio	$\bar{q}_g$	--
	Drying quality	Q_g	--
	Matrix relative density	D	--
	Outgas quality	Q_f	--
	Monotape quality	Q_T	--

TABLE 6. Tape Casting Process Parameters

Variable Type	Variable Name	Symbol	Units
	Material use efficiency	η_m	--
	Tape thickness	δ_T	mm
Efficiency and Production	Slurry production rate	$\dot{m}_s$	g/min
	Casting production rate	$\dot{m}_b$	g/min
	Outgas production rate	$\dot{m}_f$	g/min
	Production rate	$\dot{m}_{prod}$	g/min
	Materials costs	c_m	$/kg
	Consumables costs	c_c	$/kg
	Energy cost	c_e	$/kg
	Capital costs	c_{cap}	$/kg
	Monotape cost	C	$/kg

Table 7 lists material and physical properties needed for the metallic matrix, ceramic fiber, and organic slurry componentry.

TABLE 7. Material Properties

Constituent	Property	Symbol	Units
MATRIX	Density	ρ_p	g/cm^3
[illegible]	Density	ρ_b	g/cm^3
	Density	ρ_s	g/cm^3
	Molecular weight	M_s	g/mol
	Critical pressure	p_{cs}	atm
Solvent	Critical temperature	T_{cs}	K
	Diffusivity in slurry	D_{st}	m^2/s
	Diffusivity in air	D_{sa}	m^2/s
[illegible]	Density	ρ_{pl}	g/cm^3
Surfactant	Density	ρ_w	g/cm^3
[illegible]	Density	ρ_d	g/cm^3
FIBER	Density	ρ_f	g/cm^3
[illegible]	Density	ρ_T^b	g/cm^3
	Permeability	κ	m^2
	Molecular weight	M_S	g/mol
	Viscosity of liquid	μ_{Sl}	g/ms
	Viscosity of gas	μ_{Sg}	g/ms
	Shear thinning exp	n	--
	Shear thinning coefficient	k_{th}	--
	K-H coefficient	KH	--
	Blocking fraction of powder	$\bar{v}_{pb}$	--
	Density	ρ_T^g	g/cm^3
	Liquid-vapor surface tension	σ_{lv}	N/m
GREEN TAPE	Slurry-fiber wetting angle	θ_w	rad
	Preexp. constant	k_0	s^{-1}
	Activation energy for decomposition	E_{af}	J/mol-K
[illegible]	Density	ρ_T^f	g/cm^3
	Molecular weight	M_{air}	g/mol
AIR	Critical pressure	p_{cair}	atm
	Critical temperature	T_{cair}	K

As discussed previously for the plasma spray process, process variables, equipment design parameters and geometric parameters are specified by the user as input. The values chosen are arbitrary (within limits determined by physical reality and modeling assumptions), but once they are input at the start of the process, they remain unchanged. This is a consequence of the assumption of steady state conditions on which each of the process models is based. This corresponds with the actual tape casting process, which is typically operated under non-time-dependent conditions.

A number of tape features which evolve during tape casting can strongly affect the microstructural quality and performance of the final product. Figure 15 illustrates the features which are tracked by the QCM model: porosity, green tape cracking, particle/fiber rearrangement and residual contamination. These are considered to be the most important performance-defining attributes for the outgassed MMC tape.

Porosity in the outgassed tape can arise from several sources, including gas bubbles entrained in the slurry during mixing, incomplete slurry infiltration of the fiber mat, and removal of the organic slurry components during outgassing. Only gas entrainment will be neglected by the QCM model; porosity due to incomplete infiltration of the fiber mat and outgassing are considered. The ability of the slurry to infiltrate the fiber mat during casting depends primarily on the slurry viscosity (which typically depends on the temperature and shear rate), the orientation and spacing of the fibers, and the powder size relative to the fiber spacing. The ratio of infiltration depth to the thickness of the fiber mat (which is simply the fiber diameter in the case of an array of parallel fibers) is determined as one indicator of microstructural quality.

The amount of porosity produced by outgassing depends on the powder loading (i.e. the volume fraction of powder particles incorporated into the slurry); high powder loadings are desirable to minimize porosity (and shrinkage during outgassing), but create other complications by, for example, increasing slurry viscosity (often exponentially).

Porosity is unavoidable in the outgassed tape due to removal of the organic constituents and is, from that viewpoint, not regarded as a defect. However, if the porosity created is not uniformly distributed throughout the tape, nonuniform strains will develop during consolidation, leading to fiber bending and rearrangement. Fibers which are allowed to come into contact during processing lower composite strength. The cause of this is cracking of the narrow matrix ligament between the fibers, which experience the superposed residual tensile stresses associated with each of the two fibers. Fiber distortion, especially

bending, introduces residual tensile stresses into the fibers, onto which applied stresses superpose, thus reducing the useful fiber strength.

During the drying step, volatile solvent evaporates from the tape surface. The resulting concentration gradient provides a driving force for the diffusion of fresh solvent to the surface. If solvent is removed too quickly from the surface, solvent diffusion through the tape will be unable to replenish the near-surface region, leading to formation of a 'skin'. Evaporation drops off rapidly because solvent cannot readily diffuse through the more dense skin. Aside from the difficulty of having a nonuniform consistency and differential shrinkage in the tape, the skin formation traps expanding solvent (due to heating within the drying furnace). This leads to internal pressure which in turn causes failure of the brittle surface layer, resulting in surface cracks. Internal cracking and rearrangement can also occur as the interior continues to dry (and therefore to shrink). Thus shrinkage strain is calculated and, as an indirect measure of the extent of crack formation, the ratio of the solvent removal rate to the diffusional flux is determined.

Finally, the residual concentration of organic substances due to incomplete outgassing is taken as a microstructural state variable and is used to calculate a relative outgas quality index, Q_f.

The material use efficiency for the tape cast process is typically 100%, i.e. all of the powder in the slurry (and the entire fiber mat) ends up in the monotape. This is in contrast to the plasma spray and vapor deposition processes which often have much lower material use efficiencies. The slurry formulation and outgassing steps are typically batch processes while casting and drying can take place continuously. Depending on batch sizes and processing conditions therefore, production rates are different among the steps. The production rate is determined for each step, with the slowest step controlling the overall rate of production.

The same cost elements are considered as for the plasma spray process: composite constituent (material) costs, consumables, energy and capital investment.The cost of the finished tape cast product (i.e. MMC monotape that has been outgassed, but not consolidated) is given by EQ 1 in [$/kg].

Calculations of (microstructural) quality and cost for tape cast MMC produced under varying processing conditions will be used to explore the quality-cost relationship. Key process variables and other parameters for controlling quality-cost will be discussed.

4.3 Models for QCM of Tape Casting

The models needed for performing the QCM analysis (see Fig. 3) include process models (used to simulate the influence of processing conditions on microstructural evolution), resource models (used to calculate the energy consumed by processing equipment in maintaining specified processing conditions), and cost models. These models are presented, in this order, below.

4.3.1 Process (Quality) Models

The performance of the tape cast composite sheet depends on the final microstructure achieved during processing, which in turn depends on process conditions and material properties. A quality index, ranging from 0 to 1 is again defined for the finished composite monotape; the highest quality (Q_T = 1), corresponds to a microstructure which contains no porosity, no residual contaminants, no cracks, no particle or fiber rearrangement or fiber bending, and has the correct (specified) fiber volume fraction. The quality index for the tape is a weighted sum of quality indices (also ranging from 0 to 1) for each of the process steps, casting, drying and outgassing. (A quality index is not determined for the slurry formulation step; the most important property of the slurry, i.e. its viscosity, must be entered based on experimental measurement or using handbook data for the slurry composition used.)

The casting, drying and outgassing quality indices are based on the calculation of key microstructural variables or of parameters which indirectly provide a measure of the microstructural variable of interest. For the casting process, these are infiltration depth (a direct measure of porosity and tape non-uniformity) and tape thickness; for drying, the solvent flux ratio (an indirect measure of surface cracking and internal rearrangement); for outgassing, residual contamination and shrinkage strain (direct measures).

4.3.1.1 Casting

Infiltration - During casting, a fiber mat is passed beneath the casting gate through which slurry is allowed to flow. The slurry must be able to penetrate into and fill the gaps

between the fibers. This depends primarily on the magnitude of the driving force tending to push slurry into the mat, the resistance of the slurry to flow, i.e. its viscosity, and the geometry of the fiber mat (e.g. fiber spacing and weave, etc.). The infiltration process is modeled by considering the flow of a non-newtonian fluid (the slurry) between two infinite flat plates (the channel between adjacent fibers). The average infiltration velocity is given by

$$\bar{v}_l = \frac{n}{2n+1}\left(\frac{\Delta P}{\mu_{Sl} d_f}\right)^{\frac{1}{n}}\left(\frac{\lambda_s}{2}\right)^{\frac{n+1}{n}} \qquad \textbf{(EQ 44)}$$

where n is the shear thinning exponent, μ_{Sl} is the slurry viscosity, d_f is the fiber diameter, λ_s is the gap betwen adjacent fibers ($\lambda_s = \lambda - d_f$, where λ is the fiber center-to-center spacing), and ΔP is the driving force for infiltration. The slurry viscosity is described by an empirical relationship which accounts for the observed dependence of viscosity on both the powder loading (powder volume fraction, $\bar{v}_p$) and the shear strain rate, $\dot{\gamma}$:

$$\mu_{Sl} = \frac{k_{th}}{\dot{\gamma}^{|n-1|}}\left[1 - \frac{\bar{v}_p}{\bar{v}_{pb}}\right]^{-KH\bar{v}_{pb}} \qquad \textbf{(EQ 45)}$$

where k_{th} is the so-called shear thinning coefficient, KH is the Krieger-Dougherty coefficient and $\bar{v}_p$ is a critical powder loading at which the slurry "locks up", i.e. the viscosity approaches an infinite value. Physically, this condition corresponds with a transition from fluid (rheological) behavior to granular deformation as the powder volume fraction approaches the critical value. EQ 45 describes shear thinning behavior, in which the viscosity decreases as the rate of shear strain increases. This type of behavior is common in powder slurries and is desirable because it prevents sedimentation (high viscosity at low shear strain rate) while permitting complete infiltration (low viscosity at high shear strain rate) and the casting of thin tapes without tearing or rippling.

The driving force for infiltration is taken to be a combination of gravity (i.e. the weight of the slurry itself), externally applied pressure and capillary forces:

$$\Delta P = \frac{2\sigma_{lv}\cos\theta_w}{\lambda_s} + \rho_S^s g h_R + p_b \qquad \textbf{(EQ 46)}$$

where σ_{lv} is the liquid-vapor surface tension, θ_w is the wetting angle, ρ_S^s is the as-mixed slurry density, h_R is the height of the slurry column (i.e. the depth of slurry in the casting reservoir), and p_b is the externally applied pressure.

Tape Thickness - The thickness of the tape is controlled by the several factors, the most important of which are the height of the casting gate (h_b), slurry viscosity (μ_{Sl}), tape speed (v_T) and pressure (ΔP, which provides the driving force for slurry flow). The tape thickness, δ_T, (excluding fibers) following casting is determined from[1]

$$\delta_T = A h_b\left(1 + \frac{h_b^2 \Delta P}{6\bar{\mu}_{Sl} v_T \delta_b}\right) \qquad \textbf{(EQ 47)}$$

where A is a constant which depends on the amount of side flow and δ_b is the thickness of the casting gate (see Fig. 15). EQ 47 predicts that the cast tape will be thicker than than the gate height by an amount which increases with casting pressure and gate height, and decreases with increasing slurry viscosity, tape speed and gate thickness. An important consequence of this behavior is that thickness control becomes easier for very thin tapes and higher casting rates. Accurate control of cast tape thickness is important in obtaining a specified fiber volume fraction in the finished tape.

The casting quality index, Q_b, is taken as the ratio of infiltration depth to fiber mat thickness (or fiber diameter):

$$Q_b = \frac{\delta_l}{d_f} \qquad \textbf{(EQ 48)}$$

If $\delta_l / d_f > 1$, then $Q_b = 1$.

4.3.1.2 Drying

As the freshly cast tape enters the drying furnace, solvent, which is distributed reasonably uniformly through the tape thickness, begins to evaporate at the tape surface. This is controlled by the drying temperature and air flow rate. Air typically enters the furnace in a counterflow arrangement (Fig. 15) such that the incoming tape (at the furnace entrance) sees air that has already taken up solvent, so that some partial pressure of solvent exists. This lowers the evaporation rate at the outset, thereby lessening the risk of skin formation due to over-rapid solvent depletion at the

1. Y.T.Chou, Y.T.Ko and M.F.Yan, *J.Am.Cer.Soc.* 70(10), C280 (1987).

surface. Alternatively, solvent may be added to the incoming air to control the partial pressure of solvent in the air and thus the evaporation rate.

Once solvent begins to evaporate, a concentration gradient evolves with time, providing the driving force for diffusional transport of solvent from the interior of the tape. A mass balance leads to the following partial differential equation for c, the solvent concentration:

$$\frac{\partial c}{\partial t} = \frac{\partial}{\partial y}\left(D_{st}\frac{\partial c}{\partial y}\right) \qquad \text{(EQ 49)}$$

where y is the through-thickness direction in the tape and D_{st} is the diffusivity of solvent in the tape slurry. EQ 49 is subject to the following boundary conditions: the solvent flux (q) at the tape's bottom surface ($y = 0$) must be zero and at the top surface must be equal to the rate of solvent removal by evaporation. The flux at any point is given by

$$q = -D_{st}\frac{\partial c}{\partial y} \qquad \text{(EQ 50)}$$

The rate of evaporation is controlled by diffusion through a boundary layer. Effectively, the flux at the surface can be written as[1]

$$q_{sa} = a_g\sqrt{\frac{4D_{sa}u_R}{\pi L_g}} \qquad \text{(EQ 51)}$$

where a_g is an adjustable parameter (dimensionless) and u_R is the relative velocity between the tape and the air flow ($u_R = |q_g/(L_g h_g) - v_T|$, where q_g is the air flow rate and $L_g h_g$ is the cross section of the drying furnace). The required initial condition specifies the absence of any concentration gradient at $t = 0$.

EQ 49, subject to the stated initial and boundary conditions, could be solved numerically using say, an implicit finite difference scheme (e.g. Crank-Nicholson). The present objective, namely to obtain an indication of relative quality, does not warrant the computational effort required to solve the transport equation. Instead, a simplified mass balance equation is used in which the effective concentration gradient through the tape thickness is taken to be $1/\delta_T$. Setting the solvent flux within the tape (which is no longer allowed to vary with position, y) equal to the rate of solvent removal (given by EQ 51) gives

$$q_{st} = D_{st}\frac{1}{\delta_T} = a_g\sqrt{\frac{4D_{sa}u_R}{\pi L_g}}. \qquad \text{(EQ 52)}$$

The drying quality, Q_g, is then scaled with the ratio

$$\bar{q}_g = \frac{q_{sa}}{q_{st}} \qquad \text{(EQ 53)}$$

such that $Q_g = 1$ if $\bar{q}_g < 1$ and decreases linearly with increasing flux ratio until $Q_g = 0$ at a specified critical flux ratio, $\bar{q}_{gc}$. The drying quality is taken as an indirect measure of the likelihood that internal cracking and rearrangement, or surface cracking, will occur during drying. These problems are avoided by ensuring that solvent can be transported through the tape much more readily than it is removed. It is therefore in agreement with current practice in which drying rates are suppressed by limiting drying furnace temperatures and by using solvent-rich drying air.

4.3.1.3 Outgassing

Residual Contamination - Following the drying step, in which a controlled amount of solvent has been removed in order to produce a solid, yet flexible tape, the tapes are cut to a desired shape, stacked to form a laminate, and then placed within tooling to perform the final burnout (outgassing) and consolidation. During outgassing, the temperature, heating rate, and pressure are controlled to remove all of the organic slurry components (the carrier). As for drying, the rate of removal must take place slowly enough such that large temperature and concentration gradients are avoided. Outgassing is typically monitored by sampling the composition of gases exiting the tooling; the process is terminated when a specified (maximum) allowable level of residual organic material has been attained.

Several physical and chemical changes may occur during outgassing, including melting/softening, sublimation, evaporation, decomposition, depolymerization, carborization and oxidation. The mechanisms by which the organic components are removed from the green MMC laminate have not been well characterized, but they clearly depend on the green tape's microstructure (powder, organic phases and porosity). If the powder loading is high, such

1. R.B.Bird, W.E.Stewart and E.N.Lightfoot, Transport Phenomena, J.Wiley & Sons (New York), p.540, (1960).

that the ratio of the volumes of organic material to powder, $v_o/v_p < 0.1$, then diffusion of vapor products through the channels in the powder compact controls the time required for outgassing. The receding polymer/vapor interface is accompanied by a shrinkage front within the powder compact.

For the case when $v_o/v_p > 0.1$, diffusion within the organic phase is rate controlling. Weight loss is higher (with greater attendant shrinkage) and thermolysis times are much longer to avoid gas bubble formation within the organic phase.

A one-dimensional model is developed which describes the generation and removal of vapor products during outgassing.[1] The flow of gases through the powder compact and the internal pressures created if the gases are not removed (by the applied vacuum) quickly enough are modeled. Simplifying the conservation of mass equation (by assuming a parabolic dependence of pressure on x, the single in-plane coordinate, and then considering only the pressure at the center of the tooling ($x = 0$)) gives for the density of the outgas vapor

$$\frac{d\rho_v}{dt} = k_0 e^{-\frac{E_{af}}{RT}} \frac{(1-\phi_g(t)\rho_l)}{\phi_g(t)}\left(1-\frac{\rho_v}{\rho_l}\right) - \frac{2\kappa RT}{M_v \mu_{Sg} L_f^2 \phi_g(t)}\left|\rho_v - \frac{p_f}{RT}M_v\right| \qquad \text{(EQ 54)}$$

where the pressure is related to the vapor density by $p = \rho_v RT/M_v$, M_v is the molecular weight of the outgas, k_0 and E_{af} are the activation energy and pre-exponential constant characterizing the outgassing kinetics, ρ_l is the density of the liquid (carrier), κ is the permeability of the powder compact, μ_{Sg} is the viscosity of the outgas, L_f the the half-length of the tooling (distance from the center of the composite to the tooling exit, see Fig. 15), and p_f is the pressure applied at the tooling exit. The gas phase pore fraction, $\phi_g(t)$, is determined from an Arrhenius equation for the outgas kinetics

$$\frac{d\phi_g}{dt} = (1-\phi_g)k_0 e^{-\frac{E_{af}}{RT}} \qquad \text{(EQ 55)}$$

For a constant heating rate, $T(t) = T_0 + mt$, the solution to EQ 55 can be expressed as

$$\phi_g(t) = 1 - e^{-\alpha(t)} \qquad \text{(EQ 56)}$$

where α is given by

$$\alpha = k_0\left\{\frac{t}{e^{-\frac{E_{af}}{RT_0+mt}}} - \frac{T_0}{me^{-\frac{E_{af}}{RT_0}}} + \frac{T_0}{me^{-\frac{E_{af}}{RT_0+mt}}} - \frac{E_{af}}{mR}\left(-\int_{-\frac{E_{af}}{RT_0}}^{\infty}\frac{e^{-\tau}}{\tau}d\tau\right) + \frac{E_{af}}{mR}\left(-\int_{-\frac{E_{af}}{R(T_0+mt)}}^{\infty}\frac{e^{-\tau}}{\tau}d\tau\right)\right\} - \ln(1-\phi_{g0}) \qquad \text{(EQ 57)}$$

where ϕ_{g0} is the initial gas phase pore fraction. With $\phi_g(t)$ known from EQ's 56 and 57 (for an arbitrary ramp and hold heating cycle), EQ 54 is solved numerically (Runge Kutta) for the outgas density as a function of time, and this used to calculate the evolution of internal pressure. If the pressure exceeds the external pressure tending to hold all of the contents of the tooling in place (i.e. 1 atm), then cracking, rearrangement or internal voiding is expected.

Using EQ's 56 and 57, the time required to reduce the organic content to a specified (residual) fraction of its original mass fraction can be determined. If the critical pressure is not reached prior to the completion of outgassing, the outgas quality index (Q_f) is 1. If the critical pressure is reached during outgassing, the quality scales with the ratio of time to reach critical pressure divided by the outgas cycle time. Thus, the earlier in the outgassing step the critical pressure is reached, the lower the quality.

Shrinkage - The linear shrinkage strain, $\varepsilon_s = \Delta l/l$, is proportional to the mean reduction in interparticle spacing, Δl, and the mean number of interparticle liquid films per unit length, $\bar{N}_l$[2]

$$\varepsilon_s = \bar{N}_l \Delta l \qquad \text{(EQ 58)}$$

1. Based on work presented in High Performance Composites, 7th Quartely Report, prepared for ARPA (Agreement No. MDA 972-93-2-0008), p.31 (1995).

2. J.S.Reed, Principles of Ceramics Processing, 2nd ed., J.Wiley & Sons, Inc. (New York), p.552 (1995).

The number of liquid films, or gaps, is approximated (overestimated) by the reciprocal of the mean particle diameter, $1/d_p$. The interparticle spacing is the difference between the mean center-to-center particle spacing and the mean particle diameter

$$\Delta l = \lambda_p - d_p \qquad \text{(EQ 59)}$$

where λ_p is approximated by equating the known particle volume fraction with the volume fraction calculated by assuming the particles are all equally sized and spaced, and are arranged so that each particle has six nearest neighbors:

$$\lambda_p = \left(\frac{6}{\pi}\frac{c_P}{\bar{v}_p}\int_0^\infty \varphi_{dp}(x)\frac{\pi x^3}{6}(dx)\right)^{\frac{1}{3}} \qquad \text{(EQ 60)}$$

where c_p is the packing factor (= 0.74 for a close-packed assembly of uniformly sized spheres).

The final tape thickness is calculated from

$$\delta_T^f = (1-\varepsilon_s)\delta_T^g \qquad \text{(EQ 61)}$$

where the superscripts, 'f' and 'g' refer to the tape thickness in the final (outgassed) and green states.

4.3.1.4 Overall Quality

With dimensionless quality indices (each ranging from 0 to 1) for the casting (Q_b), drying (Q_g) and outgassing (Q_f) steps, the overall quality of the composite tape (Q_T) is calculated as a weighted sum:

$$Q_T = w_1 Q_b + w_2 Q_g + w_3 Q_f \qquad \text{(EQ 62)}$$

subject to the condition $\Sigma w_i = 1$. The w_i are user-specified and reflect the relative importance of microstructural defects arising from each of the process steps.

4.3.1.5 Production Rate

The tape casting process considered here (Fig. 15) may be used to continuously cast and dry, but the slurry formulation and outgassing steps are batch processes. The production rate associated with each of these three steps, slurry formulation, casting + drying, and outgassing, are determined. The production rate is defined as the rate [kg/hr] at which material is processed through the given step times the fraction of material processed which ends up in the finished tape. The slurry production rate is thus

$$\dot{m}_s = \frac{M_s}{t_s}\frac{\eta_m \bar{v}_p^s}{\bar{v}_p^f} \qquad \text{(EQ 63)}$$

where M_s is the batch size [kg], t_s is the mixing time [hr], η_m is the material use efficiency, and $\bar{v}_p^s$ and $\bar{v}_p^f$ are the volume fractions of powder in the slurry and finished tape, respectively.

The casting/drying production rate is given by the volume of tape (including powder, fiber and organic constituents) passing through the caster/dryer per hr times the tape density times the fraction of the tape which ends up in the finished composite (i.e. the sum of the mass fractions of powder and fiber):

$$\dot{m}_b = (\bar{m}_p^g + \bar{m}_f^g)(v_T \delta_T w_b)\rho_T. \qquad \text{(EQ 64)}$$

Finally, the outgassing production rate is

$$\dot{m}_f = (\bar{m}_p^g + \bar{m}_f^g + \bar{m}_{res}\bar{m}_c^g)\frac{M_f}{t_f} \qquad \text{(EQ 65)}$$

where $\bar{m}_{res}$ is the residual mass fraction of organic (carrier) materials, $\bar{m}_c^g$ is the mass fraction of carrier (organic materials) in the green tape, M_f is the outgas batch size and t_f is the time spent during outgassing. The process step with the lowest rate of production controls the actual production rate

$$\dot{m}_{prod} = Min(\dot{m}_s, \dot{m}_b, \dot{m}_f) \qquad \text{(EQ 66)}$$

4.3.2 Cost Models

The overall cost [$/kg] of tape cast MMC monotape is determined by summing the four cost elements needed for QCM, as shown in Fig. 3. Models for calculating these cost elements are presented next.

4.3.2.1 Materials Costs

The materials costs are just the sum of the costs of the powder (c_{powder} [$/kg]) and fiber ($c_{fiber}$ [$/kg]) making up the fiished tape:

$$c_m = \left(1 - \bar{v}_F\frac{\rho_F}{\rho_c}\right)c_{powder} + \bar{v}_F\frac{\rho_F}{\rho_c}c_{fiber} \qquad \text{(EQ 67)}$$

where $\rho_c = (1 - \bar{v}_F)\rho_p + \bar{v}_F\rho_F$, is the composite density.

4.3.2.2 Consumables Costs

The organic materials making up the slurry provide a vehicle for transporting the matrix powder through the tape caster and into the fiber mat. It is designed to ensure a uniform distribution of powder in the final tape. However, once the tape is cast, the organic components are no longer needed, are in fact quite undesirable and hence they are consumables in the tape casting process. Because these polymeric materials can be expensive, and because they are consumed during the process, their use must be kept to minimum from a cost standpoint.

Since it may generally be assumed that all of the powder in the slurry ends up in the final tape, the consumables cost is

$$c_c = \frac{\bar{m}_b^s}{\bar{m}_p^s}c_b + \frac{\bar{m}_s^s}{\bar{m}_p^s}c_s + \frac{\bar{m}_{pl}^s}{\bar{m}_p^s}c_{pl} + \frac{\bar{m}_w^s}{\bar{m}_p^s}c_w + \frac{\bar{m}_d^s}{\bar{m}_p^s}c_d + \quad \text{(EQ 68)}$$

$$+ c_{tooling}$$

where c_i refers to the unit costs of binder, solvent, plasticizer, surfactant, and deflocculant and $c_{tooling}$ refers to the cost of tooling used to outgas each laminate per kg of composite produced. The influence of increasing the powder loading on tape quality by reducing shrinkage has been mentioned above; here it can be seen that this also reduces cost by increasing the slurry efficiency, i.e. the amount of powder transported into the final composite by each kg of consumable organic material.

4.3.2.3 Energy Costs

The transformation of 'raw' powder and fiber into composite monotape absorbs an amount of energy per kg of tape which depends on the processing conditions used and the dimensions and properties of the powder, fiber and slurry constituents. Models for predicting the energy costs associated with each processing step are presented next.

Slurry Mixing - The cost to produce a slurry containing a given mass fraction of powder (all of which ends up in the composite) is

$$c_{mix} = \frac{P_{mixer}(\omega_s)t_s\bar{c}_E}{\bar{m}_p^f M_s} \quad \text{(EQ 69)}$$

where $P_{mixer}(\omega_s)$ is the mixer power (as a function of the mixing rate), t_s is the mixing time, and $\bar{c}_E$ is the unit cost of energy. The resource model for the mixer predicts the energy needed to provide a specified mixing rate[1]

$$P_{mixer}(\omega_s) = C_{DI}\omega_s^3\rho_S d_{mI}^5 \quad \text{(EQ 70)}$$

where C_{DI} is the impeller drag coefficient and d_{mI} is the impeller diameter.

Casting/Drying - The energy costs associated with casting and drying (i.e. the production of the 'prepreg') are given by

$$c_{prepreg} = [P_{casting}(v_T) + P_{drying}(T_g)]\frac{t_g}{(\delta_T L_g w_g \rho_T^g)}\bar{c}_E \quad \text{(EQ 71)}$$

where $P_{casting}$ and P_{drying} are process condition-dependent power requirements for the caster and drying furnace, respectively. (The other symbols are defined in Tables 6 and 7.) The power consumption associated with the casting step is not very sensitive to the casting rate or tape speed, v_T, and therefore $P_{casting}$ is assumed constant. The power requirement for the drying step is taken to be linearly dependent on the funace temperature:

$$P_{drying}(T_g) = P_0 + m_g(T_g - 20) \quad \text{(EQ 72)}$$

where P_0 is the power to start and m_g is the increase in power requirement for a unit change in furnace temperature.

Outgassing - Outgassing energy costs depend on the outgassing furnace temperature and the pressure (vacuum) maintained at the tooling exit. Thus the cost of energy to outgas enough prepreg to create 1 kg of composite tape is given by

$$c_{outgas} = \frac{P_{outgas}(T_f)t_f\bar{c}_E}{(\bar{m}_p^f + \bar{m}_f^f)M_f} \quad \text{(EQ 73)}$$

where $(\bar{m}_p^f + \bar{m}_f^f)M_f$ represents the mass of composite (powder + fiber) produced per outgassed batch (M_f [[kg]]) and P_{outgas}, the power requirement is

1. E.J.Kelly and D.J.Spottiswood, *Introduction to Minerals Processing*, Wiley-Interscience, New Yory, 1982.

$$P_{outgas} = P_{f0} + m_f(T_f - 20) + P_{p0} + m_p\left(\frac{1}{p_f}\right) \quad \text{(EQ 74)}$$

where P_{f0} and P_{p0} are the initial power requirements for the outgassing furnace and vacuum pump, respectively, and m_f and m_p are the rates at which the power consumption increases with increasing temperature and vacuum pressure, respectively.

Total Energy Costs - The total energy cost per kg of finished monotape is obtained as the sum of the costs associated with each of the steps:

$$c_e = c_{mix} + c_{prepreg} + c_{outgas} \quad \text{(EQ 75)}$$

4.3.2.4 Capital Costs

A typical tape caster is shown schematically in Fig. 18. Not shown are the slurry mixer and tape outgassing furnace/vacuum pump. The principal components of the caster include the tape casting bed, tape drive system, casting gate and reservoir and drying furnace.

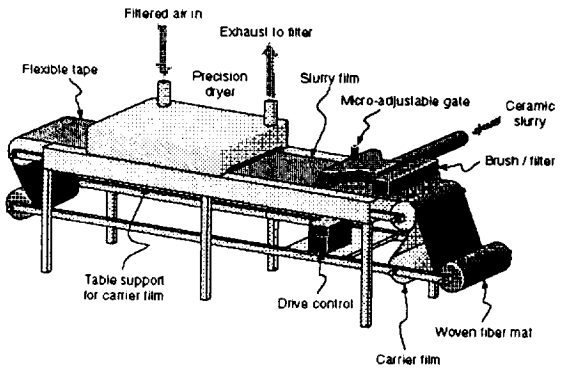

FIGURE 18. Overview of a typical (small-scale) tape casting facility. The principal components are the casting bed, tape drive system, caster, drying furnace and outgassing furnace.

Associated with these components are the capital costs, c_{capi}, giving the total capital cost as

$$c_{cap} = \sum c_{cap_i} \quad \text{(EQ 76)}$$

4.3.2.5 Total Monotape Cost per kg

As for the plasma spray deposited material, the total cost of the finished composite tape per kg is the sum of the four cost elements

$$C = c_m + c_c + c_e + \frac{c_{cap}}{M_{prod}} \quad \text{(EQ 77)}$$

4.4 Implementation

Mathematica^{TM} code containing all of the above models for predicting the cost and quality of MMC monotape by the tape casting method is included in Appendix C. The procedure for performing a QCM analysis is as follows: 1) load and run the *Mathematica* program, 2) edit material properties within *Mathematica* as desired (using standard editing procedures), 3) select Evaluate Notebook under the Action menu, 4) enter input data as requested.

4.5 Results

4.5.1 Quality-Cost Relationship

The QCM model may be used to simulate the evolution of performance-defining microstructural attributes as a function of material properties, equipment design and tape casting process conditions. The final microstructure is characterized by a dimensionless quality index (ranging from 0 to 1) and a cost ($ per kg). Conducting numerical experiments for a variety of different processing conditions, and plotting the cost and quality associated with each experiment, yields a scatter diagram like that shown in Fig. 19. Plotted on the y-axis is the cost ratio, defined as the total monotape cost [$/kg] normalized by a constant representative of the cost of raw materials. (Fig. 19 was constructed using the raw materials cost for a finished Ti-6Al-4V/SCS-6 composite tape containing 10 vol% void, 40 vol% fibers at $1000/kg and 50 vol% powder at $450/kg, giving 628 $/kg as a normalizing constant). A total production volume of 1000 kg was assumed for amortization of capital costs (cf. EQ 77).

At each cost there exists an upper limit on the quality which can be obtained; as cost decreases, so does the highest reachable quality. These outermost points define an envelope (aproximated by the curve in Fig. 19) encompassing all reachable combinations of cost and quality. Several points are shown which lie well within the reachable space. The highest quality ($Q_T = 1$) represents a tape cast composite monotape having a uniform distribution of powder and fiber, no cracks (internal or surface), and no residual organic contaminants.

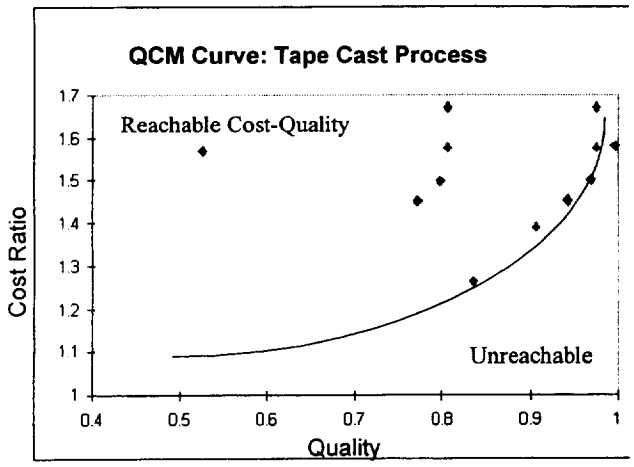

FIGURE 19. The Quality-Cost curve for the tape casting process is characterized by a slow, steady rise in cost with quality.

As can be seen from the QCM curve, the tape casting approach can potentially produce material having a high quality microstructure. The cost of this quality is about a factor of 1.7 times the cost of the powder and fiber at this total production volume. Input and output for the experimental results shown in Fig. 19 are given in Appendix D. As can be seen, the powder loading (mass fraction of powder in the slurry), gate height, particle size distribution, drying furnace temperature and flow rate, outgas temperature and fraction of residual organic material were varied. Interestingly, the results indicate that the powder size distribution exerts little influence on the highest quality attainable, but strongly affects cost (coarser particles being much cheaper). On the other hand, cost is little affected by the specified residual organic level (because the cost of the additional energy needed to ensure more complete outgassing is so low), but strongly affects the quality.

The cost ratio could approach 1 in the limit that the tape cost equals the costs of the powder and fiber, i.e. the slurry consists entirely of powder with no organic consumables. The QC curve would be expected to approach a quality of zero in this case, since without binder, it would be impossible to handle the tape to form laminated components. The QCM model, while being concerned only with the creation of the monotape (and not with laminates), indicates this trend because the viscosity becomes so great in the case of very high powder loadings, that casting and infiltration become impossible, forcing the quality to zero.

Three experiments in which the powder loading was decreased (from 40 to 30 wt%), the quality changed imperceptibly while the tape cost increased from 930 $/kg to 990 $/kg. The lower powder fraction increases the fraction of consumables (i.e. organic materials) needed to produce 1 kg of tape. The lower powder loading also resulted in a slightly thicker cast tape (by lowering the slurry viscosity) and lowered the overall production rate. Also, by lowering the volume fraction of powder in the green tape, lower powder loading increased the shrinkage strain upon outgassing from 16.7 to 21%. At the same time, the reduced powder volume fraction yielded an increased fiber volume fraction (from 34.7 to 40%).

The casting gate height is the primary means of controlling the tape thickness, but it has a strong effect on a number of other features. Three experiments are shown (Exper. Nos. 4-6, Appendix D) in which the gate height was decreased from 1 to 0.5 to 0.3 mm; as a result, the shrinkage strain decreased from 21.5 to 16.7 %. This can be expected to reduce the likelihood of warping and therefore to improve tape quality, though this has not been treated in calculating the quality at present. As expected, the volume fraction of fiber increased as the tape thickness was reduced, going from 11 to 34 vol%. Reducing tape thickness also improves drying quality since it becomes easier to maintain low solvent concentration gradients when the tape is thin (due to short overall diffusion distances through the tape). The viscosity of the powder slurry is also lowered for thinner tapes since the average rate of shear increases for a given tape speed. This has the consequence that flow is improved (for easier infiltration of the fiber mat). Thus, while the gate height is the primary means of controlling the fiber volume fraction, it is important for a number of other reasons. These results indicate that high quality should be easier to obtain for thin tapes than for thicker ones. Of course, reducing tape thickness, and thereby increasing the fiber volume fraction in the tape, does markedly increase the tape cost (by roughly 100 $/kg for the three experiments shown) due to the high cost of the fiber.

The influence of mass fraction of residual organic materials in the finished monotape ($\bar{m}_{res}$) was investigated by three experiments (Nos. 8-10, App. D) in which $\bar{m}_{res}$ was reduced from 0.01 to 0.001 to 0.0001. The tape cost was

affected only slightly while the overall tape quality improved from 0.53 to 0.97 and finally to 0.998. The outgassing time (at a constant outgassing temperature of 400 °C) increased from 9.7 to 14.5 to 19.3 hrs.

4.5.2 Cost Breakdown

Figure 20 shows the relative contributions of the four cost elements (materials, consumables, energy and capital) for the tape casting experiments listed in Appendix D. The total production volume is 1000 kg so that, for a total capital investment of $36,000 (approximate cost of a small-scale tape casting facility), the capital cost contribution is $36 per kg. It can be seen that for the relatively high cost assumed for the powder and fiber (250 - 450 $/kg and 1000 $/kg, respectively), material costs constitute roughly half of the total cost. Unlike the plasma spray process, the relative contribution of consumables to the total cost is significant for the tape casting process. Capital costs are relatively unimportant at this production volume and energy costs are insignificant. It is noteworthy that as the costs of powder and fiber drop, the relative importance of consumables (organic slurry constituents) in determining tape cost becomes predominant and studies aimed at improving the efficiency of their use will become very important.

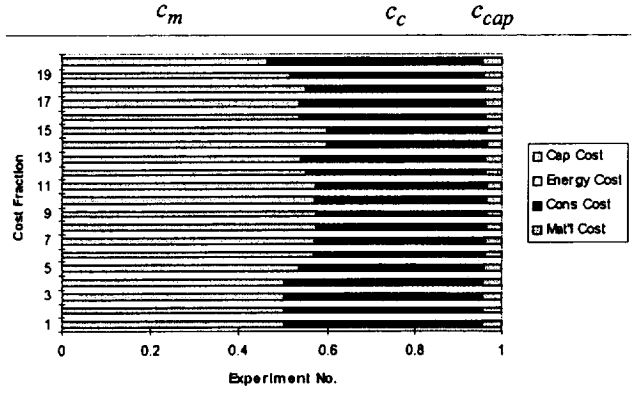

FIGURE 20. Cost breakdown among the four cost elements for tape cast experiments.

4.5.3 Key Factors Affecting QC

Some decoupling of the factors which influence quality from those that influence cost seems to be possible in the case of the tape casting process. The factors which most strongly influence quality are the temperature and air flow rate during drying and temperature during outgassing. All three of these process variables can be varied over a wide range (causing tape quality to range from uselessly low to nearly perfect) with no significant impact on overall cost. The energy costs may increase fourfold as these process variables are adjusted from one extreme to the other, but because energy costs are so small relative to the other cost elements (especially materials and consumables), the overall tape cost remains practically unaffected.

This observation leads to the conclusion that efforts to optimize these process variables (tailored to the materials used and other specifications for the composite) to obtain the highest quality possible should be most beneficial. Modeling and *in situ* monitoring (advanced sensors) which first concentrates on these factors will be most effective in improving the combination of attainable cost and quality.

The casting gate height is also seen to be a key control parameter, influencing both cost and quality, but primarily quality for fixed fiber volume fraction. Increasing the fiber spacing while decreasing tape thickness to achieve the same fiber volume fraction as a thicker tape with more closely spaced fibers may be an easy way to achieve quality improvements (within a fairly narrow range of fiber volume fractions) with no penalty in cost.

The clear cost advantage of the tape casting process will most likely be realized for low production volumes when the relatively small initial investment needed for tape casting leads to low capital costs. For large production volumes, tape casting will most likely be at a cost disadvantage because of its heavy reliance on consumable polymeric materials for production. This observation underscores the importance of research and modeling in identifying optimal slurry compositions (as opposed to process design refinements or process optimization). These consumable constituents will be low cost and will allow the greatest mass fraction of powder to be transported into the final product, without sacrificing rheological properties such as shear thinning behavior.

5.0 Comparison of Plasma Spray Deposition and Tape Casting Processes

Figure 21 shows a plot of EQ 43 comparing the cost of monotape of similar properties and quality as a function of production volume for the plasma spray and tape casting processes. The low capital costs associated with the tape

casting approach make it the preferred choice for production volumes below about 10^3 kg. Above this, the much lower reliance of consumable materials gives the plasma spray deposition route the cost advantage.

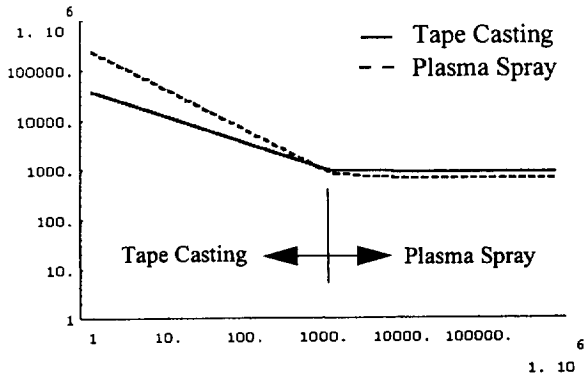

FIGURE 21. MMC cost as a function of production volume: tape casting offers lower cost for small production volumes.

Figure 21 is based on averaged costs for materials, consumables, and energy for all of the "experiments" listed in Appendices B and D. Capital costs were fixed at \$36K for the tape casting facility and \$227.5K for the plasma spray facility. In terms of production capacity, these are comparable facilities.

Comparison of the QCM curves for the two processes (Fig. 22) at a production volume of 10^3 kg, illustrates the very comparable range of total cost in the region where the two curves cross over in Fig. 21. The extra detail available with the QCM curves shows that although overall costs are similar, the choice ultimately depends on the quality required by the application. A component requiring a relative quality of greater than 0.85 could be obtained more cheaply by plasma spray deposition. If lower quality is acceptable, the tape casting method should provide the lowest overall cost. Figure 21 indicates that as the production volume decreases, the point in Figure 22 where the curves intersect will shift to the right until at sufficiently low production volume, the tape casting process would be preferred regardless of the application. Conversely, the plasma spray process will be preferred regardless of application for sufficiently high production volumes. Figure 23 shows QCM curves for the two processes at a production volume of 10^6 kg; the plasma spray process has become the clear choice regardless of quality.

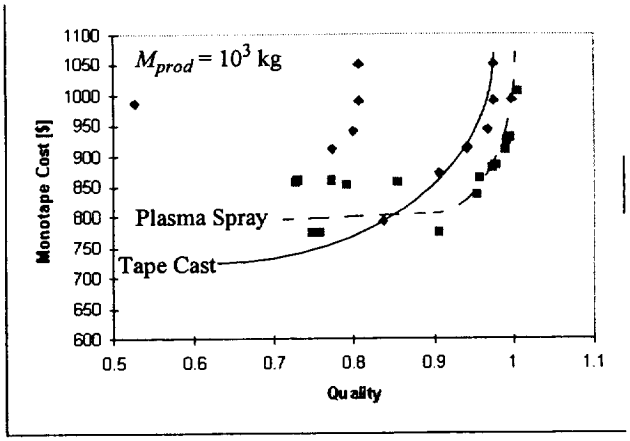

FIGURE 22. Comparison of QCM curves for the plasma spray and tape casting processes at a production volume of 10^3 kg.

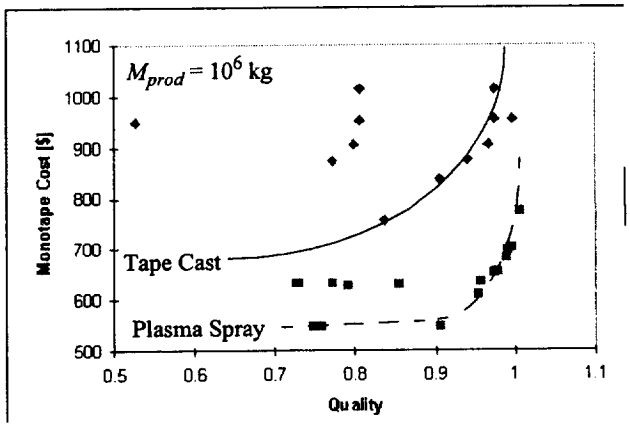

FIGURE 23. QCM curves for the two processes at a production volume of 10^6 kg confirming the trend seen in Figure 21.

The quality-cost relationship (i.e. the QCM curve) should be a unique characterization of a given process/material system. The numerical experiments which have been performed using the QCM tool indicate a relatively flat curve for the plasma spray process over a wide range of quality followed by a sharp, exponential increase in cost above a

quality of around 0.9. The tape cast process appears to possess a more gradually increasing cost-quality relationship. A flat QCM curve indicates that much higher quality can be achieved at little extra cost. However, one must be able to understand and predict the influence of the relevant factors on product quality in order to consistently achieve these improvements. As noted previously, the opportunity to influence quality without impact on cost is a strong argument for modeling, sensing and process optimization - these are the only tools needed to exploit the potential improvement.

On the other hand, a strongly sensitive cost-quality relationship (as exhibited by the plasma spray process for $Q_{PS} > 0.9$) may indicate the need to alter the interaction between the processing environment and the materials system, possibly by process design refinements. The steeply rising QC curve for the plasma spray process is due to the need to achieve greater superheat in the powder particles in order to lower internal porosity and surface roughness by improving the flow characteristics of the impacting droplets. As the plasma temperature is increased (to improve superheating), material use efficiency decreases since more and more of the smaller particles are vaporized. Reducing the size variation can help, but is an expensive approach, adding cost to each kg of finished composite. A design refinement allowing improved control of the energy distribution (such that larger particles recieve proportionately more energy) within the plasma spray would require a single (initial) investment.

The QC curve for the tape casting process shows a more steady, gradual increase in cost with quality. Material use efficiency is not an issue for the tape casting approach (almost all powder in the slurry winds up in the finished tape), but efficient use of consumables (organic slurry components) clearly is. A combination of intelligent processing and carefully directed process refinement might be the best approach to improving cost and quality of tape cast product.

Sharply rising QC curves render conventional cost model predictions (in which quality-related parameters are assumed, or are based on empirical observations) unreliable because the costs are so sensitive to assumptions regarding quality. In the region where the QC curve is relatively flat, conventional cost models are more likely to be accurate since cost is little affected by these assumptions.

6.0 Summary and Recommendations

Quality-Cost Modeling (QCM) has been proposed as a means to obtain approximate yet quantitative information regarding the potential of emerging manufacturing processes for advanced materials. The QCM concept is based on the development of relatively simple (first order) models intended to capture the essential interactions between the material and its processing environment and their use in calculating the final microstructure (and relating this to quality) and the associated cost. Both cost and quality are functions of the starting state of the material, process conditions used and the design of the process. The QCM tool allows numerical experiments to be conducted in which the influence of these variables on cost and quality can be explored.

The QCM concept has been developed and applied to two emerging processes for the manufacture of continuous fiber reinforced metal matrix composites. The plasma spray deposition process is a semi-solid process in which a metallic powder is melted within a plasma and spray deposited onto a ceramic fiber substrate. The tape casting process employs a viscous organic carrier to entrain the solid (metallic) powder, allowing it to be infiltrated into a ceramic fiber substrate. The resulting 'green' tape is subsequently heated to remove all organic constituents. Both processes result in fiber reinforced MMC monotapes which can be laminated and consolidated (e.g. by Hot Isostatic Pressing) to produce a fully dense, near net shape component.

Quality and Cost models have been presented for both MMC manufacturing processes and the resulting predicted quality-cost curves presented and discussed. The tape casting process is characterized by a steadily increasing (nonlinear) QC curve, while for the plasma spray process, the QC curve exhibited a wide flat region followed by steeply rising cost as quality is made to approach 1 (highest quality). Both processes are predicted to be capable of producing high quality composite material.

The most affordable process depends strongly on the anticipated production volume: at low volumes ($M_{prod} < 10^3$ kg), tape casting offers the most economical route while plasma spraying becomes the preferred route at higher production volumes. At low production volumes, the high capital costs associated with plasma spraying (roughly 4 - 5 times that needed for tape casting) result in

higher product cost for the plasma spray process. At high production volumes, the capital costs are much less due to amortization of the initial costs. Here, the heavy reliance of the tape casting route on expensive consumables (organic slurry materials) to produce composite tape make it more costly than plasma spraying. For intermediate production volumes (on the order of 10^3 kg), the preferred route was shown to depend on the intended application (i.e. on the quality required); for applications requiring lower quality, tape casting appears most economical while for applications demanding higher quality, plasma spray deposition is most affordable.

The greatest potential for improving the affordability of tape cast MMC's is expected to lie in improved slurry compositions. It is important to identify optimal slurry compositions which maximize the powder transport efficiency and which can do so at the lowest cost. Basic research aimed at improved understanding of the role of slurry constituents and their interactions with the powder and fiber mat during tape casting is likely to be most helpful. Identification of low cost slurries, (possibly aqueous-based compositions for some applications), should be pursued. Next, improved sensing and on-line controls should be developed. Here, the key process variables are casting gate height (affects infiltration, final fiber volume fraction, shrinkage strain, and tape drying), drying temperature and outgassing temperature. Increasing the duration of the outgassing cycle can dramatically improve quality with little impact on final cost.

The plasma spray deposition process is seen to possess an intrinsic cost-quality tradeoff: as the plasma temperature is increased (to improve particle superheat and thereby to improve the flow properties of the droplets on impact), internal porosity and surface roughness are reduced, but smaller particles in the powder size distribution are increasingly vaporized, resulting in reduced deposition efficiency (and therefore higher cost) and higher radiation losses (lower energy efficiency). For this reason, the plasma operating conditions (RF powder, gas flow rates and composition) must be tailored to the thermal properties and size distribution of the matrix powder particles. While advanced sensing and control concepts may be very useful, an improved torch design which allows more control of the energy and mass distributions within the torch is expected to provide the greatest cost-quality improvement.

The results show clearly that tape cast and plasma spray deposited MMC's will not become affordable alternatives to more conventional high performance materials as a result of process refinement, on-line sensing and control, and/or predictive modeling for process optimization unless the costs of high strength fiber reinforcement and fine alloy powders can be greatly reduced; otherwise, the resulting improvements in affordability will not be tangible. Processing routes which avoid powder processing, such as the e-beam vapor deposition of alloy bar stock, are attractive for this reason, if other factors such as product quality, deposition efficiency and production rate are adequate.

APPENDIX A

■ Vers. 2.1 QCM (D.M.Elzey, University of Virginia, 1996)

Plasma Spray Process

The quality-model for the RF Plasma Spray Deposition process allows the relative density, surface roughness, fiber/coating damage, residual stresses and tape thickness to be predicted for an arbitrary plasma spray deposition schedule. The process schedule is characterized by the powder flow rate, plasma forming gas flow rate, RF power, and mandrel position and temperature as a function of time.
The spray deposition process is broken down into two steps: 1) creation of the plasma spray, and 2) deposition.

■ Plasma Spray Creation

The plasma spray is defined by the steady state, spatial distribution of temperature, particle and plasma velocities, and mass. These distributions can be treated as steady state and axisymmetric. Turbulence and non-steady flow will not be treated. The factors that can affect these distributions include material parameters (e.g. thermal conductivity of the powder), geometric parameters (e.g. the particle size distribution, nozzle/torch geometry), process variables (e.g. RF power, powder flow rate).

After defining constants, dimensionless numbers and material property functions, a routine for calculating the particle velocity as a function of time (or position) is given. Only axial velocity is considered. The initial velocity of the powder is determined from the injection nozzle size and carrier gas flow rate. The velocity is affected through the drag coefficient, which is written as a function of the Reynolds number (Re). Drag is inversely proportional to Re. (Re increases with the relative velocity between plasma and particle, plasma density, particle size and decreases with plasma viscosity.) The plasma velocity is determined from conservation of mass and depends on the the plasma temperature (initially unknown).

The temperature history of a powder particle of a given size is then determined for a given plasma temperature. Powder heating is determined by heat conduction from the plasma and radiative losses to the surroundings. The heat transfer coefficient (governing heat conduction) depends on the Reynolds number (increases with Re), the thermal conductivity of the powder and the powder size. The dependence on Re requires that the velocity history first be solved, then the temperature history. Depending on the plasma conditions, powder size, material properties, etc., the particle may melt partially or fully, arrive at the substrate as a superheated liquid, be partially or fully vaporized. If the melting point is reached, the fraction of liquid is calculated; if the boiling point is reached, the mass fraction lost by evaporation is determined.

With functions for calculating the velocity and temperature histories of individual particles now available, a distribution function (arbitrary) for particle size is introduced. The total heat energy absorbed by the powder distribution per unit time (power consumption) can then be calculated. Next, the plasma temperature is determined by balancing the power consumption to heat the powder with the input RF power. An iterative (root finding) routine starts with a 10,000 K plasma temperature and iterates the temperature until a power equilibrium is obtained.

■ Plasma Spray Deposition

Relative density of the substrate is calculated based on Madejski's model for flow and solidification of single droplets applied to representative particle sizes within the particle size distribution. Interfacial reaction zone thickness and fiber thermal shock due to impingement of molten droplets on the relatively cool fibers are determined as additional quality-defining parameters.

```
<< Graphics\Graphics.M
```

Quality Models

■ Data for Quality Models

```
matrixproperties := (
  kps = 33.0; (*[W/mK].....thermal conductivity (solid Ti) *)
  kpl = 20.0; (*[W/mK].....thermal conductivity (liquid Ti) *)
  as = 8.0*10^-6; (*[m^2/s]....thermal diffusivity of
                                  solid (Ti@1500K) *)
  al = 7.0*10^-6; (*[m^2/s]....thermal diff of liquid *)
  rhops = 4.5*10^6; (*[g/m^3]..solid particle density *)
  rhopl = 4.5*10^6; (*[g/m^3]..liquid particle density *)
  cpps = 0.52; (*[J/gK].....specific heat (solid Ti) *)
  cppl = 0.70; (*[J/gK].....specific heat (liquid Ti) *)
  e = 0.5; (*.....emissivity *)
  tm = 1800.0; (*[K].....melting temp (Ti) *)
  tb = 2500.0; (*[K].....boiling temp (Ti) *)
  hm = 200.0; (*[J/g].....latent heat of melting (Ti) *)
  hv = 5000.0; (*[J/g].....latent heat of vaporization (Ti) *)
  sten = 1470.0; (*[g/s^2].....surface tension (Ti) *)
  mup = 5.1; (*[g/ms].....dynamic viscosity @ Tm (Ti) *)
  hof = 437.0; (*[J/g].....heat of fusion *)
  );
General::spell1: Possible spelling error: new symbol name "rhopl"
    is similar to existing symbol "rhops".
General::spell1: Possible spelling error: new symbol name "cppl"
    is similar to existing symbol "cpps".
powdersize =.
powdersize := (
  dp = 180.0*10^-6; (*[m].....mean particle size *)
  dpsd = 35.0*10^-6; (*[m].....size deviation *)
  );
fiberproperties := ((* SiC FIBER *)
  weibullmod = 13; (*.....Weibull modulus *)
  refstrength = 4.5*10^9; (*[Pa]..fiber reference strength *)
  emodfiber = 4.0*10^11; (*[Pa]...fiber stiffness ???value???*)
  nufiber = 0.3; (*.....fiber Poisson's ratio *)
  ctefiber = 4.5*10^-6; (*[1/C]...fiber CTE *)
  kfiber = 5.0; (*[W/mK].....fiber thermal conductivity ???value???*)
  rhof = 3.9*10^6; (*[g/m^3].....fiber density *)
  );
General::spell1: Possible spelling error: new symbol name "rhof"
    is similar to existing symbol "hof".
fibermat := (
  fiberdiameter = 142.0*10^-6; (*[m]*)
  fiberspacing = 2.5*fiberdiameter; (*[m]*)
  fibergap = fiberspacing  - fiberdiameter; (*[m]*)
  );
interfacialproperties := (
  kappa0 = 3.53*10^-3; (*[m/s^0.5].....preexponential
                                        constant *)
  rztactenergy = 257.0*10^3; (*[J/mol]..activation
```

```
                                                    energy *)
  allowablerzt = 1.0*10^-6; (*[m].......acceptable
                      interfacial reaction thickness *)
  );
physicalconstants := (
  sbc = 5.7*10^-8; (*[W/m^2*K^4]..Stefan Boltzmann constant *)
  g = 9.8; (*[m/s^2].............acceleration due to gravity*)
  rgas = 8.315; (*[J/mol-K].......Universal gas constant *)
  rtemp = 293.15; (*[K]...........room temperature *)
  tamb = 293.15; (*[K]............ambient chamber temperature *)
  );
mandrelproperties := (
  meltpointmandrel = 1550.0; (*[K]..melting temperature *)
  );
designdata := (
  r1 = 1.7*10^-3; (*[m]...........radius of injection probe orifice *)
  ls = 0.4; (*[m].................spraying distance *)
  r0 = 35.0*10^-3; (*[m]..........torch internal radius *)
  lmandrel = 0.25; (*[m]..........spray deposit length *)
  dmandrel = 0.2; (*[m]...........mandrel diameter *)
  areaofdeposit = lmandrel*N[Pi,10]*dmandrel;
  );
General::spell1: Possible spelling error: new symbol name "dmandrel"
    is similar to existing symbol "lmandrel".
```

Dimensionless numbers

```
re[v_,x_,dynvis_,dens_] := dens*Abs[v]*x/dynvis; (* Reynold's number *)
nuss[htc_,x_,k_] := htc*x/k; (* Nusselt number *)
biot[kplasma_,kpart_] := kplasma/kpart; (* Biot number *)
we[v_,x_] := rhopl*Abs[v]^2*x/sten;       (* Weber number *)
pe[v_,x_] := Abs[v]*x/as;                 (* Peclet number *)
```

Calculated Physical Parameters

```
nu[dynvis_,density_] := dynvis/density; (* kinematic viscosity *)
hc[reynum_,dia_,t_] := k[t]/dia*(2.0 + 0.515*reynum^0.5); (*
                    plasma-particle heat transfer coefficient *)
hcapp[dia_] := Which[ (* Heat capacity of matrix powder *)
  (tp < tm) || (tm<tp && tp<tb), N[Pi,6]/6*rhops*dia^3*cpps,
  (tp == tm), N[Pi,6]/6*rhops*dia^3*hm,
  (tp == tb), -N[Pi,6]/2*rhops*dia^2*hv];
cd[rn_] := Which[rn<=0.2, 24/rn, (* Drag coefficient *)
                 rn<=2.0, 24/rn*(1+0.189*rn),
                 rn<=21.0, 24/rn*(1+0.11*rn^0.81),
                 rn<=200.0, 24/rn*(1+0.189*rn^0.62),
                 rn>200.0, 0.0];
fiberpof[stress_] := 1.0 - Exp[-(stress/refstrength)^weibullmod];
```

Plasma Properties

```
mu = 0.01; (*[g/m*s].....dynamic viscosity (Ar-plasma) *)
rho[tempx_] := 1.783*((273/tempx) - 2.06*10^-7*tempx +
  6.71*10^-11*tempx^2 - 5.21*10^-15*tempx^3)*10^3;
            (*[g/m^3].....plasma density *)
cp[temp_] := Which[temp < 6000, 0.519,
  6000.0 <= temp && temp < 10^4, 0.519 + 0.996*(temp/10^4)^11,
  temp >= 10^4, 0.519 + 0.996*(temp/10^4)^7];
          (*[J/gK].....plasma heat capacity *)
k[temp_] := Which[temp < 6000, -0.024*(temp/10^4)^2 +
  0.262*(temp/10^4) + 0.0165,
  temp >= 6000, 0.248*(temp/10^4)^6 + 0.372*(temp/10^4)^3 + 0.074];
            (*[W/mK].....thermal conductivity (plasma) *)
```

■ Calculated Process Conditions

Average inlet gas velocity

The factor 10^-3/60 converts slpm to m^3/s

```
u0 = (q1+q2+q3)*10^-3/60/(N[Pi,6]*r0^2);
```

Temperature dependent plasma velocity

```
u[tmpl_] := rho[tamb]/rho[tmpl]*u0;
```

Initial powder velocity

```
up0 = q1*(10^-3/60)/(N[Pi,6]*r1^2); (* initial powder speed;
            factor of (10^-3/60) converts lit/min to m^3/s *)
```

■ Plasma Spray Creation

■ Particle velocity history

Particle position function

```
Clear[dist];
dist[t_] := First[NIntegrate[Evaluate[y[x]/.usol],{x,0.0,t}]];
```

Particle velocity

```
Clear[pvel];
pvel[psize_,tmp_] := Module[{initre,eta},
  initre = re[(u[tmp]-up0),psize,mu,rho[tmp]]; (* initial Reynolds no. *
  eta = ls/Min[up0,u[tmp]]; (*[s]....maximum time to reach substrate *)
  usol = NDSolve[{y'[x] == -3/4*
    cd[re[Abs[u[tmp]-y[x]],psize,mu,rho[tmp]]]*(y[x]-u[tmp])*
    Abs[y[x]-u[tmp]]*rho[tmp]/(rhops*psize)+g, y[0] == up0},y,
    {x,0.0,eta}];
  tof = tf /. First[FindRoot[dist[tf] == ls, {tf,{10^-8,ls/up0}}]];
  upf = First[Evaluate[y[tof]/.usol]]; (* particle vel at impact *)
  ];
```

■ Particle temperature history

```
Clear[ptemp];
```

```
General::spell: Possible spelling error: new symbol name "ptemp"
    is similar to existing symbols {rtemp, temp}.
```

```
ptemp[psize_,plt_] := Module[{},
  Off[General::spell];
  lfrac = 0.0; (* liquid fraction reset to zero *)
  tsolid = 0.0; tliq = 0.0; tvapor = 0.0; tevap = 0.0;
  (* Calculate temperature history for Tp < Tm *)
  tp = rtemp;
  tsol = NDSolve[{yt'[x] == 1/hcapp[psize]*
         N[Pi,6]*psize^2*
         hc[re[u[plt]-First[Evaluate[y[x]/.usol]],
           psize,mu,rho[plt]],psize,plt]*
         (plt-yt[x]) - N[Pi,6]*psize^2*sbc*e*
         (yt[x]^4-tamb^4),
         yt[0] == tp},yt,{x,0.0,tof}];

  (* Particle temperature predicted at impact *)
  tempf = Re[First[Evaluate[yt[tof]/.tsol]]];

  If[tempf >= tm,
    (* time at which melting begins *)
    tsolid = x /. First[FindRoot[First[
      Evaluate[yt[x]/.tsol]] == tm,
      {x,{0.0,tof/100.0},0,tof}]];
    tp = tm;
    (* Rate of melting *)
    dxdt = 1/hcapp[psize]*
      N[Pi,6]*psize^2*
      hc[re[u[plt]-First[Evaluate[y[tsolid]/.usol]],
          psize,mu,rho[plt]],psize,plt]*
      (plt-tm) - N[Pi,6]*psize^2*sbc*e*
      (tm^4-tamb^4);
    (* time at completion of melting *)
    tliq = tsolid + 1/dxdt;

    If[tliq < tof,
      tp = tm/0.9999;
      (* Temp history for T > Tm but T < Tb *)
      tmbsol = NDSolve[{ytmb'[x] == 1/hcapp[psize]*
          N[Pi,6]*psize^2*
          hc[re[u[plt]-First[Evaluate[y[x]/.usol]],
            psize,mu,rho[plt]],psize,plt]*
          (plt-ytmb[x]) - N[Pi,6]*psize^2*sbc*e*
          (ytmb[x]^4-tamb^4),
          ytmb[tliq] == tp},ytmb,{x,tliq,tof}];
      (* Calculate temperature at impact *)
      tempf = Re[First[Evaluate[ytmb[tof]/.tmbsol]]];

      If[tempf >= tb,
        (* time to begin vaporization *)
        tvapor = x /. First[FindRoot[First[
        Evaluate[ytmb[x]/.tmbsol]] == tb,
```

```
        {x,{tliq,tliq/0.9999},tliq,tof}]];
        tp = tb;
        (* Particle size history during vaporization *)
        vapsol = NDSolve[{ydp'[x] == 1/hcapp[ydp[x]]*
          N[Pi,6]*ydp[x]^2*
          hc[re[u[plt]-First[Evaluate[y[x]/.usol]],
            ydp[x],mu,rho[plt]],ydp[x],plt]*
          (plt-tb) - N[Pi,6]*ydp[x]^2*sbc*e*
          (tb^4-tamb^4),
          ydp[tvapor] == psize},ydp,{x,tvapor,tof}];
        tevap = x /. First[FindRoot[Re[First[
        Evaluate[ydp[x]/.vapsol]]] == 2.*10^-6,
        {x,{tvapor,tvapor/0.9999},tvapor,tof}]];
        (* particle size at impact *)
        If[tevap > tof,
          dpf = Re[First[Evaluate[ydp[tof]/.vapsol]]];
          msg = "Partial vaporization.";
          lfrac = 1.0,
          dpf = 0.0;
          msg = "Particle vaporized."],
        msg = "Complete melting. No vaporization.";
        lfrac = 1.0;
        dpf = psize;
        tp = tempf],
      lfrac = dxdt*(tof-tsolid);
      msg = "Partial melting.";
      dpf = psize;
      tp = tm],
    msg = "Particle unmelted on impact.";
    dpf = psize;
    tp = First[Evaluate[yt[tof]/.tsol]]
    ];
  If[diagnostics, Print[msg];
    Print["dp = ",N[dpf*10^6,4]," [um]"];
    Print["lfrac = ",N[lfrac,4]];
    Print["start melting at ",tsolid];
    Print["complete melting at ",tliq];
    Print["start vaporization at ",tvapor];
    Print["complete vaporization at ",tevap];
    Print[""];
    ];
  On[General::spell]
];
General::spell1: Possible spelling error: new symbol name "tsol"
    is similar to existing symbol "usol".
General::spell: Possible spelling error: new symbol name "tempf"
    is similar to existing symbols {temp, tempx}.
General::spell1: Possible spelling error: new symbol name "dpf"
    is similar to existing symbol "DPF".
```

```
Clear[ptemphist];
ptemphist[time_] := Which[time < tsolid, First[Evaluate[yt[time]/.tsol]]
  time >= tsolid && time < tliq, tm,
  time >= tliq && time < tvapor, First[Evaluate[ytmb[time]/.tmbsol]],
  time >= tvapor, tb];
```

■ Plasma particle history function

Uses the particle velocity and temperature subroutines to calculate the particle velocity and temperature history for a particle of size (partsize).

```
pspart =.
pspart[partsize_,pltmp_] := Module[{},
  pvel[partsize,pltmp];
  ptemp[partsize,pltmp];
  If[diagnostics,
    Print["Time of flight:          ",N[tof,3]," [s]"];
    Print["Speed at impact:         ",N[upf,3]," [m/s]"];
    Print["Particle size at impact: ",N[dpf*10^6,4]," [um]"];
    Print["Temperature at impact:   ",N[tp,5]," [K]"] ];
  ];
```

■ Number of particles in a given mass

The number of particles (of all sizes) entering the plasma per second can be determined as follows: the mass flow rate = Sum(total no. of particles/sec x fraction of particle population of size dpi x volume of particle x particle density). The fraction of the particle population of size dpi is the probability density function (PDF) evaluated at dpi x delta-dp. This equation can be solved for the number of particles, which becomes a function of the mass flow rate.

Define a Gaussian particle size distribution:

```
pdfdp=.
pdfdp[dia_] := Exp[-0.5((dia-dp)/dpsd)^2]/(Sqrt[2*N[Pi,6]]*dpsd);
```

Number of particles

```
np=.
np[mass_] := mass/NIntegrate[pdfdp[x]*N[Pi,6]/6*x^3*
             rhops,{x,0,0.01}]/60.0; (* gives the no. of
                 particles's being processed per second for
                 a given powder flow rate ('mass'),
                 which is entered in g/min *)
```

■ Power consumption per particle by heat absorption during flight

The rate at which energy is transferred to a powder particle of a given size = (the energy required to raise the temperature to the final particle temperature + the energy required to melt + any energy required to vaporize)/the time of flight.

```
qp=.
qp[dia_,tpl_] := Module[{},
  pvel[dia,tpl];
  ptemp[dia,tpl];
  qpheat = cpps*rhops*N[Pi,6]/6*dia^3*tp; (*[J].....
                          .........energy to raise temp *)
  qpm = lfrac*hm*rhops*N[Pi,6]/6*dia^3;  (*[J].....
                          .........energy to melt *)
  qpv = N[Pi,6]/6*(dia^3-dpf^3)*hv*rhops;(*[J].....
```

```
                              .........energy to vaporize *)
  (*Print[N[dia*10^6,3],"      ",*)
 (qpheat + qpm + qpv)/tof (* [J/s] or [W].........
                              .........power consumption *)
];
```

■ Total particle power consumption

With the power consumption for a particle of arbitrary size given by 'qp', the total power consumption by all particles in the particle size distribution can be determined by discretizing the distribution into bins (each represented by the midpoint or average particle size) and summing the power consumption calculated for each average particle size.

```
Clear[qloss];

qloss[mdot_,tplasma_,prnt_:False] := Module[{mdpts,pwr},
  nbins = 20; (* number of bins in pdf discretization *)
  dpl = x /. First[FindRoot[pdfdp[x] == 0.01,{x,0.01*dp,0.9*dp}]];
  If[dpl < 0, dpl = 0];
  dpu = x /. First[FindRoot[pdfdp[x] == 0.01,{x,1.1*dp,2*dp}]];
  deldp = (dpu - dpl)/nbins;
  mdpts = Table[dpl+deldp/2.0+(i-1)*deldp,{i,nbins}]; (* bin midpoints *
  numpart = np[mdot];
  pwr = Sum[numpart*pdfdp[mdpts[[i]]]*deldp*qp[mdpts[[i]],tplasma],{i,nb
  If[prnt == True,
    Print["Power consumption due to particle processing: ",
      N[pwr/10^3,4]," [kW]"] ];
  pwr
  ];
```

■ Plasma-particle interaction

The powder particles absorb heat, cooling the plasma. This routine determines the equilibrium temperature of the plasma for a given mass flux and RF power. Powder mass flow rate entered in [g/min], RF power entered in [kW].

```
rfeff = 0.5; (*.............RF coupling efficiency *)

Clear[ppi];

ppi[mrate_,rfpwr_] := Module[{t},
  t = 10^4; (* Unloaded plasma temperature *)
  xfr /. First[FindRoot[qloss[mrate,xfr] ==
    rfeff*rfpwr*10^3,{xfr,{2000,2100},tamb,t}]]
  ];
```

■ Deposition and melting efficiency

Determines the fraction of powder mass vaporized in flight. The remainder, normalized by the input mass flow rate is the deposition eficiency. Also determines the melt ratio: the fraction of deposited material which is molten on impact.

```
nbins = 20;
impact = Table[i*j*0.0, {i,nbins},{j,4}]; (* Array for
                storing particle conditions at impact *)
Clear[depchar];
```

```
depchar[mdot_,eqtemp_] := Module[(*

  Discretizes the particle size distribution into n
  bins. Determines particle velocity, temperature,
  diameter and solid fraction at impact. Uses final
  particle size and solid fraction to calculate the
  deposition and melting efficiency. Uses the fiber-
  shock routine to determine the fraction of droplets
  impacting which cause thermal shock damage to the
  fibers. *)

  {nbins = 20,
  dpl,dpu, (*[m].............particle size limits *)
  vpf, (*[m^3]...............particle volume at impact *)
  mpf, (*[g].................particle mass at impact *)
  mtotal = 0, ltotal = 0, ntotal = 0,
  numpart, (* ................No. of particles of size
              dpi (= mdpts[[i]]) impacting per second *)
  numshockpart = 0.0 (* number of particles causing thermal shock *)
  },
  dpl = x /. First[FindRoot[pdfdp[x] == 0.01,{x,0.01*dp,0.9*dp}]];
  If[dpl < 0, dpl = 0];
  dpu = x /. First[FindRoot[pdfdp[x] == 0.01,{x,1.1*dp,2*dp}]];
  deldp = (dpu - dpl)/nbins;
  mdpts = Table[dpl+deldp/2.0+(i-1)*deldp,{i,nbins}]; (* bin midpoints *
  Do[pvel[mdpts[[i]],eqtemp];
     ptemp[mdpts[[i]],eqtemp];
     fibershock[tp]; (* determine if thermal shock damage
            occurs upon impact with the fiber substrate *)
     impact[[i]] = {upf,tp,dpf,1-lfrac}; (* Store ith particle
       velocity, temperature, diameter and fraction of solid *)
     Print[i,"  ",N[upf,3],"  ",N[tp,5],"  ",
       N[mdpts[[i]]*10^6,3],"  ",N[dpf*10^6,3],"  ",
       N[lfrac,3],"  ",thermalshock];
     vpf = N[Pi,6]/6*dpf^3;
     mpf = rhops*vpf;
     numpart = np[mdot]*pdfdp[mdpts[[i]]]*deldp;
     numshockpart = numshockpart + numpart*thermalshock; (*
       Total number of particles causing thermal shock damage *)
     ntotal = ntotal + numpart; (* Total no. of particles per sec *)
     mtotal = mtotal + numpart*mpf; (* Total mass deposited per sec *)
     ltotal = ltotal + numpart*mpf*lfrac;(* Total melted mass per sec *)
     ,{i,nbins}];
  shockdamage = numshockpart/ntotal; (* fraction of particles
          deposited causing thermal shock damage to fibers *)
  depeff = mtotal/(mdot/60.0); (* Deposition efficiency *)
  mue = depeff; (* Materials use efficiency *)
  deprate = powderrate/(60.0)*mue; (*[g/s].....
                           actual mass deposition rate *)
  depliq = ltotal/(depeff*mdot/60.0);  (* Melting ratio *)
```

```
];
General::spell1: Possible spelling error: new symbol name "ltotal"
    is similar to existing symbol "mtotal".
General::spell: Possible spelling error: new symbol name "ntotal"
    is similar to existing symbols {ltotal, mtotal}.
```

Creates a bar chart showing particle temperature at impact vs particle size

```
GeneralizedBarChart[Transpose[{mdpts*10^6,Transpose[impact][[2]],
  Table[deldp*10^6,{i,nbins}]}], PlotRange -> {0,3000} ]
Transpose::nmtx: The first two levels of the one dimensional list {1000000 mdpts, <<2>>
    cannot be transposed.
```

Particle temperature at impact vs particle size (90 +/- 15 um, Teq = 2800)

■ Plasma Spray Deposition

■ Effective normalized splat diameter

Determines an effective normalized splat size by taking a weighted sum of the normalized splat sizes for each discrete particle in the size distribution.

Note: Requires generation of the array, (impact), using routine, "depchar".

```
splatstats = Table[i*j*0.0, {i,nbins},{j,4}]; (* Array for
               storing particle splat parameters *)

effsplat=.

effsplat[massdot_] := Module[
  {vel,temp,size,mfrac,splatrat,numpart},
  wtdsplat = 0.0;           (* weighted sum of splat sizes *)
  Do[vel = impact[[i,1]];   (* impact velocity of particle i *)
    temp = impact[[i,2]];   (* temperature at impact *)
    size = impact[[i,3]];   (* particle size at impact *)
    mfrac = impact[[i,4]]; (* solid fraction at impact *)
    vpf = N[Pi,6]/6*size^3;
    mpf = rhops*vpf;        (* particle mass at impact*)
    numpart = np[massdot]*pdfdp[mdpts[[i]]]*deldp;
                    (* no. frac. of part's of size dpi *)
    massfrac = numpart*mpf/(depeff*massdot/60.0);
         (* fraction of deposited mass due to particles of size dpi *)
    splatrat = Which[temp < tm || mfrac >= 0.4, 1.0, (* no spreading if
      size < 20.0*10^-6, 1.0, (* very small droplets freeze instantly *)
      size < 40.0*10^-6 && vel < 8.0, 1.0, (* small, slow droplets *)
      size < 0.01*mdpts[[i]], 0.0, (* no splat if fully vaporized *)
      True, splat[vel,temp,size,mfrac]];
                                        (* else call splat routine *)
    wtdsplat = wtdsplat + massfrac*splatrat;
    splatstats[[i]] = {numpart,massfrac,splatrat,massfrac*splatrat};
    Print[wtdsplat],
    {i,nbins}];
  Print["Weighted normalized splat diameter: ",N[wtdsplat,4]]
  ];
General::spell1: Possible spelling error: new symbol name "size"
    is similar to existing symbol "psize".
General::spell1: Possible spelling error: new symbol name "mfrac"
    is similar to existing symbol "lfrac".
```

splatstats//MatrixForm

Creates a bar chart of number fraction of particles vs particle size

```
GeneralizedBarChart[Transpose[{mdpts*10^6,Transpose[splatstats][[1]],
  Table[deldp*10^6,{i,nbins}]}], PlotRange -> {0,40000} ]
Transpose::nmtx: The first two levels of the one dimensional list {1000000 mdpts, <<2>>
    cannot be transposed.
```

Number fraction of part's vs particle size (90 +/- 15 um)

Creates a bar chart of mass fraction of particles vs particle size

```
GeneralizedBarChart[Transpose[{mdpts*10^6,Transpose[splatstats][[2]],
  Table[deldp*10^6,{i,nbins}]}], PlotRange -> {0,0.3} ]
Transpose::nmtx: The first two levels of the one dimensional list {1000000 mdpts, <<2>>
    cannot be transposed.
```

Mass fraction vs particle size (130 +/- 45 um) (Teq = 3000)

Creates a bar chart of splat diameter vs particle size

```
GeneralizedBarChart[Transpose[{mdpts*10^6,Transpose[splatstats][[3]],
  Table[deldp*10^6,{i,nbins}]}], PlotRange -> {0.0,2} ]
```

```
Transpose::nmtx: The first two levels of the one dimensional list {1000000 mdpts, <<2>>
    cannot be transposed.
```

Normalized splat diameter vs particle size (130 +/- 45 um) (Teq = 3000)

■ Droplet Impact Model

```
c1 = 0.5; (* ............sphere-to-cylinder constant *)
tsub = 1000.0; (*[K].....substrate temperature *)
General::spell1: Possible spelling error: new symbol name "tsub"
     is similar to existing symbol "Stub".
```

Parameter kappa in the Madejski-model

```
ckap=.
ckap[cf_,pvelc_,pdia_] := 6*c1^2*cf*(rhops/rhopl)*
  Sqrt[c1/pe[pvelc,pdia]];
```

Dimensionless temperatures

```
t0[substratetemp_] := kps*(tm-substratetemp)/(as*rhops*hof);
tpn[liquidtemp_] := kps*(liquidtemp-tm)/(as*rhops*hof);
```

Freezing constant

```
Clear[freeze];
freeze[tpl_] := x /. First[FindRoot[x - 2/Sqrt[Pi]*
  (t0[tsub]/(Erf[x/2]*Exp[x^2/4]) -
  (tpn[tpl]*Sqrt[(kpl*cppl*rhopl)/(kps*cpps*rhops)]/
  Erfc[x/2*Sqrt[as/al]]*Exp[-x^2*as/(4*al)])) == 0,{x,0.01,2.0}]];
```

Dimensionless thickness of liquid layer

```
Clear[phi];
phi[zfcn_,pfcn_,time_,tp1_,vp_,dp_,mfrac_] := 1/(6*c1^2*zfcn^2)*
  (1 - mfrac - ckap[freeze[tp1],vp,dp]*(Sqrt[time] +
  2*NIntegrate[zfcn*pfcn*Sqrt[time-x],{x,0,time}]));
```

Dimensionless splat diameter

```
splat=.
```

```
splat[vel_,tem_,dia_,fsm_:0.0] := Module[{cnt = 1,
  results,tstopnorm},
  Off[NIntegrate::precw]; Off[NIntegrate::nlim];
  tstopnorm = cnt;
  Print[tstopnorm];
  etasol = NDSolve[{p'[t] == 1/(z[t]^2*p[t])*
  (3/(2*phi[z[t],p[t],t,tem,vel,dia,fsm]*c1)*
  (-2/we[vel,dia]*(z[t]*p[t]+phi[z[t],p[t],t,tem,vel,dia,fsm]*p[t]) -
  1/(phi[z[t],p[t],t,tem,vel,dia,fsm]*re[vel,dia,mup,rhopl])*z[t]^2*p[t]
  z[t]*p[t]^3),
  z'[t] == p[t],
  z[0] == 1, p[0] == Sqrt[(3/2)/(1+1/(30c1^6))]},
  {z,p},{t,0,tstopnorm}];
  cnt++;
  While[First[Evaluate[p[tstopnorm] /. etasol]] > 0,
    tstopnorm = cnt; (* *10^-6*vel/(dia/2.0);*) (* convert to dim'nless
    Print[tstopnorm];
    etasol = NDSolve[{p'[t] == 1/(z[t]^2*p[t])*
    (3/(2*phi[z[t],p[t],t,tem,vel,dia,fsm]*c1)*
    (-2/we[vel,dia]*(z[t]*p[t]+phi[z[t],p[t],t,tem,vel,dia,fsm]*p[t]) -
    1/(phi[z[t],p[t],t,tem,vel,dia,fsm]*re[vel,dia,mup,rhopl])*z[t]^2*p[
    z[t]*p[t]^3),
    z'[t] == p[t],
    z[0] == 1, p[0] == Sqrt[(3/2)/(1+1/(30c1^6))]},
    {z,p},{t,0,tstopnorm}];
    cnt++
    ];
  results = FindMinimum[First[
      10 - Evaluate[z[x] /. etasol]],{x,0,0,tstopnorm}];
  zeta = 10. - First[results];
  dsplat = zeta*dia; (* splat size in [m] *)
  tsplat = (x /. Part[results[[2]]])*(dia/2)/vel; (* time to freeze in [
  If[diagnostics,
    Print["SINGLE DROPLET IMPACT RESULTS"];
    Print["At impact: dia. = ",N[dia*10^6,4]," [um]   vel. = ",
    N[vel,3]," [m/s]   frac. sol. = ",N[fsm,2]];
    Print["Normalized splat diameter: ",N[zeta,3]];
    Print["Splat diameter:            ",N[dsplat*10^6,4]," [um]"];
    Print["Time to freeze:            ",N[tsplat*10^6,4]," [us]"];
    Print["Dim'nless time:            ",N[tsplat*vel/(dia/2),3]] ];
  On[NIntegrate::precw]; On[NIntegrate::nlim];
  zeta
  ];
General::spell: Possible spelling error: new symbol name "zeta"
    is similar to existing symbols {eta, Zeta}.
General::spell1: Possible spelling error: new symbol name "dsplat"
    is similar to existing symbol "splat".
General::spell: Possible spelling error: new symbol name "tsplat"
    is similar to existing symbols {dsplat, splat}.
fibershock =.
```

```
fibershock[tdroplet_] := Module[(* Determines if the
    temperature difference between an incoming droplet
    and the fiber is great enough to cause thermal
    shock damage to the fiber or coating. Returns a
    value of 1 is damage occurred, 0 if not. *)

  {deltemp, (*[C].....temperature difference between
                      fiber and droplet *)
  strength, (*[Pa].....tensile strength of fiber as
             determined using a Monte Carlo estimate *)
  heatxfercoeff = 215000.0, (*[W/m^2-K].....
                     heat transfer coefficient ???value???*)
  biotshock, (*.....Biot number for thermal contact *)
  logb, (*.....base 10 logarithm of Biot *)
  sshock, (*.....dim'nless stress *)
  shocklimit (*[C].....temperature difference needed
                  to cause thermal shock damage *)
  },
  deltemp = tdroplet - tfiber; (* tfiber = substrate
                   temperature, a global variable *)
  biotshock = heatxfercoeff*(fiberdiameter/2.0)/kfiber;
  strength = refstrength*(-Log[1-x])^(1/weibullmod) /. x -> Random[];
  logb = Log[10,biotshock];
  If[deltemp >= 0.0, (* Hot Shock *)
    sshock = 0.31 + 0.129*(logb -
      Sqrt[logb^2 - 2.5*logb + 1.7]),
    (* else Cold Shock *)
    sshock = 0.58 + 0.163*(logb -
      Sqrt[logb^2 - 5.2*logb + 6.9])];
  shocklimit = strength*(1.0 - nufiber)/
    (sshock*biotshock*ctefiber*emodfiber);
  If[deltemp > shocklimit && shocklimit > 0.0,
    thermalshock = 1,
    thermalshock = 0];
  (*Print["deltemp: ",deltemp];
  Print["strength: ",strength];
  Print["sshock: ",sshock];
  Print["shocklimit: ",shocklimit];
  Print["thermalshock: ",thermalshock];*)
  ];
General::spell1: Possible spelling error: new symbol name "tfiber"
    is similar to existing symbol "kfiber".
reaction[rztime_,rztemp_] := Module[(* Calculates the
    interfacial reaction zone thickness (RZT)using
    experimentally determined reaction kinetics. Input
    to the RZT model is time and temperature: time is
    determined using the routine 'runduration' and the
    temperature is the user-input preheat temperature.
    The interfacial quality is calculated as a number
```

```
    between 0 and 1: it equals 1 if RZT < allowable
    and degrades to 0 as RZT grows beyond allowable. *)

  {rztratio, (* dimensionless ratio of actual reaction
                      zone thickness to allowable RZT *)
  degradationrange = 1.0 (* range of rztratio over which
            the interfacial quality goes from 1 to 0 *)
  },
  rztrateconstant = kappa0*Exp[-rztactenergy/
                               (2rgas*(rztemp+273.15))];
  rzt = rztrateconstant*Sqrt[rztime];
  rztratio = rzt/allowablerzt;
  ifacequality = Which[rztratio <= 1.0, 1.0,
       rztratio >= 1.0 + degradationrange, 0.0,
       True, 1.0 - (rztratio - 1.0)/degradationrange];
  ];
tapequality =.
tapequality := Module[
  {w1 = 0.5, (*............weighting factor for importance
              of the relative density in determining tape
              quality *)
  w2 = 0.3, (*............weighting factor for thermal shock *)
  w3 = 0.2 (*.............weighting factor for inter-
                                    facial quality *)
  },

  matrixproperties;
  powdersize;
  fiberproperties;
  interfacialproperties;
  physicalconstants;
  designdata;
  fibermat;

  (*Print["Thinking (about how hot this plasma is getting) ..."];
  equiltemp = ppi[powderrate,torchpower]; (* Determine
                        plasma equilibrium temperature *)
  Print["Plasma equilibrium temperature: ",N[equiltemp,4]," [K]"];*)
  Print["Thinking (about how much RF juice we need) ..."];
  torchpower = qloss[powderrate,equiltemp]/10^3;
  Print["RF Power: ",N[torchpower/rfeff,4]," [kW]"];
  Print["Thinking (about how much powder's really gonna' reach the subst
  depchar[powderrate,equiltemp]; (* Determine deposition
    efficiency, molten mass fraction, deposition rate
              and fiber quality due to thermal shock *)
  effsplat[powderrate]; (* Calculates the weighted splat size *)
  depositreldensity = 0.3*wtdsplat + 0.5; (* estimate relative
        density of the deposit based on flow character of
        impacting droplets, as given by 'wtdsplat' *)
```

```
  runduration; (* calculate time of plasma spray run *)
  reaction[timeofspray, preheattemp]; (* calculate dimensionless reactio
                    thickness and interfacial quality *)
  actualquality = w1*depositreldensity +
    w2*(1 - shockdamage) + w3*ifacequality;
  ];
runduration =.
runduration := Module[(* Determines the duration of
    plasma spray run needed to give a specified volume
    fraction of fiber. The relative density of the
    deposit and the rate of deposition are known. *)
  {hf, (*[m].....effective fiber thickness *)
  hdeposit, (*[m].....effective matrix thickness *)
  ff = fibervolfracspec},
  hf = N[Pi,6]*fiberdiameter^2/(4fiberspacing); (* an effective
    fiber thickness assuming fiber volume is concentrated
    in a solid plate at the bottom of the tape *)
  hdeposit = hf/depositreldensity*((1.0 + ff)/ff);
  tapethickness = hdeposit + hf;
  timeofspray = (rhops*depositreldensity*areaofdeposit*
                          hdeposit)/deprate; (*[s]*)
  ];
```

Cost Model

■ Production Rate

```
prate := Module[(* Calculates the production rate of
    spray deposited monotape [kg/s] for a given fiber
    volume fraction (specified for the fully dense
    composite) and deposit relative density. *)
  {hf, (*[m].....effective fiber thickness *)
  hm, (*[m].....effctive matrix thickness *)
  hdeposit, (*[m].....effective deposit (matrix+void) thickness *)
  ff = fibervolfracspec (* specified fiber vol fraction *)
  },
  hf = N[Pi,6]*fiberdiameter^2/(4fiberspacing); (* an effective
    fiber thickness assuming fiber volume is concentrated
    in a solid plate at the bottom of the tape *)
  hdeposit = hf/depositreldensity*((1.0 - ff)/ff);
  hm = depositreldensity*hdeposit;
  arealrateofcoverage = deprate/(depositreldensity*rhops*hdeposit);
  fibercoatingrate = ff*arealrateofcoverage*(hm+hf)*rhof; (*
                          .....[g of fiber/s]*)
  productionrate = deprate + fibercoatingrate; (*[g/s]*)
  netproductionrate = productionrate*yield;
  ];
General::spell1: Possible spelling error: new symbol name "prate"
    is similar to existing symbol "mrate".
```

■

```
costdata =.

costdata := (
  costofpowder = 500.0 - 1.5*10^6*dp; (*[$/kg].....cost of low
    volume Ti-6Al-4V powder *)
  costoffiber = 1000.0; (*[$/kg].....cost of SiC fiber *)
  costofelec = 0.01; (* [$/kWh].....cost of electric power *)
  costofgas = 0.0055; (*[$/litre]....cost of Argon gas *)
  );

facilitycostdata := (
  costofchamber = 95000;
  costoftorch = 20000;
  costoffeeder = 15000;
  costofpumps = 10000;
  costofpowersupply = 80000;
  costofsensors = 7500;
  );
```

Cost Models

```
cm =.

cm := Module[(* Material costs [$/kg] *)
  {fibervolfrac = fibervolfracspec,
  powdervolfrac = 1.0 - fibervolfracspec},
  materialcost = costofpowder*powdervolfrac/mue +
    fibervolfrac*costoffiber;
  ];

ccon := Module[(* Consumables cost [$/kg] *)
  {gascostrate},
  gascostrate = (q1+q2+q3)*costofgas/60.0; (*[$/s]*)
  consumablescost = gascostrate/productionrate*10^3;
  ];

cc := ((* Capital cost [$] *)
  capitalcost = costofchamber + costoftorch +
    costoffeeder + costofpumps + costofpowersupply +
    costofsensors;
  );

ce := Module[(* Energy cost [$/kg] *)
  {hrtosec = 1/3600.0,
  rfpwr},
  rfpwr = torchpower/rfeff;
  powercost = rfpwr*costofelec*hrtosec; (*[$/s]*)
  energycost = powercost/productionrate*10^3;
  ];

tapecost[m_] := Module[(* Cost to produce plasma
    sprayed MMC monotape [$/kg] (unconsolidated) *)
  {},
  costdata;
  facilitycostdata;
  cm;
```

```
    ccon;
    cc;
    ce;
    costoftape = (materialcost + consumablescost +
      energycost) + capitalcost/m;
    ];
  costvol[amt_] := (materialcost + consumablescost +
      energycost) + capitalcost/amt; (* Calculates tape cost as
      a function of production volume *)
```

Quality-Cost: Plasma Spray Deposition

■ INPUT

```
  processvariable := Module[
    {preheattemp = meltptmandrel,
    preheatlimit = 0.8*meltptmandrel},
    q1 = Input["Enter carrier gas flow rate [litres/min]"];
    q2 = Input["Enter central gas flow rate [litres/min]"];
    q3 = Input["Enter sheath gas flow rate [litres/min]"];
    powderrate = Input["Enter particle mass flow rate [g/min]"];
    (*torchpower = Input["Enter RF power [kW]"];*)
    equiltemp = Input["Enter plasma equilibrium temperature [K]"];
    While[preheattemp > preheatlimit,
      preheattemp = Input["Enter mandrel preheat temperature [deg C]"];
      preheattemp = preheattemp + 273.15;
      If[preheattemp > preheatlimit,
        Print["Preheat temperature cannot exceed ",
          preheatlimit-273.15," C"] ];
    ];
    tfiber = preheattemp; (* fiber temperature used to
                  assess thermal shock during spraying *)
    fibervolfracspec = Input["Enter target fiber volume fraction"];
    ];
  defaultinput =.
  defaultinput := (
    q1 = 10.0; q2 = 5.0; q3 = 35.0; (*[slpm]*)
    powderrate = 20.0; (*[g/min]*)
    (*torchpower = 20.0;*)
    equiltemp = 2850.0; (*[K]*)
    preheattemp = 1200.0; (*[C]*)
    tfiber = preheattemp;
    fibervolfracspec = 0.4;
    );
```

■ Quality-Cost Model

```
  plasmasprayqcm =.
  plasmasprayqcm[req1_,req2_] := Module[{
    },
    diagnostics = False; (* Prints intermediate results during simulation
```

```
    acceptablequality = req1; (* Must be between 0 and 1; sets
                        the cutoff used to determine the yield *)
    prodvol = req2; (* required production volume *)
    mandrelproperties;
    (*defaultinput;*)
    processvariable; (* Enter process variables *)
    tapequality;
    yield = If[actualquality < acceptablequality, 0.0, 1.0];
    prate;
    tapecost[prodvol];
    printinput;
    printreport;
    results = {q1,q2,q3,powderrate,torchpower/rfeff,equiltemp,preheattemp,
    results >> psqcm; (* export results to file *)
    ];
```

■ OUTPUT

```
printinput =.
```

```
printinput := (
  Print[""];
  Print["INPUT DATA"];
  Print["    Cumulative production volume [kg]: ",prodvol];
  Print["    Acceptable quality (0 - 1): ",acceptablequality];
  Print[""];
  Print["EQUIPMENT DESIGN PARAMETERS"];
  Print["  Torch"];
  Print["    Radius of injection probe orifice [mm]: ",r1*10^3];
  Print["    Torch internal radius [mm]: ",r0*10^3];
  Print["  Spray distance [cm]: ",ls*10^2];
  Print["  Mandrel"];
  Print["    Length [cm]: ",lmandrel*10^2];
  Print["    Diameter [cm]: ",dmandrel*10^2];
  Print["    Deposit area [cm^2]: ",areaofdeposit*10^4];
  Print[""];
  Print["PROCESS SCHEDULE"];
  Print["  Process variable settings"];
  Print["    Carrier gas flow rate [slpm]: ",N[q1,3]];
  Print["    Central gas flow rate [slpm]: ",N[q2,3]];
  Print["    Sheath gas flow rate [slpm]:  ",N[q3,3]];
  Print["    Powder mass flow rate [g/min]: ",N[powderrate,3]];
  Print["    RF power [kW]: ",N[torchpower/rfeff,3]];
  Print["    Mandrel preheat temperature [C]: ",preheattemp];
  Print["  Powder/Fiber Data"];
  Print["    Mean particle size [um]: ",N[dp*10^6,4]];
  Print["    Particle size std. dev. [um]: ",N[dpsd*10^6,4]];
  Print["    Fiber diameter [um]: ",N[fiberdiameter*10^6,4]];
  Print["    Fiber spacing [s/d]: ",N[fiberspacing/fiberdiameter,3]];
  Print["    Fiber gap [um]: ",N[fibergap*10^6,4]];
  Print["    Specified fiber volume fraction: ",fibervolfracspec];
  Print[""]; (* newline *)
  );

printreport =.
printreport := (
  Print["QUALITY-COST"];
  Print["  Quality: ",N[actualquality,3]];
  Print["  Yield: ",yield];
  Print["  Material use efficiency: ",N[mue,3]];
  Print["  Cost of tape [$/kg]: ",costoftape];
  Print[""];
  Print["COST ELEMENTS"];
  Print["  Material cost [$/kg]: ",materialcost];
  Print["  Consumables cost [$/kg]: ",consumablescost];
  Print["  Energy cost [$/kg]: ",energycost];
  Print["  Capital cost [$/kg]: ",capitalcost/prodvol];
  Print[""];
  Print["PRODUCTION RATE"];
```

```
    Print["  Deposition time [min]: ",N[timeofspray/60.0,3]];
    Print["  Matrix deposition rate [kg/hr]: ",N[deprate*3.6,3]];
    Print["  Production rate [kg/hr]: ",N[productionrate*3.6,3]];
    Print["  Net production rate [kg/hr]: ",N[netproductionrate*3.6,3]];
    Print[""];
    Print["PLASMA SPRAY QUALITY PARAMETERS"];
    Print["  Interface"];
    Print["    Reaction zone thickness [um]: ",N[rzt*10^6,4]];
    Print["    Interface quality: ",ifacequality];
    Print["  Deposit"];
    Print["    Tape thickness [mm]: ",N[tapethickness*10^3,4]];
    Print["    Relative density: ",N[depositreldensity,3]];
    Print["    Melt fraction on impact: ",N[depliq,3]];
    Print["  Fiber"];
    Print["    Thermal shock damage: ",shockdamage]; (* fraction of partic
      deposited causing thermal shock damage to fibers *)

);
```

plasmasprayqcm[0.5,1000.0]

```
Thinking (about how much RF juice we need) ...
RF Power: 26.18 [kW]
Thinking (about how much powder's really gonna' reach the substrate) ...
1  2.13  2500.  9.12  0.  0.  0
2  2.42  2500.  27.4  0.  0.  0
3  8.34  2500.  45.6  0.  0.  0
4  12.1  2500.  63.8  9.6  1.  0
5  14.  2500.  82.1  21.6  1.  0
6  15.3  2500.  100.  68.5  1.  0
7  16.  2263.6  119.  119.  1.  0
8  16.5  1964.8  137.  137.  1.  0
9  16.9  1800.  155.  155.  0.698  0
10  17.2  1800.  173.  173.  0.149  0
11  17.4  1695.9  192.  192.  0.  0
12  17.5  1556.2  210.  210.  0.  0
13  17.6  1434.7  228.  228.  0.  0
14  17.7  1329.  246.  246.  0.  0
15  17.8  1237.  265.  265.  0.  0
16  17.9  1156.6  283.  283.  0.  0
17  18.  1086.1  301.  301.  0.  0
18  18.  1024.  319.  319.  0.  0
19  18.1  969.02  337.  337.  0.  0
20  18.1  920.23  356.  356.  0.  0
0.
0.
0.
          -7
1.15257 10
1
         -6
7.6637 10
1
2
0.00113518
1
2
3
0.0204198
1
2
3
0.0877291
1
2
3
0.242758
0.406739
0.620298
0.826543
0.974927
1.05473
1.08691
1.09666
1.09888
1.09926
1.09931
1.09931
Weighted normalized splat diameter: 1.099

INPUT DATA
    Cumulative production volume [kg]: 1000.
    Acceptable quality (0 - 1): 0.5
```

```
EQUIPMENT DESIGN PARAMETERS
  Torch
    Radius of injection probe orifice [mm]: 1.7
    Torch internal radius [mm]: 35.
  Spray distance [cm]: 40.
  Mandrel
    Length [cm]: 25.
    Diameter [cm]: 20.
    Deposit area [cm^2]: 1570.8

PROCESS SCHEDULE
  Process variable settings
    Carrier gas flow rate [slpm]: 10.
    Central gas flow rate [slpm]: 5.
    Sheath gas flow rate [slpm]:  35.
    Powder mass flow rate [g/min]: 20.
    RF power [kW]: 26.2
    Mandrel preheat temperature [C]: 1200.
  Powder/Fiber Data
    Mean particle size [um]: 180.
    Particle size std. dev. [um]: 35.
    Fiber diameter [um]: 142.
    Fiber spacing [s/d]: 2.5
    Fiber gap [um]: 213.
    Specified fiber volume fraction: 0.4

QUALITY-COST
  Quality: 0.757
  Yield: 1.
  Material use efficiency: 0.998
  Cost of tape [$/kg]: 774.653

COST ELEMENTS
  Material cost [$/kg]: 538.282
  Consumables cost [$/kg]: 8.73259
  Energy cost [$/kg]: 0.13858
  Capital cost [$/kg]: 227.5

PRODUCTION RATE
  Deposition time [min]: 5.53
  Matrix deposition rate [kg/hr]: 1.2
  Production rate [kg/hr]: 1.89
  Net production rate [kg/hr]: 1.89

PLASMA SPRAY QUALITY PARAMETERS
  Interface
    Reaction zone thickness [um]: 1.788
    Interface quality: 0.212462
  Deposit
    Tape thickness [mm]: 0.2328
    Relative density: 0.83
    Melt fraction on impact: 0.14
  Fiber
    Thermal shock damage: 0.
FindRoot::regex: Reached the point {0.0320385} which is outside the region
    {{0.0103295, 0.0269254}}.
FindRoot::regex: Reached the point {0.0286297} which is outside the region
    {{0.0159932, 0.0249349}}.
FindRoot::regex: Reached the point {0.0254293} which is outside the region
    {{0.0225992, 0.0239061}}.
General::stop: Further output of FindRoot::regex will be suppressed during this calcul
OpenWrite::noopen: Can't open psqcm.
```

APPENDIX B Plasma Spray QCM Experiments

Exper. No.	Carrier gas flow [slpm]	Central gas flow [slpm]	Sheath gas flow [slpm]	Powder flow rate [g/min]	Torch power [kW]	Equil Plasma Temp [C]	Preheat Temp [C]
1	10	5	35	20	41.89987	2700	800
2	10	5	35	20	41.89987	2700	1000
3	10	5	35	20	51.8331	2750	1000
4	10	5	35	20	54.123	2800	1000
5	10	5	35	20	55.3675	2850	1000
6	10	5	35	20	66.4721	2900	1000
7	10	5	35	20	72.761	2950	1000
8	10	5	35	20	75.0636	3000	1000
9	10	5	35	20	76.4002	3050	1000
10	10	5	35	20	97.5989	3150	1000
11	10	5	35	25	52.3748	2700	200
12	10	5	35	30	62.8498	2700	200
13	10	5	35	35	73.3248	2700	200
14	10	5	35	20	36.0705	2700	200
15	10	5	35	20	29.224	2700	200
16	10	5	35	20	35.9702	2700	800
17	10	5	35	20	24.3274	2700	800
18	10	5	35	20	24.3274	2700	1200
19	10	5	35	20	26.1844	2850	1200

Exper. No.	Mean Powder Size [um]	Std Dev [um]	Fiber Dia [um]	Fiber Spacing	Fiber vol fraction	Actual Quality	Cost Ratio	Yield
1	100	35	142	2.5	0.4	0.959474	1.412228	1
2	100	35	142	2.5	0.4	0.959474	1.412228	1
3	100	35	142	2.5	0.4	0.974549	1.442103	1
4	100	35	142	2.5	0.4	0.976813	1.44771	1
5	100	35	142	2.5	0.4	0.978877	1.449569	1
6	100	35	142	2.5	0.4	0.990071	1.489805	1
7	100	35	142	2.5	0.4	0.992139	1.515008	1
8	100	35	142	2.5	0.4	0.994231	1.522995	1
9	100	35	142	2.5	0.4	0.995997	1.526454	1
10	100	35	142	2.5	0.4	1.0057	1.647738	1
11	100	35	142	2.5	0.4	0.772284	1.409175	1
12	100	35	142	2.5	0.4	0.727181	1.407139	1
13	100	35	142	2.5	0.4	0.854874	1.405685	1
14	100	55	142	2.5	0.4	0.728798	1.407875	1
15	100	75	142	2.5	0.4	0.79164	1.398664	1
16	120	35	142	2.5	0.4	0.954533	1.370141	1
17	180	35	142	2.5	0.4	0.90555	1.439398	1
18	180	35	142	2.5	0.4	0.748342	1.439398	1
19	180	35	142	2.5	0.4	0.757389	1.439875	1

Exper. No.	MUE	Tape Cost [$/kg]	Mat'l Cost [$/kg]	Consumables Cost [$/kg]	Energy Cost [$/kg]	Capital Cost [$]	Spray Time [min]	Dep Rate [g/min]
1	0.935787	861.4593	624.41	9.312791	0.236488	227500	5.897007	1.122944
2	0.935787	861.4593	624.41	9.312791	0.236488	227500	5.897007	1.122944
3	0.86837	879.683	641.832	10.0358	0.315264	227500	6.35483	1.04204
4	0.8568	883.103	645.098	10.1713	0.333638	227500	6.44064	1.02816
5	0.853042	884.237	646.178	10.2161	0.342813	227500	6.46901	1.02365
6	0.778814	908.781	669.641	11.1898	0.450795	227500	7.08557	0.934577
7	0.738566	924.155	684.335	11.7996	0.520334	227500	7.47169	0.88628
8	0.726673	929.027	688.988	11.9927	0.545586	227500	7.59398	0.872008
9	0.721645	931.137	691.002	12.0763	0.55917	227500	7.6469	0.865973
10	0.580553	1005.12	761.724	15.0112	0.887925	227500	9.50532	0.696663
11	0.935787	859.597	624.41	7.45023	0.236488	227500	4.71761	1.40368
12	0.935787	858.355	624.41	6.20853	0.236488	227500	3.93134	1.68442
13	0.935787	857.468	624.41	5.32159	0.236488	227500	3.36972	1.96515
14	0.946395	858.804	621.895	9.20841	0.201304	227500	5.83091	1.13567
15	0.969801	853.185	616.539	8.98616	0.159158	227500	5.69018	1.16376
16	0.964561	835.786	599.054	9.03498	0.196964	227500	5.72109	1.15747
17	0.999638	774.396	538.05	8.71795	0.128536	227500	5.52034	1.19957
18	0.999638	774.396	538.05	8.71795	0.128536	227500	5.52034	1.19957
19	0.997962	774.653	538.282	8.73259	0.13858	227500	5.52961	1.19755

Exper. No.	Prod Rate [g/min]	RZT [um]	Interface Quality	Tape thickness [mm]	Relative Density	Melt Fraction	Shock
1	1.771757	0.036989	1	0.214519	0.918948	0.714774	0
2	1.771757	0.036989	1	0.214519	0.918948	0.714774	0
3	1.64411	0.368777	1	0.209122	0.949099	0.72995	0
4	1.62221	0.371259	1	0.208341	0.953626	0.765597	0
5	1.61509	0.372075	1	0.207635	0.957754	0.812543	0
6	1.47455	0.389403	1	0.203911	0.980142	0.820739	0
7	1.39835	0.399872	1	0.203242	0.984277	0.838182	0
8	1.37583	0.403131	1	0.20257	0.988461	0.866063	0
9	1.36631	0.404534	1	0.202008	0.991993	0.897275	0
10	1.09918	0.45102	1	0.198987	1.01141	0.907778	0
11	2.2147	3.88E-10	1	0.214519	0.918948	0.714774	0.623965
12	2.65764	3.54E-10	1	0.214519	0.918948	0.714774	0.77431
13	3.10057	3.28E-10	1	0.214519	0.918948	0.714774	0.348666
14	1.79184	4.31E-10	1	0.224081	0.86999	0.386895	0.687323
15	1.83616	4.26E-10	1	0.233108	0.828326	0.203531	0.40841
16	1.82624	0.036433	1	0.216366	0.909067	0.526742	0
17	1.89265	0.035788	1	0.237111	0.811099	0.080311	0
18	1.89265	1.78604	0.213961	0.237111	0.811099	0.080311	0
19	1.88947	1.78754	0.212462	0.232774	0.829794	0.13987	0

APPENDIX C

■ **QCM (D.M.Elzey, University of Virginia, 1996)**

Tape Casting Process

This program calculates the quality and cost of metal matrix composite monotape manufactured by the tape casting process. The overall structure of the program consists first, of models for determining the quality, followed by cost models and finally the quality-cost relation. The process is treated as a four-step sequence of slurry formulation, casting, drying and outgassing. The quality is determined by microstructural state variables: degree of slurry infiltration into the fiber mat, uniformity of solvent removal during drying, and cracking or rearrangement of constituents during outgassing. In addition, the model also estimates overall shrinkage and calculates the final tape thickness. Cost models estimate the cost of materials, consumables, energy and equipment investment per kg of finished tape. Finally, the program outputs a relative quality index (0-1) and cost of tape per kg, depending on material properties, processing schedule and equipment design parameters.

Quality Models

Model Data

```
slurrycomposition =.

slurrycomposition := ((* mass fractions of slurry components *)
                  powderfracs = 0.3;
                  binderfracs = 0.3;
                  solventfracs = 0.35;
                  plasticizerfracs = 0.02;
                  surfactantfracs = 0.01;
                  deflocculantfracs = 0.02;
  If[(powderfracs+binderfracs+solventfracs+plasticizerfracs+
    surfactantfracs+deflocculantfracs) != 1.0,
    Print["Warning: Slurry mass fractions do not sum to 1"]]);

bladedcomposition =.

bladedcomposition := Module[(* Recalculates the mass fractions
    of all components following casting (i.e. introduction
    of the fibers), but prior to drying. The subscript 'b',
    denotes "bladed" or as-cast. *)
  {pf = 1.0 + powderfracs/(1.0-powderfracs)},
  fibervolfracb = N[Pi,6]*fiberdiameter^2/
                  (4*fiberspacing*tapethicknessc);
  slurryvolfracb = 1. - fibervolfracb;
  powdervolfracs = slurrydensity*powderfracs/powderdensity;
  carrierdensity = (* density of slurry excluding powder *)
                  1/(solventfracs*pf/solventdensity +
                  binderfracs*pf/binderdensity +
                  plasticizerfracs*pf/plasticizerdensity +
                  surfactantfracs*pf/surfactantdensity +
                  deflocculantfracs*pf/deflocculantdensity);
  tapedensityb = fibervolfracb*fiberdensity +
       slurryvolfracb*slurrydensity;
  fiberfracb = fibervolfracb*fiberdensity/tapedensityb;
  slurryfracb = slurryvolfracb*slurrydensity/tapedensityb;
  powderfracb = powderfracs*slurryfracb; (* Note: powder,
    slurry, etc. are conserved from mixing to casting *)
  binderfracb = binderfracs*slurryfracb;
  solventfracb = solventfracs*slurryfracb;
  plasticizerfracb = plasticizerfracs*slurryfracb;
  surfactantfracb = surfactantfracs*slurryfracb;
  deflocculantfracb = deflocculantfracs*slurryfracb;
  If[(powderfracb+binderfracb+solventfracb+plasticizerfracb+
    surfactantfracb+deflocculantfracb+fiberfracb) != 1.0,
    Print["Warning: Bladed mass fractions do not sum to 1"]]
  ];

driedcomposition =.

driedcomposition := Module[(* Calculate composition following
    drying based on assumption that only solvent is
    removed during drying. The subscript 'g' denotes "green". *)
```

```
    {pf},
    driedmass = 1.0 - evapsolvent; (* evapsolvent = the mass
        of solvent lost by evaporation during drying per kg
        of as-bladed tape *)
    solventfracg = (solventfracb - evapsolvent)/driedmass;
    powderfracg = powderfracb/driedmass;
    fiberfracg = fiberfracb/driedmass;
    binderfracg = binderfracb/driedmass;
    plasticizerfracg = plasticizerfracb/driedmass;
    surfactantfracg = surfactantfracb/driedmass;
    deflocculantfracg = deflocculantfracb/driedmass;
    carrierfracg = (binderfracg+solventfracg+plasticizerfracg+
      surfactantfracg+deflocculantfracg);
    carrierdensityg = carrierfracg/(binderfracg/binderdensity +
                    solventfracg/solventdensity +
                    plasticizerfracg/plasticizerdensity +
                    surfactantfracg/surfactantdensity +
                    deflocculantfracg/deflocculantdensity);
    tapedensityg = 1/(carrierfracg/carrierdensityg +
                    powderfracg/powderdensity +
                    fiberfracg/fiberdensity);
    carriervolfracg = tapedensityg*carrierfracg/carrierdensityg;
    powdervolfracg = tapedensityg*powderfracg/powderdensity;
    fibervolfracg = tapedensityg*fiberfracg/fiberdensity;
    ];
outgassedcomposition =.
outgassedcomposition := ((* Knowing the fraction of
    carrier (i.e. all organics) removed during
    outgassing and the shrinkage strain, calculate final mass
    and volume fractions. Shrinkage is assumed to be plane
    strain, with no shrinkage in the fiber direction. *)
    carriervolfrac = residbinder*carriervolfracg/
      (1.0 - shrinkagestrain)^2;
    powdervolfrac = powdervolfracg/(1.0 - shrinkagestrain)^2;
    fibervolfrac = fibervolfracg/(1.0 - shrinkagestrain)^2;
    voidvolfrac = 1.0 - (carriervolfrac+powdervolfrac+fibervolfrac);
    If[voidvolfrac < 0.0,
      Print["Warning: void fraction after outgassing less than zero."]];
    tapereldensity = 1.0 - voidvolfrac;
    tapedensity = carriervolfrac*carrierdensityg +
      powdervolfrac*powderdensity + fibervolfrac*fiberdensity;
    carrierfracf = carrierdensityg*carriervolfrac/tapedensity;
    powderfracf = powderdensity*powdervolfrac/tapedensity;
    fiberfracf = fiberdensity*fibervolfrac/tapedensity;
    );

fibermat =.
fibermat := ((* design parameters for fiber mat *)
```

```
            fiberdiameter = 142.0*10^-6;
            fiberspacing = 2.0*fiberdiameter;
            fibergap = fiberspacing - fiberdiameter; );
powdersizedist =.
powdersizedist := ((* parameters characterizing powder size
    distribution *)
  dp = 300.0*10^-6; (*[m].....mean powder particle size *)
  dpsd = 75.0*10^-6; (*[m].....std deviation in particle size *)
  );
physicaldata =.
physicaldata := ((* Densities are entered in [g/cm^3] and
     are converted to [kg/m^3] using a conversion factor of 10^3 *)
  solventdensity = 4.3 *10^3;
  binderdensity = 3.6 *10^3;
  plasticizerdensity = 3.5 *10^3;
  surfactantdensity = 3.4 *10^3;
  deflocculantdensity = 3.0 *10^3;
  powderdensity = 4.6 *10^3;
  fiberdensity = 2.8 *10^3;
  molwtair = 28.97; (* molecular wt of dry air *)
  pcair = 36.4; (*[atm]...critical pressure air *)
  tcair = 132.0; (*[K]....critical temp air *)
  molwtsol = 28.05; (* molecular wt of solvent *)
  pcsol = 50.0; (*[atm]...critical pressure solvent *)
  tcsol = 282.4; (*[K]....critical temp solvent *)
  diffsolintape = 4.*10^-7; (*[m^2/s]...
                  diffusivity of solvent in tape *)
  (* Binder Thermolyis Parameters *)
  k0 = 6.0*10^0; (*[1/s]..........preexp constant:
                        binder vaporization kinetics *)
  q = 60.0*10^3; (*[J/mol].......activation energy:
                        binder vaporization kinetics *)
  rhol = carrierdensity*10^3; (*[g/m^3]...density
                                   of liquid binder *)
  permeability = 3.33*10^-13; (*[m^2]..permeability *)
  mwgas = 1200.0; (*[g/mol].........molecular weight of vapor
                                   product *)
  viscgas = 1.0*10^-1; (*[Pa*s]....viscosity of decomposed
                           (gaseous) carrier in poise *)
  nominalslurryviscosity = 10.0; (*[Pa*s]*)
  );
solairdiffusivity[temp_] := Module[(* Use Slattery-Bird
    theory to estimate diffusivity of solvent in air *)
  {t,
  molwtfac,
  pcfac,
  tcfac,
  a = 2.745*10^-4,
```

```
    b = 1.823},
    t = temp + 273.15; (* convert temp deg C to K *)
    molwtfac = Sqrt[1/molwtair + 1/molwtsol];
    pcfac = (pcair*pcsol)^0.33;
    tcfac = (tcair*tcsol)^0.42;
    tfac = a*(t/Sqrt[tcair*tcsol])^b;
    diffsolinair = tfac*molwtfac*pcfac*tcfac; (*[cm^2/s]*)
    diffsolinair = diffsolinair*10^-4; (*[m^2/s]*)
    ];
physicalconstants := (
                    accelgravity = 9.81; (*[m/s^2]*);
                    rgas = 8.315; (*[J/mol-K]*);
    );
designdata =.
designdata := ((* Equipment design parameters *)
    mixerimpellerdiameter = 0.2; (*[m]*)
    castingreservoirdepth = 0.1; (*[m]*)
    castinggatethickness = 0.05; (*[m]*)
    gatewidth = 0.25; (*[m] *)
    furnacelength = 1.0; (* [m] *)
    furnaceheight = 0.1; (* [m] *)
    furnacewidth = 0.3; (* [m] *)
    ltool = 0.15; (*[m].....half-length of outgassing/
                                consolidation tooling *)
    );
```

Quality Models

Data for Quality Models

```
slurryproperties =.

slurryproperties := (
    shearthinexp = 0.5;
    shearthincoeff = 10.0;
    khcoeff = 2.7;
    powdervolfractoblock = 0.45; (* powder volume fraction
                in the slurry which causes blocking *)
    liqvapsurfenergy = 1.0; (* [J/m^2] *)
    theta = 35.0*N[Pi]/180.0; (*[rad]..slurry-on-fiber wetting angle *)
    slurrydensity = 1/(powderfracs/powderdensity +
                solventfracs/solventdensity +
                binderfracs/binderdensity +
                plasticizerfracs/plasticizerdensity +
                surfactantfracs/surfactantdensity +
                deflocculantfracs/deflocculantdensity);
    dryslurrydensity = 1/(powderfracg/powderdensity +
                solventfracg/solventdensity +
                binderfracg/binderdensity +
                plasticizerfracg/plasticizerdensity +
                surfactantfracg/surfactantdensity +
                deflocculantfracg/deflocculantdensity);
    powdervolfracs = powderfracs*slurrydensity/powderdensity;
);
```

Casting Quality

```
infiltration =.

infiltration := Module[(* Calculates the velocity at which
    slurry infiltrates the fiber mat, which is then
    used to estimate the completeness of infiltration
    during casting *)
  {n,
  plug = dp/fibergap, (* ratio of mean powder size to fiber gap *)
  qfac = 1.0, (* influence of plug on cast quality: ranges 0 to 1 *)
  pvf},
  If[plug > 1.0,
    Print["Warning: Mean powder size larger than fiber gap."];
    If[plug < 3.0, qfac = 1.0-0.5*(plug-1.0), qfac = 0.0]];
  n = shearthinexp;
  shearstrainrate = tapespeed/gateheight; (* nominal shear rate *)
  If[powdervolfracs >= powdervolfractoblock,
    Print["Warning: high powder loading may cause blocking."];
    pvf = 0.999*powdervolfractoblock,
    pvf = powdervolfracs];
  slurryviscosity = shearthincoeff/shearstrainrate^
    Abs[shearthinexp-1]*(1.0 - pvf/powdervolfractoblock)^
    -(khcoeff*powdervolfractoblock);
```

```
    capillary = 2*liqvapsurfenergy*Cos[theta]/fibergap;
    gravity = slurrydensity*accelgravity*castingreservoirdepth;
    drivingforce = capillary + gravity + appliedpressure;
    infiltrationspeed = n/(2n+1)*
      (drivingforce/(slurryviscosity*fiberdiameter))^(1/n)*
        (fibergap/2)^((n+1)/n);
    infiltrationtime = castinggatethickness/tapespeed;
    infiltrationdepth = infiltrationspeed*infiltrationtime;
    castquality = If[
      infiltrationdepth >= fiberdiameter, qfac*1.0,
      qfac*infiltrationdepth/fiberdiameter]; (* = 1 if fibermat
        is fully infiltrated; between 0 and 1 otherwise. *)
    ];
  cast =.
  cast := Module[(* Uses Chou-Ko-Yan model to calculates the
      tape thickness upon casting *)
    {densityratio = slurrydensity/slurrydensity},
    sideflow = 1.0;
    drivingforce = gravity + appliedpressure;
    tapethicknessc = sideflow*densityratio*gateheight*
      (1.0 + gateheight^2*drivingforce/
      (6*slurryviscosity*tapespeed*castinggatethickness));
    ];
```

■ Drying Quality

```
  drying =.
  drying := Module[(* Calculates a dimensionless drying
      quality factor which lies in the range 0 to 1.
      Quality is determined by the relative magnitudes
      of the diffusive flux of solvent in the drying air
      and that of solvent in the tape. If the flux of
      solvent in air exceeds that in the tape, a skin
      is assumed to form on the tape surface, leading
      to reduced quality (residual stresses, cracking) *)
    {qsa, (*[m/s].....solvent flux in air *)
    qst, (*[m/s].....solvent flux in tape *)
    c = 5 (* critical flux ratio, i.e. the ratio at
      which solvent removal becomes too high and a skin
      forms on the tape during drying *)
    },
    dryingtime = furnacelength/tapespeed; (*[s]...time spent
                                          during drying *)
    solairdiffusivity[dryingtemp]; (* determine diffusivity
              of solvent in air at drying temperature *)
    dryairvel = airflowrate/(furnaceheight*furnacewidth); (*[m/s]*)
    relvel = Abs[dryairvel - tapespeed];
    qsa = Sqrt[4*diffsolinair*relvel/(N[Pi,6]*furnacelength)];
    qst = diffsolintape/tapethicknessc;
    fluxratio = qsa/qst; (* ratio of solvent flux in air to
```

```
                    solvent flux in tape *)
  dryquality = If[qsa < qst, 1.0, 1/(c-1)*(c - fluxratio)];
  evapsolvent = qsa*solventdensity*dryingtime/
    (tapethicknessc*tapedensityb); (* evapsolvent: mass of
                  solvent removed per kg of as-bladed tape *)
  If[evapsolvent > solventfracb, evapsolvent = solventfracb];
  ];
```

■ Outgassing Quality

```
temp[time_] := 293.15 + (1.0 - Exp[-time/(holdstart/3)])*
  outgastemp; (* temperature function for outgassing *)

pressure[tx_] := First[Evaluate[y[tx] /. outgassol]*rgas*temp[tx]/mwgas]
  (* Pressure at the center of the tooling at time, tx *)

gasfrac[t_] := Module[(* Predicts the fraction of binder
    transformed to the vapor phase at time, t, or
    alternatively, the fraction of binder remaining.
    The outgassing temperature schedule must be available
    as well as the kinetic parameters for the given
    binder. *)
  {
  isotemp = outgastemp + 273.15,(*[K]..hold temperature *)
  th, (*[s].....................start time for hold *)
  phi0 = 0.0, (*...............initial gas phase fraction *)
  initemp = 293, (*[K].........initial temperature *)
  m, (*[K/s]...................heating rate *)
  e1, e2, e3, e4, e5,
  alpha1, alpha2
  },
  m = heatrate;
  th = holdstart;
  If[t < th,
    e1 = t/Exp[q/(rgas*(initemp + m*t))];
    e2 = initemp/(Exp[q/(rgas*initemp)]*m);
    e3 = initemp/(Exp[q/(rgas*(initemp + m*t))]*m);
    e4 = q/(m*rgas)*ExpIntegralEi[-q/(rgas*initemp)];
    e5 = q/(m*rgas)*ExpIntegralEi[-q/(rgas*(initemp+m*t))];
    alpha1 = k0*(e1 - e2 + e3 - e4 + e5) - Log[1 - phi0];
    phig = N[1 - Exp[-alpha1],5],
  (*Else*)
    e1 = th/Exp[q/(rgas*(initemp + m*th))];
    e2 = initemp/(Exp[q/(rgas*initemp)]*m);
    e3 = initemp/(Exp[q/(rgas*(initemp + m*th))]*m);
    e4 = q/(m*rgas)*ExpIntegralEi[-q/(rgas*initemp)];
    e5 = q/(m*rgas)*ExpIntegralEi[-q/(rgas*(initemp+m*th))];
    alpha1 = k0*(e1 - e2 + e3 - e4 + e5) - Log[1 - phi0];
    phigh = N[1 - Exp[-alpha1],5];
    alpha2 = k0*(t-th)/Exp[q/(rgas*isotemp)] - Log[1 - phigh];
    phig = N[1 - Exp[-alpha2],5]
  ];
```

```
  (*Print["Start soak at ",th];
  Print["Soak temp: ",isotemp-273.15," [C]"];
  If[t>th, Print["phig at start of soak: ",phigh];
    Print["phig at end of soak: ",phig] ];*)
  phig*1.0
];
outgas =.
outgas := Module[(* Solves a simplified continuity
    equation for the production and removal of vapor
    products during outgassing. As vapor products are
    produced during heating of the binder, they are
    removed by flow through the porous powder/fiber
    compact with the aid of a vacuum applied to the
    tooling (Darcy Flow).
    Internal pressure is generated as the gases are
    created and expand, which can cause cracking or
    voiding within the tape if the rate of removal is
    too slow relative to the rate of vapor creation.
    Predicts whether a pre-defined critical pressure is
    reached during outgassing and relates this to
    the quality of the outgassed tape. *)
  {tcrit = 10^8, (*[s].........critical time *)
  pcrit = 1.01*10^5, (*[Pa].....critical pressure *)
  contaminationfactor (* influence of residual organics on quality *)
  },
  holdstart = (outgastemp - 20.0)/heatrate; (*[s]...time at
                                        which soak begins *)

  rhog0 = pexit/(rgas*temp[0.0])*mwgas;
  contaminationfactor = Exp[-residbinder/0.02];
  outgastime = (* Uses "gasfrac" to determine
    the time required to remove all binder except a given
    remaining fraction, residbinder *)
    xs /. First[
    FindRoot[1.0-gasfrac[xs] == residbinder,{xs,{1.0,1.0*10^5}}]];
  outgassol = NDSolve[{y'[x] == k0*Exp[-q/(rgas*temp[x])]*
    (1.0-gasfrac[x])*rhol/gasfrac[x]*(1.0-y[x]/rhol) -
    2*permeability*rgas*temp[x]/
    (mwgas*viscgas*ltool^2*gasfrac[x])*
    Abs[(y[x] - pexit/(rgas*temp[x])*mwgas)]*y[x],
    y[0] == rhog0}, y, {x,0,1.2*outgastime}];
  If[pressure[outgastime] < pcrit,
    tcrit = 10^8,
    tcrit = xs /. First[FindRoot[pressure[xs] == pcrit,
    {xs,{1.0,1.2*outgastime},0,1.2*outgastime}]] ];
  If[tcrit < outgastime,
    outgasquality = tcrit/outgastime*contaminationfactor,
    outgasquality = 1.0*contaminationfactor];
  (*Print["Time to outgas: ",outgastime/3600.0," [hr]"];
  Print["Critical pressure: ",pcrit/10^3," [kPa]"];
```

```
  If[tcrit < outgastime,
    Print["Critical time: ",tcrit/3600.0," [hr]"],
    Print["Critical pressure not reached."] ];
  Print["Outgas Quality: ",outgasquality];*)
  shrinkage; (* estimate shrinkage due to binder removal *)
  outgassedcomposition; (* vol fractions after outgassing *)
  tapethickness = (1.0 - shrinkagestrain)*tapethicknessc;
  ];
pdfdp[dia_] := (* Probability Density Function describing the
    powder particle size distribution *)
  Exp[-0.5*((dia-dp)/dpsd)^2]/(Sqrt[2*N[Pi,6]]*dpsd);
```

Tape Shrinkage

```
shrinkage =.
shrinkage := Module[(* Calculates the linear shrinkage as a
    result of binder removal during outgassing. Assumes all
    binder is removed. *)

  {np, (*.............number of particles per unit volume*)
  ls, (*[m]...........mean center-to-center particle spacing *)
  pf = 0.74, (*........particle packing fraction for a close-
    packed assembly of uniformly sized spheres *)
  ngaps, (*[1/m].......number of interparticle gaps per m *)
  gapreduction (*[m]...mean reduction in interparticle gap *)
  },
  np = powdervolfracs/
    NIntegrate[pdfdp[x]*N[Pi,6]/6.0*x^3,{x,0,0.01}];
  ls = (6.0/N[Pi,6]*pf/np)^(1.0/3.0);
  ngaps = 1/dp;
  gapreduction = ls - dp;
  shrinkagestrain = ngaps*gapreduction; (* linear strain due
    to shrinkage *)
  maxstrain = 1.0 - Sqrt[(residbinder*carriervolfracg +
    powdervolfracg + fibervolfracg)/(1-(1-0.74)*carriervolfracg)];
    (* maxstrain = the maximum shrinkage strain based on 100%
       removal of organic material and a close-packed powder
       structure (packing factor = 0.74) *)
  If[shrinkagestrain > maxstrain, shrinkagestrain = maxstrain];
  (* relate shrinkage strain to quality? *)
  ];
```

■ Tape Quality

```
tapequality =.

tapequality := Module[(* Uses process models to predict
    the as-processed microstructure for a given material
    and process schedule. The output of the routine is
    a relative quality index, 0 to 1, 1 being the best. *)
  {castingimportance = 0.25, (* Weighting factors determine *)
  dryingimportance = 0.25, (* the relative importance of *)
  outgasimportance = 0.5}, (* quality during each process step *)
  slurryproperties;
  infiltration;
  Print["Infiltration complete."];
  cast;
  Print["Casting complete."];
  bladedcomposition; (* reevaluate vol/mass fractions
    after combining slurry with fibers *)
  drying;
  driedcomposition; (* reevaluate vol/mass fractions
    after evaporating solvent, evapsolvent [kg] per
    kg of as-bladed tape *)
  Print["Drying complete."];
  outgas;
  Print["Outgas complete."];
  actualquality = castingimportance*castquality +
            dryingimportance*dryquality +
            outgasimportance*outgasquality;
  mue = 1.0;
  ];
```

■ Resource Models

```
(* Resource models based on a small scale production unit *)

mixerpower =.

mixerpower[rate_] := Module[(* [W] to power slurry mixer *)
  {cd = 1.0 (*.......impeller drag coefficient *)},
  cd*(rate/60.0)^3*slurrydensity*(mixerimpellerdiameter)^5];

casterpower[rate_] := 500.0; (* [W] to power tape drive *)

dryingovenpower[t_] := 800.0 + 16.0*(t-20.0); (* [W] to power drying
      oven; 800W to start, increasing at 16.0 W/degree C above 20 *)

thermolysispower[t_] := 2000.0 + 20.0*(t-20.0) +
  (500.0 + 10.0*133.0/pexit); (* [W] to power thermolysis furnace and
    vacuum pump to maintain a specified exit pressure *)
```

Cost Model

■ Production Rate

```
prate =.
prate := ((*
    Calculates the rate of tape production as
    controlled by each of the steps in the process:
    slurry formulation, casting/drying, outgassing.
    The slowest process is rate-controlling. *)
  slurryrate = (powderfracs/powderfracf)*mue*
      mixerbatchsize/mixingtime; (* rate at which MMC
            tape can be produced based on the rate of
                                  slurry production *)
  castrate = (tapespeed*tapethicknessc*gatewidth)*
        tapedensity;
  outgasrate = outgasbatchsize*
    (powderfracg + fiberfracg + residbinder*carrierfracg)/
                outgastime; (* outgas batch size refers to the
              mass [kg] of green tape placed in the tooling *)
  productionrate = Min[slurryrate,castrate,outgasrate];
  netproductionrate = productionrate*yield;
  );
```

■ Cost Data

```
tapecostdata =.
tapecostdata := ((* A conversion factor of 2.2 is used
     where input in [$/lb] is converted to units of [$/kg] *)
  costofpowder = 500.0 - 1.5*10^6*dp; (*[$/kg].....cost of low
    volume Ti-6Al-4V powder *)
  costoffiber = 1000.0;                (*[$/kg]*)
  costofbinder = 45.0;                 (*[$/kg]*)
  costofplasticizer = 50.0;            (*[$/kg]*)
  costofsolvent = 5.0;                 (*[$/kg]*)
  costofsurfactant = 12.0;             (*[$/kg]*)
  costofdeflocculant = 12.0;           (*[$/kg]*)
  costoftooling = 150.0 *2.2;          (*[$/kg] of
    composite tape produced *);
  costofenergy = 0.016; (* [$/kWh] *));
facilitycostdata =.
facilitycostdata = (
                costofmixer = 1000.0; (*[$]*)
                costofcaster = 10000.0;
                costoffurnace = 25000.0; );
```

■ Cost Models

```
cm =.
cm := ((*
    Calculates the material costs (powder + fiber) in [$/kg]
    given the  volume fractions of powder and fiber in the
```

```
    finished (outgassed) tape and the material use efficiency *)
  materialcost = costofpowder/mue*powderfracf + costoffiber*fiberfracf
  );
ccon =.
ccon := ((*
    Calculates the cost of consumables per kg of finished
    (outgassed) tape *)
  consumablescost = binderfracs/(mue*powderfracs)*costofbinder +
  solventfracs/(mue*powderfracs)*costofsolvent +
  plasticizerfracs/(mue*powderfracs)*costofplasticizer +
  surfactantfracs/(mue*powderfracs)*costofsurfactant +
  deflocculantfracs/(mue*powderfracs)*costofdeflocculant +
  costoftooling;
  );
cc := ((* Calculates capital costs *)
  capitalcost = costofmixer + costofcaster + costoffurnace;
  );
ce =.
ce :=  ((*
    Calculates the total process energy cost per kg of final
    (outgassed) composite tape *)
  costofenergy = costofenergy/(3.6*10^6); (* convert $/kWh
                                    to $/(W*s) = $/Joule *)
  mixedpowdermass = powderfracf/mixerbatchsize;
  costofmixing = mixerpower[mixerrpm]*mixingtime*costofenergy*
    mixedpowdermass/mue; (* cost of mixing per kg powder produced *)
  tapevolume = tapethicknessc*furnacelength*furnacewidth;
  costofprepreg = (casterpower[tapespeed] + dryingovenpower[dryingtemp])
    dryingtime/(tapevolume*tapedensity)*costofenergy;
  costofthermolysis = thermolysispower[outgastemp]*outgastime*
    costofenergy/outgasbatchsize;
  energycost = costofmixing + costofprepreg + costofthermolysis;
  );
tapecost =.
tapecost[m_] := Module[(*
    Calculates the total cost (per kg) of continuous fiber
    reinforced metal matrix composite tape produced by
    slurry casting for an arbitrary set of processing
    conditions *)
  {density},
  tapecostdata;
  facilitycostdata;
  cm;
  ccon;
  cc;
  ce;
  costoftape = (materialcost + consumablescost +
```

```
  energycost) + capitalcost/m;
density = fibervolfrac*fiberdensity + (1.0-fibervolfrac)*powderdensity
basematcost = fibervolfrac*fiberdensity/density*costoffiber +
(1.0-fibervolfrac)*powderdensity/density*costofpowder; (* cost of powd
  and fiber per kg of tape *)
costratio = costoftape/basematcost; (* total cost of tape
  normalized by the cost of the powder and fiber *)
];
```

Quality-Cost: Tape Casting Process

■ INPUT

```
processvariable := (
  Input["Enter mix batch size [kg]:",mixerbatchsize];
  Input["Enter mixing time [hr]:",mixingtime];
    mixingtime = mixingtime/3600.0; (* [s] *)
  Input["Enter mixer speed [RPM]:",mixerrpm];
  Input["Enter tape speed [cm/s]:",tapespeed];
    tapespeed = tapespeed*0.01; (* [m/s] *)
  Input["Enter gate height [mm]:",gateheight];
    gateheight = gateheight*0.001; (* [m] *)
  Input["Enter gatewidth [m]:",gatewidth];
  Input["Enter applied casting pressure [Pa]:",appliedpressure];
  Input["Enter drying temperature [C]:",dryingtemp];
  Input["Enter air flow rate [liter/min]:",airflowrate];
    airflowrate = airflowrate*(0.001/60); (* [m^3/s] *)
  Input["Enter outgas batch size [kg]:",outgasbatchsize];
  Input["Enter outgas heating rate [C/min]:",heatrate];
    heatrate = heatrate/60.0; (* [C/s] *)
  Input["Enter outgas temperature [C]:",outgastemp];
  Input["Enter outgas pressure [torr]:",pexit]; (* Pressure
    imposed by the applied vacuum at the tooling exit *)
    pexit = pexit*133.0; (*[Pa]*)
  Input["Enter allowable residual binder fraction [e.g. 0.01]:",
    residbinder];
    );

defaultprocdata =.

defaultprocdata := (
  mixerbatchsize = 15.0;
  mixingtime = 24.0*3600.0; (*[s]*)
  mixerrpm = 500.0;
  tapespeed = 1.0*0.01; (*[m/s]*)
  gateheight = 0.0003;
  appliedpressure = 0.0;
  dryingtemp = 100.0;
  airflowrate = 55.0*(0.001/60); (*[m^3/s]*)
  outgasbatchsize = 5.0;
  outgastemp = 300.0; (*[C]*)
  heatrate = 200.0/60.0; (*[C/s]*)
  pexit = 10^1(*[torr]*)*133.0; (*[Pa]*)
  residbinder = 0.001;
  );
```

■ Quality-Cost Model

```
tapecastqcm =.

tapecastqcm[req1_,req2_] := Module[(*
    Determines the cost (per kg) and quality of MMC tape
    produced by slurry casting for a given set of processing
```

```
    conditions *)
  {},
  physicalconstants;
  physicaldata;
  designdata;
  printdesigndata;
  fibermat;
  powdersizedist;
  slurrycomposition;
  acceptablequality = req1; (* Must be between 0 and 1; sets
      the cutoff used to determine the yield *)
  prodvol = req2; (* Required production volume *)
  (*defaultprocdata;*)
  processvariable;
  printinput;
  tapequality; (* returns actual tape quality on a scale
    of 0 to 1 as well as other values calculated using
    the quality models *)
  yield = If[actualquality < acceptablequality, 0.0, 1.0];
  tapecost[prodvol];
  prate;
  printreport;
  results = {powderfracs,tapespeed*10^2,gateheight*10^3,dp*10^6,dpsd*10^
    fiberdiameter*10^6,fiberspacing/fiberdiameter,dryingtemp,
    airflowrate/(0.001/60.0),outgastemp,heatrate,pexit/133.0,residbinder
    actualquality,costratio,yield,materialcost,consumablescost,
    energycost,capitalcost,slurryrate*3600.0,castrate*3600.0,outgasrate*
    productionrate*3600.0,infiltrationdepth/fiberdiameter,castquality,
    tapethicknessc/gateheight,slurryviscosity,fluxratio,
    evapsolvent/solventfracb,dryquality,outgastime/3600.0,
    shrinkagestrain,outgasquality,tapethickness*10^3,1.0-voidvolfrac,
    fibervolfrac,powdervolfrac};
  ];
tapecostfcn[pvol_] := (tapecost[pvol];costoftape);
(*Plot[tapecostfcn[x],{x,1,10000},PlotRange->{0,40000}]*)
```

■ OUTPUT

```
printdesigndata =.
printdesigndata := (
  Print["EQUIPMENT DESIGN PARAMETERS"];
  Print["  Mixer impeller diameter [cm]: ",mixerimpellerdiameter*10^2];
  Print["  Casting reservoir depth [cm]: ",castingreservoirdepth*10^2];
  Print["  Gate thickness [cm]: ",castinggatethickness*10^2];
  Print["  Gate width [cm]: ",gatewidth*10^2];
  Print["  Drying furnace length [m]: ",furnacelength];
  Print["  Drying furnace height [cm]: ",furnaceheight*10^2];
  Print["  Drying furnace width [cm]: ",furnacewidth*10^2];
  Print["  Outgas tooling length [cm]: ",2.0*ltool*10^2];
  );
```

```
printinput =.
printinput := (
  Print[""];
  Print["INPUT DATA"];
  Print["    Cumulative production volume [kg]: ",prodvol];
  Print["    Acceptable quality (0 - 1): ",acceptablequality];
  Print["  Slurry Formulation"];
  Print["    Mass Fractions"];
  Print["      powder: ",powderfracs];
  Print["      binder: ",binderfracs];
  Print["      solvent: ",solventfracs];
  Print["      plasticizer: ",plasticizerfracs];
  Print["      surfactant: ",surfactantfracs];
  Print["      deflocculant: ",deflocculantfracs];
  Print["    Mixing batch size [kg]: ",mixerbatchsize];
  Print["    Mixing time [hr]: ",mixingtime/3600.0];
  Print["    Mixing speed [RPM]: ",mixerrpm];
  Print["  Casting"];
  Print["    Tape speed [cm/s]: ",tapespeed*10^2];
  Print["    Gate height [mm]: ",gateheight*10^3];
  Print["    Applied pressure [kPa]: ",appliedpressure/10^2];
  Print["    Fiber diameter [um]: ",fiberdiameter*10^6];
  Print["    Fiber spacing [um]: ",fiberspacing*10^6];
  Print["  Drying"];
  Print["    Drying temperature [C]: ",dryingtemp];
  Print["    Air flow rate [slpm]: ",airflowrate/(0.001/60)];
  Print["  Thermolysis"];
  Print["    Outgas batch size [kg]: ",outgasbatchsize];
  Print["    Outgas temperature [C]: ",outgastemp];
  Print["    Heating rate [C/s]: ", heatrate];
  Print["    Exit pressure [torr]: ",pexit/133.0];
  Print["    Allowable residual binder: ",residbinder];
  Print[""];
  );
printreport =.
printreport := (
  Print[""];
  Print["QUALITY-COST"];
  Print["  Quality: ",actualquality];
  Print["  Yield: ",yield];
  Print["  Cost of tape [$/kg]: ",costoftape];
  Print[""];
  Print["COST ELEMENTS"];
  Print["  Material cost [$/kg]: ",materialcost];
  Print["  Consumables cost [$/kg]: ",consumablescost];
  Print["  Energy cost [$/kg]: ",energycost];
  Print["  Capital cost [$/kg]: ",capitalcost/prodvol];
  Print[""];
  Print["PRODUCTION RATE based on"];
```

```
Print["  Slurry production [kg/hr]: ",N[slurryrate*3600.0,4]];
Print["  Casting production [kg/hr]: ",N[castrate*3600.0,4]];
Print["  Outgassing production [kg/hr]: ",
  N[outgasrate*3600.0,4]];
Print["  Production rate [kg/hr]: ",N[productionrate*3600.0,4]];
Print["  Net production rate [kg/hr]: ",
  N[netproductionrate*3600.0,4]];
Print[""];
Print["TAPE CAST QUALITY PARAMETERS"];
Print["  Infiltration: ",If[infiltrationdepth > fiberdiameter,
  1.0, N[infiltrationdepth/fiberdiameter,3]]];
Print["  Casting Quality: ",castquality];
Print["  Tape thickness/gate height: ",tapethicknessc/gateheight];
Print["  Slurry viscosity [Pa*s]: ",slurryviscosity];
Print["  Flux ratio (qsa/qst): ",N[fluxratio,4],
  "  (Should be less than 1)"];
Print["  Fraction of solvent evaporated: ",
  N[evapsolvent/solventfracb,3]];
Print["  Drying Quality: ",dryquality];
Print["  Time to outgas to ",residbinder,"[hr]: ",
  N[outgastime/3600,4]];
Print["  Shrinkage strain: ",N[shrinkagestrain,3]];
Print["  Outgas Quality: ",outgasquality];
Print["  Tape thickness [mm]: ",tapethickness*10^3];
Print["  Relative density: ",1.0 - voidvolfrac];
Print["  Fiber volume fraction: ",fibervolfrac];
Print["  Powder volume fraction: ",powdervolfrac];
);
```

tapecastqcm[0.5,1000]

```
EQUIPMENT DESIGN PARAMETERS
  Mixer impeller diameter [cm]: 20.
  Casting reservoir depth [cm]: 10.
  Gate thickness [cm]: 5.
  Gate width [cm]: 25.
  Drying furnace length [m]: 1.
  Drying furnace height [cm]: 10.
  Drying furnace width [cm]: 30.
  Outgas tooling length [cm]: 30.

INPUT DATA
    Cumulative production volume [kg]: 1000
    Acceptable quality (0 - 1): 0.5
  Slurry Formulation
    Mass Fractions
      powder: 0.3
      binder: 0.3
      solvent: 0.35
      plasticizer: 0.02
      surfactant: 0.01
      deflocculant: 0.02
    Mixing batch size [kg]: 15.
    Mixing time [hr]: 24.
    Mixing speed [RPM]: 500.
  Casting
    Tape speed [cm/s]: 1.
    Gate height [mm]: 0.3
    Applied pressure [kPa]: 0.
    Fiber diameter [um]: 142.
    Fiber spacing [um]: 284.
  Drying
    Drying temperature [C]: 100.
    Air flow rate [slpm]: 55.
  Thermolysis
    Outgas batch size [kg]: 5.
    Outgas temperature [C]: 300.
    Heating rate [C/s]: 3.33333
    Exit pressure [torr]: 10.
    Allowable residual binder: 0.001

Warning: Mean powder size larger than fiber gap.
Infiltration complete.
Casting complete.
Drying complete.
Outgas complete.

QUALITY-COST
  Quality: 0.83653
  Yield: 1.
  Cost of tape [$/kg]: 793.583

COST ELEMENTS
  Material cost [$/kg]: 369.766
  Consumables cost [$/kg]: 385.367
  Energy cost [$/kg]: 2.45063
  Capital cost [$/kg]: 36.

PRODUCTION RATE based on
  Slurry production [kg/hr]: 0.283
  Casting production [kg/hr]: 9.22
  Outgassing production [kg/hr]: 0.03005
  Production rate [kg/hr]: 0.03005
  Net production rate [kg/hr]: 0.03005
```

```
TAPE CAST QUALITY PARAMETERS
  Infiltration: 1.
  Casting Quality: 0.443662
  Tape thickness/gate height: 1.02339
  Slurry viscosity [Pa*s]: 5.13074
  Flux ratio (qsa/qst): 0.6075  (Should be less than 1)
  Fraction of solvent evaporated: 1.
  Drying Quality: 1.
  Time to outgas to 0.001[hr]: 93.9
  Shrinkage strain: 0.212
  Outgas Quality: 0.951229
  Tape thickness [mm]: 0.242052
  Relative density: 0.882503
  Fiber volume fraction: 0.401158
  Powder volume fraction: 0.480618
```

APPENDIX D Tape Cast QCM Experiments

Exper. No.	Powder Fraction	Tape Speed [cm/s]	Gate Height [mm]	Mean Part Size [um]	Standard Deviation	Fiber Dia [um]	Fiber Spacing	Dry Temp [C]
1	0.4	1	1	100	55	142	2	165
2	0.4	1	1	100	55	142	2	100
3	0.4	1	1	100	55	142	2	100
4	0.4	1	1	100	55	142	2	100
5	0.4	1	0.5	100	55	142	2	100
6	0.4	1	0.3	100	55	142	2	100
7	0.35	1	0.3	100	55	142	2	100
8	0.3	1	0.3	100	55	142	2	100
9	0.3	5	0.3	100	55	142	2	100
10	0.3	1	0.3	100	55	142	2	150
11	0.3	1	0.3	100	55	142	2	100
12	0.3	1	0.3	150	55	142	2	100
13	0.3	1	0.3	180	55	142	2	100
14	0.3	1	0.3	40	25	142	2	100
15	0.3	1	0.3	40	25	142	2	100
16	0.3	1	0.3	180	55	142	2	100
17	0.3	1	0.3	180	55	142	2	100
18	0.3	1	0.3	150	55	142	2	100
19	0.3	1	0.3	220	55	142	2	100
20	0.3	1	0.3	300	75	142	2	100

Exper. No.	Drying Temp [C]	Air Flow Rate [slpm]	Outgas Temp [C]	Heat Rate [C/s]	Pexit [torr]	Residual Binder	Actual Quality	Cost Ratio
1	165	65	450	3.33333	10	0.001	0.698202	2.02386
2	100	65	450	3.33333	10	0.001	0.721504	2.02385
3	100	25	450	3.33333	10	0.001	0.806836	2.02385
4	100	25	400	3.33333	10	0.001	0.975615	2.02441
5	100	25	400	3.33333	10	0.001	0.975615	1.92605
6	100	25	400	3.33333	10	0.001	0.975615	1.82859
7	100	25	400	3.33333	10	0.001	0.975615	1.84103
8	100	25	400	3.33333	10	0.001	0.975615	1.83995
9	100	25	400	3.33333	10	0.0001	0.997506	1.83772
10	150	25	400	3.33333	10	0.01	0.526693	1.83797
11	100	55	450	3.33333	10	0.001	0.806737	1.83953
12	100	55	450	3.33333	10	0.001	0.799695	1.93914
13	100	55	450	3.33333	10	0.001	0.773286	2.01015
14	100	55	450	3.33333	10	0.001	0.806737	1.74327
15	100	55	350	3.33333	10	0.001	0.975615	1.74452
16	100	55	350	3.33333	10	0.001	0.942164	2.01181
17	100	55	300	3.33333	10	0.001	0.942164	2.01498
18	100	55	300	3.33333	10	0.001	0.968572	1.94365
19	100	55	300	3.33333	10	0.001	0.906953	2.12737
20	100	55	300	3.33333	10	0.001	0.83653	2.44053

Exper. No.	Yield	Mat'l Cost [$/kg]	Cons Cost [$/kg]	Energy Cost [$/kg]	Cap Cost [$]	Tape Cost [$/kg]	Slurry Prod Rate	Cast Rate [kg/hr]
1	1	405.473	365.275	0.265226	36000	807.0132	0.273642	36.6516
2	1	405.473	365.275	0.264848	36000	807.0128	0.273642	36.6516
3	1	405.473	365.275	0.264848	36000	807.0128	0.273642	36.6516
4	1	405.473	365.275	0.487323	36000	807.2353	0.273642	36.6516
5	1	461.279	365.275	0.48673	36000	863.0407	0.301988	16.9555
6	1	529.14	365.275	0.486232	36000	930.9012	0.345512	9.61454
7	1	547.494	376.743	0.485594	36000	960.7226	0.314706	9.37906
8	1	568.543	385.367	0.484988	36000	990.395	0.28298	9.21969
9	1	571.203	385.367	0.638063	36000	993.2081	0.284277	45.4581
10	1	564.615	385.367	0.330201	36000	986.3122	0.284949	9.2155
11	1	568.543	385.367	0.262512	36000	990.1725	0.28298	9.21969
12	1	518.849	385.367	0.262512	36000	940.4785	0.28298	9.21969
13	1	489.032	385.367	0.262512	36000	910.6615	0.28298	9.21969
14	1	628.176	385.367	0.262512	36000	1049.806	0.28298	9.21969
15	1	628.176	385.367	1.01285	36000	1050.556	0.28298	9.21969
16	1	489.032	385.367	1.01285	36000	911.4119	0.28298	9.21969
17	1	489.032	385.367	2.45063	36000	912.8496	0.28298	9.21969
18	1	518.849	385.367	2.45063	36000	942.6666	0.28298	9.21969
19	1	449.277	385.367	2.45063	36000	873.0946	0.28298	9.21969
20	1	369.766	385.367	2.45063	36000	793.5836	0.28298	9.21969

Exper. No.	Outgas Rate [kg/hr]	Prod Rate [kg/hr]	Infiltration	Cast Quality	Tape/ Gate	Viscosity [Pa*s]	Flux Ratio	Frac Sol Evap
1	0.428664	0.273642	75959.7	1	1.06052	22.3734	2.73814	1
2	0.428664	0.273642	75959.7	1	1.06052	22.3734	2.36531	1
3	0.428664	0.273642	75959.7	1	1.06052	22.3734	0.912825	1
4	0.204808	0.204808	75959.7	1	1.06052	22.3734	0.912825	1
5	0.21293	0.21293	151919	1	1.0214	15.8204	0.439575	1
6	0.223718	0.223718	253199	1	1.00994	12.2544	0.260788	1
7	0.203613	0.203613	722719	1	1.01665	7.23004	0.262518	1
8	0.194669	0.194669	1.43E+06	1	1.02339	5.13074	0.264259	1
9	0.146245	0.146245	1.43E+06	1	1.01046	2.29454	0.795089	1
10	0.29376	0.284949	1.43E+06	1	1.02339	5.13074	0.296351	1
11	0.407444	0.28298	1.43E+06	1	1.02339	5.13074	0.607548	1
12	0.407444	0.28298	1.43E+06	0.971831	1.02339	5.13074	0.607548	1
13	0.407444	0.28298	1.43E+06	0.866197	1.02339	5.13074	0.607548	1
14	0.407444	0.28298	1.43E+06	1	1.02339	5.13074	0.607548	1
15	0.0824689	0.0824689	1.43E+06	1	1.02339	5.13074	0.607548	1
16	0.0824689	0.0824689	1.43E+06	0.866197	1.02339	5.13074	0.607548	1
17	0.0300467	0.0300467	1.43E+06	0.866197	1.02339	5.13074	0.607548	1
18	0.0300467	0.0300467	1.43E+06	0.971831	1.02339	5.13074	0.607548	1
19	0.0300467	0.0300467	1.43E+06	0.725352	1.02339	5.13074	0.607548	1
20	0.0300467	0.0300467	1.43E+06	0.443662	1.02339	5.13074	0.607548	1

Exper. No.	Dry Quality	Outgas Time [hr]	Shrinkage Strain	Outgas Quality	Tape thickness	Rel Density	Fiber vol fraction	Powd vol fraction
1	0.565466	6.92432	0.215211	0.613671	0.832286	0.880949	0.117548	0.762658
2	0.658673	6.92432	0.215211	0.613671	0.832286	0.880949	0.117548	0.762658
3	1	6.92432	0.215211	0.613671	0.832286	0.880949	0.117548	0.762658
4	1	14.4927	0.215211	0.951229	0.832286	0.880949	0.117548	0.762658
5	1	14.4927	0.193404	0.951229	0.411928	0.890528	0.225991	0.663889
6	1	14.4927	0.167437	0.951229	0.252253	0.902565	0.347415	0.554609
7	1	14.4927	0.198587	0.951229	0.244426	0.888209	0.37123	0.51631
8	1	14.4927	0.2116	0.951229	0.242052	0.882503	0.401158	0.480618
9	1	19.3223	0.210833	0.995012	0.239226	0.882961	0.405072	0.477817
10	1	9.67083	0.208682	0.0533863	0.242947	0.882503	0.398206	0.477081
11	1	6.92432	0.2116	0.613474	0.242052	0.882503	0.401158	0.480618
12	1	6.92432	0.2116	0.613474	0.242052	0.882503	0.401158	0.480618
13	1	6.92432	0.2116	0.613474	0.242052	0.882503	0.401158	0.480618
14	1	6.92432	0.2116	0.613474	0.242052	0.882503	0.401158	0.480618
15	1	34.2101	0.2116	0.951229	0.242052	0.882503	0.401158	0.480618
16	1	34.2101	0.2116	0.951229	0.242052	0.882503	0.401158	0.480618
17	1	93.8964	0.2116	0.951229	0.242052	0.882503	0.401158	0.480618
18	1	93.8964	0.2116	0.951229	0.242052	0.882503	0.401158	0.480618
19	1	93.8964	0.2116	0.951229	0.242052	0.882503	0.401158	0.480618
20	1	93.8964	0.2116	0.951229	0.242052	0.882503	0.401158	0.480618

DISTRIBUTION LIST

1 - 4	Mr. Glen M. Williams, Contracting Officer Technology Support Branch, MS 500-306 National Aeronautics and Space Administration Lewis Research Center 21000 Brookpark Road Cleveland, OH 44135
5	Dr. Hugh R. Gray Materials Division National Aeronautics and Space Administration Lewis Research Center 21000 Brookpark Road Cleveland, OH 44135
6 - 7	D. Elzey
8	H. N. G. Wadley
9	W. A. Jesser
10 - 11*	NASA Scientific and Technical Information Facility P. O. 8757 Baltimore/Washington International Airport Baltimore, MD 21240
12 - 13	M. Rodeffer, Clark Hall
**	SEAS Postaward Research Administration
14	SEAS Preaward Research Administration

*1 unbound copy
**Cover Letter

JO#7020:ph